

ASSESSMENT OF DEBRIS-FLOW HAZARDS, NORTH MOUNTAIN, PHOENIX, AZ

by

Kathryn Jeanette Reavis

December, 2014

Director: Thad Wasklewicz, Ph.D.

Department of Geography, Planning, and Environment

Population increases in many western cities have led to urban sprawl, which has been a constant issue in metropolitan Phoenix, AZ. The Metropolitan Phoenix Area (MPA) has sprawled exponentially since its initial development and in doing so has expanded into surrounding mountainous areas and onto alluvial fans. Alluvial fans, particularly in the western US, provide cooler, more scenic environments for people to live. Alluvial fans are conic-shaped features occurring in piedmont areas prone to floods and debris-flows. Debris-flows often supply large quantities of material to alluvial fans and are critical to the long-term development of alluvial fans. A key to understanding alluvial fan evolution is quantifying debris-flow dynamics above and below the fan apex.

The addition of humans and built structures into these environments increases the risk of exposure to debris-flows, and therefore the vulnerability of people and their housing structures. This scenario magnifies the importance of understanding debris-flow hazards from a holistic multidisciplinary perspective. The scientific understanding of the evolution of alluvial fan systems needs to be instilled to protect society via engineered solutions and planning decisions.

These management schemes must be grounded in a quantitative understanding of debris-flow behavior.

A 2D debris-flow modeling approach, aided by high-resolution air-borne laser scanning (ALS) and terrestrial laser scanning (TLS) topographic data, is implemented to examine debris-flow behavior in a densely populated portion of the MPA and to assess the vulnerability of the built infrastructure to debris-flow damage. A calibrated 2D debris-flow model is developed for a recent debris-flow at an undeveloped site and applied to a developed site - Shaw Butte at North Mountain, a populated area with historical evidence of debris-flow activity. Several values were maintained from the calibrated model and these include: antecedent moisture conditions; an estimated volume; and sediment concentration by volume (C_v). Four separate scenarios were applied to the developed site with variations in precipitation events, including the historical rainstorm that initiated the debris-flow at Elephant Mountain, two higher magnitude seasonally average rainstorms, and one maximum event that made use of the largest recorded rainstorm for the area.

Overall the results show that the highest debris-flow depths and velocities, and therefore the highest debris-flow intensities occur at the fan apex and within the existing debris-flow channel, directly below the fan apex. The complexity of the alluvial fan topography plays a major role in the flow direction. For instance, in all four scenarios, the flow did not exit into the developed neighborhood perpendicular to the fan apex (a northerly direction at the site), rather the topography steered flows in a northwesterly direction. Homes on the western side of the neighborhood are the most vulnerable to debris-flow inundation. The addition of impervious surfaces such as roadways on the alluvial fan also has an influence on debris-flow behavior as these areas provide an ideal surface for maintaining high velocities and therefore have an impact

by amplifying the runout distances and the areal extent of inundation. The building vulnerability index results show that, depending on the magnitude of a potential debris-flow, a range of 22 to 44 homes are potentially in danger of damage.

These results have scientific and applied merit. The 2D debris-flow modeling provides new insight into how drainage basin and alluvial fan topography influence debris-flow inundation, velocity, and runout. The 2D modeling coupled with the building vulnerability index provides a broader understanding of societal implications. These results are important in that they can provide communities and hazard management agencies with decision-making data and mitigation information based upon the degree of risk and therefore vulnerability associated with different debris-flow magnitudes.

ASSESSMENT OF DEBRIS-FLOW HAZARDS, NORTH MOUNTAIN, PHOENIX, AZ

A Thesis

Presented To

The Faculty of the Department of Geography, Planning, and Environment

East Carolina University

In Partial Fulfillment of the Requirements for the Degree

M. A. Geography, Planning and Environment

by

Kathryn Jeanette Reavis

December, 2014

©Kathryn Jeanette Reavis, 2014

ASSESSMENT OF DEBRIS-FLOW HAZARDS, NORTH MOUNTAIN, PHOENIX, AZ

by

Kathryn Jeanette Reavis

APPROVED BY:

DIRECTOR OF THESIS: _____
Thad Wasklewicz, Ph.D.

COMMITTEE MEMBER: _____
Burrell Montz, Ph.D.

COMMITTEE MEMBER: _____
Paul Gares, Ph.D.

CHAIR OF THE DEPARTMENT OF GEOGRAPHY, PLANNING, AND ENVIRONMENT:

Burrell Montz, Ph.D.

DEAN OF THE GRADUATE SCHOOL:

Paul Gemperline, Ph.D.

ACKNOWLEDGEMENTS

First of all, I would like to thank my committee members, Dr. Burrell Montz and Dr. Paul Gares for their help and support and for pushing me to think more critically about my research. I would also like to extend a special thanks to Dr. Ron Dorn of Arizona State University for his intellectual input, inspirational enthusiasm, and generous assistance with travel, field work, and in general support. I would also like to give special recognition to my dear friend Mitch Haynes for not only emotional and technical support but also for sacrificing his back and legs during our long hikes with research equipment. I would also like to thank all of the faculty members of the Department of Geography, Planning, and Environment for always being available to help and provide support, especially Dr. Scott Lecce for his assistance with the sediment laboratory analysis. I would also like to thank my mother Della Reavis, my father Charles Reavis, my ECU cousins Matthew, Kristin, Brian, Sandra, and Christopher Meyerhoeffer, and my dearest friends Cal and Elizabeth Scheinert, Alex Smith, Mike and Jennifer Griffin, Holly Lussenden, Elliot Wickham, and Laura Havener for their steadfast support and comic relief.

And finally, above all, I would like to thank my advisor, Dr. Thad Wasklewicz for his support and guidance throughout my time here at East Carolina University. Thad is a one in a million teacher, advisor, and friend and I am lucky to have had the opportunity to work with and learn from him. Without his guidance and influence my successful academic and professional careers would not have been possible.

TABLE OF CONTENTS

TITLE PAGE.....	i
COPYRIGHT PAGE.....	ii
SIGNATURE PAGE.....	iii
ACKNOWLEDGEMENTS.....	iv
LIST OF TABLES.....	viii
LIST OF FIGURES.....	ix
CHAPTER 1: INTRODUCTION.....	1
CHAPTER 2: CURRENT STATE OF KNOWLEDGE.....	5
Alluvial Fans.....	5
Debris-flows.....	6
Debris-flow and Alluvial Fan Research.....	9
Key Debris-flow Parameters.....	10
Research Methods.....	11
Debris-flow and Alluvial Fan Hazards.....	16
Clarification of Hazard Terminology.....	16
Debris-flow Hazard Research.....	18
2D Modeling and Hazard Mapping.....	20
Quantifying Building Vulnerability.....	22
CHAPTER 3: STUDY AREA.....	26
Metropolitan Phoenix AZ (MPA).....	26
Elephant Mountain.....	30
Shaw Butte.....	32
CHAPTER 4: METHODOLOGY.....	36

Summary of Methods.....	37
Fieldwork and Sediment Analysis.....	38
Sediment Laboratory Analysis.....	38
Terrestrial Laser Scanning (TLS) and Volumetric Calculations.....	39
Airborne Laser Scanning (ALS) Data Collection.....	40
FLO-2D Modeling.....	41
Shaw Butte Modeling Scenarios.....	41
Building Vulnerability Index.....	48
CHAPTER 5: RESULTS.....	50
Results from Initial Data Acquisition.....	50
FLO-2D Modeling.....	54
Calibrated Model at Elephant Mountain.....	54
Scenario 1: Historical Debris-flow Recorded at Elephant Mountain.....	58
Scenario 2: Lower Average Event (AVG1).....	62
Scenario 3: Higher Average Event (AVG2).....	65
Scenario 4: Maximum Historical Rainfall.....	68
CHAPTER 6: DISCUSSION.....	72
Field work and Sediment Analysis.....	72
2D Debris-Flow Modeling.....	73
Model Calibration.....	74
Shaw Butte Scenarios.....	75
Building Vulnerability Index.....	78
Limitations of Research.....	80
Strengths and Weakness of FLO-2D.....	81

CHAPTER 7: CONCLUSIONS.....	82
Future Research.....	83
Broader Impacts and Geographical Context.....	84
REFERENCES.....	85

LIST OF TABLES

Table 2.1. Damage Classes with corresponding qualitative description and percent of insured loss for each (Jakob et al., 2012).....	24
Table 2.2. The percent probability of damage occurring for a specified debris-flow intensity (I_{DF}) (Jakob et al., 2012).....	24
Table 4.1. Outline of each model scenario applied to the Shaw Butte site at North Mountain based on differences in rainfall.....	42
Table 4.2. The percent probability of damage occurring for a specified debris-flow intensity (I_{DF}) (Jakob et al., 2012).....	50
Table 4.3. Damage Classes with corresponding qualitative description and percent of insured loss for each (Jakob et al., 2012).....	50
Table 5.1. Table of the results of the laboratory sediment analysis. High percentages of fine particles such as silt and clay provide evidence of debris-flow activity.....	53
Table 5.2. Number of homes affected and their corresponding damage class description and percent of insured loss for all four scenarios.....	62
Table 6.1. Number of homes affected and their corresponding damage class description and percent of insured loss for all four scenarios.....	79

LIST OF FIGURES

Figure 2.1. Basic operation of an ALS (Petrie and Toth, 2008).....	14
Figure 2.2. Basic operation of a pulse based TLS (Petrie and Toth, 2008).....	15
Figure 3.1. Maps of AZ representing average annual precipitation (A) and average monsoonal precipitation (B) for the past ~57 years (Flood Control District of Maricopa County, 2013).....	27
Figure 3.2. Map of MPA with the undeveloped model calibration site at Elephant Mountain in red and the developed hazard analysis site at Shaw Butte in blue.....	29
Figure 3.3. Map of the undeveloped model calibration site at Elephant Mountain (circle) and its closest rain gage (triangle) that was used for rainfall data.....	31
Figure 3.4. Images of the Elephant mountain debris-flow site that occurred in 2010 (Dorn, 2010).....	32
Figure 3.5. Map of the developed hazard analysis site at Shaw Butte on North Mountain.....	33
Figure 3.6. Images of the developed site at Shaw Butte on North Mountain, one looking south towards the mountain and debris-flow levees (top) and one looking north towards the potentially at risk neighborhood from the top of the right levee (bottom).....	34
Figure 3.7. Slope map of the drainage basin at the Elephant Mountain study site (right) and Shaw Butte study site.....	35
Figure 4.1. 2010 debris-flow inducing rainstorm at Elephant Mountain; with the Elephant Mountain gage located in the yellows and reds of the northeastern section and Shaw Butte located just south of Elephant Mountain in the yellow and lighter greens (Flood Control district of Maricopa County’s Alert System Data Report Generator, 2013).....	43
Figure 4.2. Mean Annual Precipitation recorded from gage stations with 10 or more years on record; with the Elephant Mountain gage located in the yellows and greens of the northeastern section and Shaw Butte located just south of Elephant Mountain in the lighter browns (Flood Control District of Maricopa County’s Alert System Data Report Generator, 2013).....	44
Figure 4.3. 24 hour rainstorm extremes from gage stations with 10 or more years on record; with Elephant Mountain gage located in the yellows and reds of the northeastern section and Shaw Butte located just south of Elephant Mountain in the lighter blues and greens (Flood Control District of Maricopa County’s Alert System Data Report Generator, 2013).....	45

Figure 4.4. Top left: image of rain gage 4920 at cave creek; top right: map of rain gage 4920; bottom: Average monthly rainfall for the past 2 decades at this gage, years in grey represent an incomplete dataset due to gage malfunction. Data provided by the Flood Control District of Maricopa County (2013).....	47
Figure 5.1. Graph of a total of 96 AxBxC particle size measurements made every one-meter along the top of the right levee looking downslope for a total of 88 meters at the undeveloped site at Elephant Mountain.....	51
Figure 5.2. Graph of a total of 51 AxBxC particle size measurements made within the matrix of the levee from a section of the upper channel at the undeveloped site at Elephant Mountain.....	52
Figure 5.3. Graph of 100 AxBxC particle size measurements made every one-meter along the top of the right debris-flow levee at the developed site at Shaw Butte.	53
Figure 5.4. Graph of 48 AxBxC particle size measurements made within the matrix of the left levee.	53
Figure 5.5. Rainfall event that led to the debris-flow at Elephant Mountain in 2010. Resulted in a total of 105.41 mm of precipitation (top). The combination of rainfall, Cv values, and topographic data develops the debris-flow hydrograph (bottom).....	55
Figure 5.6. Shows the mapped FLO-2D results of the 2010 debris-flow at Elephant Mountain including flow depth (top left), flow velocity (top right), raw intensity values (IDF) (bottom left), and intensity in terms of the building vulnerability index (bottom right).....	57
Figure 5.7. Rainfall event that led to the debris-flow at Elephant Mountain in 2010. Resulted in a total of 105.41 mm of precipitation (top). The combination of rainfall, Cv values, and topographic data develops the debris-flow hydrograph (bottom).....	58
Figure 5.8. Shows the mapped FLO-2D results at the Shaw Butte site with application of the rain event of 2010 at Elephant Mountain. The results include flow depth (top left), flow velocity (top right), raw intensity values (bottom left), and intensity in terms of the building vulnerability index (bottom right).....	60
Figure 5.9. The lower average (avg1) rainfall event that resulted in a total of 52.07 mm of precipitation (top). The combination of rainfall, Cv values, and topographic data develops the initially peaked debris-flow hydrograph (bottom).....	63
Figure 5.10. Shows the mapped FLO-2D results at the Shaw Butte site with application of the lower average rain event (avg1). The results include flow depth (top left), flow velocity (top right), raw intensity values (bottom left), and intensity in terms of the building vulnerability index (bottom right).....	64

Figure 5.11. The Higher Average (avg2) rainfall event that resulted in a total of 67.56 mm of precipitation (top). The combination of rainfall, Cv values, and topographic data develops the peaked debris-flow hydrograph (bottom).....66

Figure 5.12. Shows the mapped FLO-2D results at the Shaw Butte site with application of the higher average rain event (avg2). The results include flow depth (top left), flow velocity (top right), raw intensity values (bottom left), and intensity in terms of the building vulnerability index (bottom right).....67

Figure 5.13. The maximum recorded historical rainfall event that resulted in a total of 205.29 mm of precipitation (top). The combination of rainfall, Cv values, and topographic data develops the resulting debris-flow hydrograph (bottom).....69

Figure 5.14. Shows the mapped FLO-2D results at the Shaw Butte site with application of the maximum historical rain event. The results include flow depth (top left), flow velocity (top right), raw intensity values (bottom left), and intensity in terms of the building vulnerability index (bottom right).....70

CHAPTER 1: INTRODUCTION

One of the most dangerous events of all natural hazardous phenomena is a debris-flow (Takahashi, 1981) because of their unpredictability of onset and destructive power. Debris-flows are considered the most lethal, destructive, and common hazards in many mountainous regions of Latin America, China, former USSR, New Zealand, Japan, Pakistan, Afghanistan, and India. In the US, debris-flows are estimated to cause over \$2 billion in damages and 25-50 deaths annually, with worldwide annual deaths totaling approximately 1,000 (Santi et al., 2011). Debris-flows are rapid gravity induced mass movements of saturated sediment. Debris-flows occur in areas with steep relief and play a significant role in the geomorphology of the surrounding landscape, and more specifically, on alluvial fan evolution and development. Alluvial fans in the Metropolitan Phoenix Arizona (MPA) region typically form at the mouth of steep canyons as a result of deposition from debris-flows and sediment-laden floods. These particular features commonly provide readily developable land for urban expansion in mountainous regions because of their gentle slopes (in relation to the steep drainage areas), aquifer accessibility, and desirable views (Jakob, 2005; Santi et al., 2011; Welsh and Davies, 2010). However, when humans encroach upon these regions, debris-flows evolve from a natural phenomenon of sediment transportation to an environmental hazard. In the past, societies would learn about debris-flows through direct exposure, and would respond to the hazard by avoiding areas susceptible to them (Jakob and Hungr, 2005). Presently, the combination of, population growth, urban sprawl, and lack of knowledge, has led to an increase in residents in these areas. This has given rise to an increase in exposure to debris-flows and therefore, an increase in vulnerability of life and property (Dorn, 2011). The devastating power of debris-flows can be catastrophic and are made even more dangerous their rapid initiation and substantial gap between

the initiation site and the area of deposition where the destruction occurs. Direct debris-flow damage includes casualties, damage to property and infrastructure, environmental destruction, loss of crops in agricultural areas, disruption of water supply, and many others (Jakob and Hungr, 2005).

The worldwide urban sprawl onto alluvial fans has prompted a need to research debris-flow initiation and propagation, prediction methods, and where applicable, mitigation techniques (Jakob and Hungr, 2005). Restraining or managing debris-flows by modifying the fan is difficult, expensive, and often times unreliable. Therefore, it is more appropriate to identify areas vulnerable to debris-flows first and make sustainable land-use decisions accordingly based upon a qualitative and quantitative understanding of the risks.

Airborne laser scanning (ALS) and Terrestrial laser scanning (TLS) are revitalizing interests in the quantification of geomorphological landforms such as alluvial fans because they allow for high-resolution topographic modeling. The unprecedented detail of ALS and TLS allows for the construction of very accurate digital elevation models (DEMs), which provide detailed information on small-scale features and landscape patterns (Jakob, 2005; Frankel and Dolan, 2007; Wasklewicz et al., 2008). This is especially useful on alluvial fans because the small-scale surficial features and patterns (boulder trains, levees, slope, surface roughness, etc.) provide important geomorphic evidence of past debris-flows that aid in our ability to predict future debris-flows as well as provide important information about the timing of debris-flows. Detailed alluvial fan topography is vital as alluvial fans play a significant role in the debris-flow hazard analysis because the topography represents important “boundary conditions” critical to the development of accurate models to predict future debris-flow runout scenarios.

Despite recent advances in research, knowledge, awareness, and detailed data, debris-flows are still not officially considered a hazard in many areas even with obvious information to

the contrary (City of Phoenix, 2009; Dorn 2010, 2011). Furthermore, a methodology for conducting a debris-flow hazard analysis has not been universally defined (Dorn, 2011). For example, there is debate among researchers and government organizations, such as Maricopa County Flood Control District and the Arizona Geological Survey, whether to consider areas of Arizona at risk to debris-flows. Underlying this debate is an assumption that debris-flow activity is limited to wetter climates in other more humid regions or in arid settings wetter periods like that of the Pleistocene and early Holocene (Pearthree and Youberg, 2006; Magril et al., 2009). Recent extreme rainstorms in Arizona and in Phoenix specifically have led to debris-flows and this has brought this debate back to the forefront. Recent debris-flows, within the past three decades have also been recorded in other parts of Arizona and these include debris-flows in the Picacho Mountains in 1983 after Tropical Storm Octave (Youberg, 2010), at the Gila-Maricopa county line in 2004 after a monsoonal storm (Pearthree and Youberg, 2006), in the Ajo Mountains in 2008 following a summer convective storm (Youberg, 2010), in Southern Arizona and in the Santa Catalina Mountains in 2006 (Magirl et al., 2007; Griffiths et al., 2009), and at Cave Creek in 2010 after a 4 day precipitation event (Dorn, 2011). Maricopa County, specifically, is characterized by low lying mountain ranges, slow sediment recharge rates, and low annual rainfall totals. Because of its geomorphological and climatic characteristics, the return intervals for debris-flow events in this region are on the order of >1,000 years (Dorn, 2010; Webb et al., 2008; Youberg et al., 2008; Youberg, 2010). However, while these events are intermittent in this area, many of the identified debris-flow sites in the area have evidence of activity during the 20th century. Therefore, if the meteorological and geomorphological conditions are present, the resulting debris-flow will have a significant impact on neighboring residents (Dorn, 2010; Youberg, 2010). This study uses and tests existing debris-flow hazard analysis methods (Jakob, 2005; Jakob et al., 2012) while simultaneously providing a hazard

assessment for the area of Shaw Butte in MPA by concluding with a building vulnerability assessment and debris-flow hazard vulnerability maps. First, two sites were selected that were geographically similar. One site serves as the control for the study as it is an undeveloped site with a recent debris-flow event. The second site, serves as a developed site in which the debris-flow hazard analysis can be conducted. A calibrated model was developed using FLO-2D software at the undeveloped site. Once calibrated, this model was applied to the developed site under four separate rainfall magnitude scenarios: historical debris-flow rainfall, a lower average rainfall and a higher average rainfall to display a range of a typical summer monsoon rainstorm, and a maximum historical rainstorm. For each scenario, a series of maps were made to display the key variables: maximum flow depth, maximum velocity, debris-flow intensity, and debris-flow intensity scaled to Jakob et al.'s (2012) building vulnerability index. A building vulnerability analysis was then conducted within each rainfall magnitude scenario to give an overall assessment of the potential damage.

This research aims to address the following questions:

1. Is a historically documented non-urban debris flow capable of inundating and damaging buildings on the alluvial fan at Shaw Butte in MPA?
2. What is the potential for building damage under modeled scenarios under average and extreme rainfall conditions?

CHAPTER 2: REVIEW OF LITERATURE

Alluvial Fans

Alluvial fans can be located in a variety of settings including alpine, tropical, Mediterranean, periglacial, and paraglacial settings (Dorn, 2009). Alluvial fans occur at the mouths of channels adjacent to steep drainage basins in the piedmont adjacent to many mountainous regions (Jakob, 2005; Frankel and Dolan, 2007; Blair and McPherson, 2009; Marcato et al., 2012; Scheinert et al., 2012). An alluvial fan can expand 0.5-20 km from its adjacent mountain range and provide a site for a variety of desert vegetation such as cacti, grass, and shrubs (Blair and McPherson, 2009). They are created through the deposition and layering of eroded sediment transported from an adjacent drainage basin via debris-flow, fluvial flows, or a mixture of both (Volker et al., 2007; Wasklewicz et al., 2008; Marcato et al., 2012; Scheinert et al., 2012). Alluvial fan deposits tend to be poorly sorted coarse-grained material that originates from eroded uplifted bedrock or colluvium located in the upstream catchment (Blair and McPherson, 2009).

Alluvial fans are distinguished from other piedmont features by characteristics such as topographic surface features, stratigraphy, soil condition, clast rubification, and desert varnish accumulation (Frankel and Dolan, 2007). They have identifiable sub-features such as debris dams, incised channels, levees, gullies, depositional lobes, and the fan apex (Staley et al., 2006; Cavalli and Marchi, 2008; Blair and McPherson, 2009). The fan apex is the highest part of the fan and is located where the upper feeder channel debouches from the catchment area.

Alluvial fans are often compared on the basis of drainage basin lithology and shape and other morphometric variables such as basin area (Van Dine, 1985; Kostaschuck et al., 1986; Jackson et al., 1987; De Scally and Owens, 2004; Wilford et al., 2004; Staley et al., 2006) slope and fan gradient (Desloges and Gardner, 1984; Kostaschuck et al., 1986; Jackson et al., 1987; de Scally et al., 2001; de Scally and Owens, 2004; Staley et al., 2006; Prochaska et al., 2008),

watershed length (Wilford et al., 2004), and the Melton Ratio (Melton, 1965; Jackson et al., 1987; De Scally and Owens, 2004; Wilford et al., 2004; Welsh and Davies, 2010). Bedrock lithology within the drainage basin controls the rate at which colluvial volume accumulates and therefore influences the recharge rate of subsequent debris-flows and sediment entrainment via fluid flows. The shape and topographic characteristics of the drainage basin determines the contour of the main channel, slope gradient, flooding susceptibility, and the volume of sediment storage; and, weather patterns can be influenced by basin elevation (Hashimoto et al., 2008; Blair and McPherson, 2009).

Debris-flows

Debris-flows are a common source of material that constitutes alluvial fans and is one of the most destructive forces, next to flooding, that is related to urban development on alluvial fans (Larsen et al., 2001). Debris-flows, often associated with steep drainage basins, are gravity induced mass movements that move as a viscous slurry and consist of poorly sorted material such as sand, gravel, boulders, some silt and clay (<10%), and organic material mixed with small amounts of water and air (Takahashi, 1981; Costa, 1984; Whipple and Dunne, 1992; Iverson, 1997; Hungr, 2005; Sosio et al., 2007; Blair and McPherson, 2009; Youberg, 2010;). Debris-flow initiation is dependent on sediment availability, steep slopes, and water availability either from rainfall, snowmelt, or stream flow (Welsh and Davies, 2010). The interaction between both solid and fluid forces controls the mobility of debris-flows, which is what differentiates them from other related events such as rock falls and sediment rich floods that are specifically controlled by solid grain forces and fluid forces respectively (Iverson, 1997).

Debris-flows have three stages: initiation, transport, and deposition. Debris-flows are initiated from the failure of colluvium on steep hillslopes (20° to 45°) (Hungr, 2005). The likelihood of debris-flow initiation is increased by steeper slopes, exposed bedrock, which

increases the velocity of runoff and flow of debris, high antecedent moisture conditions, and sustained and/or extreme rainfall (Giraud, 2005; Youberg, 2010). The two most common initiation processes are: (1) a colluvial failure event (rock fall or landslide) in the debris basin that transforms into a debris-flow (Iverson et al., 1997; Reid et al., 2003; Gabet and Mudd, 2006); or (2) by liquefaction or a massive introduction of water into the system either by a precipitation event or by rapid snow melt that leads to flash flooding through infiltration and runoff (Takahashi, 1981; Costa, 1984; Iverson, 1997; Hungr, 2005; Coe et al., 2008). The difference between a debris-flow and a landslide is in the function of the pore water which influences mobility of a mass to flow or slide. While a debris-flow moves in a fluid-like state, landslides tend to have more rigid mobility with localized zones of movement restrained by the basal slip surface. On the other hand, when a debris-flow is initiated by liquefaction, the shear strength of the surface reduces as the pore pressure increases until slope failure occurs. However, level of saturation is not the only variable that determines debris-flow initiation; debris also needs to be available to the system (Costa, 1984). The material that makes up a debris-flow originates from a number of different processes such as physical and chemical weathering, till, volcanism, anthropogenic activities, or from past mass wasting events (Hungr, 2005). Debris availability in the source area is mostly dependent on the weathering rates of the surrounding steep relief and on the history of past flows.

Once initiated, debris-flows travel downslope through an existing main channel, generating enough force to scour out channels down to the bedrock for up to hundreds of meters (Dorn, 2011). The head or leading section of the debris-flow is made up of a coarse boulder front, where the body and tail of the debris-flow is a liquefied slurry and watery hyperconcentrated flow. Debris-flows are usually 1-10 m thick in the drainage basin channels (Blair and McPherson, 2009) and can exceed 10^9 m³ in volume releasing more than 10^{16} J of

potential energy (Iverson, 1997). Debris-flows tend to progress downslope in a series of irregular violent surges or in a wave-like pattern caused by the periodic accretion of sediment or from the continuous production and rupturing of natural dams created by larger components such as boulders and logs (Hung, 2000; Hurlimann et al., 2003; McCoy et al., 2010; Welsh and Davies, 2010).

Debris-flows move in a non-Newtonian laminar fashion and tend to have a higher viscosity, much like wet concrete, due to their higher clay content. Their fluid nature, however, allows debris-flows to travel long distances and inundate large areas (Costa, 1984; Iverson, 1997; Blair and McPherson, 2009). During both the transport and deposition stages, features such as levees, dams, and snouts are created at the base of the bedrock channel and out along the flow boundaries from frictional resistance when coarse particles or boulder debris collect at the premier of the flow (Costa, 1984; Iverson, 1997; Major and Iverson, 1999; Hung, 2005; Staley et al., 2006; Wasklewicz et al., 2008; Blair and McPherson, 2009; Youberg, 2010; Dorn, 2011; Scheinert et al., 2012). The larger boulder sized particles tend to ride on the top and front of the flow because of internal buoyant forces and because the flow moves faster at the top because of frictional forces at the bottom. The strength and density of the debris-flow, maintained by cohesive, dispersive, and buoyant forces, support the debris-flow particles as a whole. However, levees and other depositional features such as debris dams and snouts are created through frictional resistance when the larger particles on top are pushed to the side as a result of marginal friction and diminished pore water pressure, which is an agent that helps initiate and sustain debris mobility (Iverson, 1997; Major and Iverson, 1999). Levees help to confine the flow volume as they usually form into pairs of parallel ridges that are 2-10 m apart, each ridge standing 1-2 m wide and 1-4 m tall (Blair and McPherson, 2009). The resulting depositional features frequently comprise the coarsest particles generating distinct geographic features

important in the study of debris-flows as they can be used to reveal the history and characteristics of past flows (Youberg, 2010; Dorn, 2011).

While final debris-flow deposition commonly occurs from laminar flow, dewatering, and thinning out of the flow as the slope angle declines to a specific threshold where the plastic yield strength and the shear strength are equal (Costa, 1984; Iverson et al., 1997; Hungr, 2005; Youberg, 2010), deposition can also occur due to fluctuating channel dimensions. As the dimension of the channel varies, debris-flows can overtop the channel and slow or debouch from the confinement of the channel. This would allow the flow to maintain a greater depth and higher velocity, therefore resulting in a longer runout distance.

Each debris-flow can have a significant effect on the surface topography of the alluvial fan. As a result, debris-flow characteristics such as run-out, inundation, trajectory, and magnitude of future flows are greatly affected on an event-to-event basis. The addition of urban development onto alluvial fans further complicates the interaction of these processes and converts this phenomenon from a natural event to a dangerous hazard (Pelletier et al., 2005). Therefore, there is a need in the literature to expand on existing research to enhance our scientific understanding of debris-flow mechanics and the geomorphology of alluvial fan topography to provide needed information for land use planning and mitigation in at risk areas.

Debris-flow and Alluvial Fan Research

The highly unpredictable and magnitude of debris-flows limits the compilation of real-time debris flow data such as measurements of velocity, depths, and surge heights. The study of debris-flows is also made difficult because of the long time intervals between flows. This makes studying a debris-flow environment on an event-by-event basis very rare in a researcher's lifetime. Also, because of the unpredictability and scale fluctuations of these events many debris-flows go unnoticed. All of these factors coupled with limitations of technology and dating

techniques, have historically restricted the scientific understanding of debris-flows to qualitative observations, lab reconstructions, photographic techniques and unsophisticated quantitative modeling (Hooke, 1967; Costa, 1984; Iverson, 2003). However, our understanding of key debris-flow parameters such as rheology, velocity, runout, and peak discharge has been improved by technological advances in field based methods such as observation stations, GIS, aerial photography, and laser scanning. These advances have made way for the widespread use of 2D debris-flow modeling as an accurate tool for predicting and measuring debris-flow activity.

Key Debris-flow Parameters

Debris-flows are classified based on sediment concentration and flow rheology (Youberg, 2010). Rheology is often considered the main key to successful modeling of debris-flows and allows for better interpretation and prediction of events because it provides information on mechanical parameters to help describe debris-flow behavior (O'Brien et al., 1993; Iverson, 2003; Sosio et al., 2007; Sosio and Crosta, 2009). Rheology is the study of sediment concentration as a function of viscosity and yield strength (stress or cohesion between fine grained particles). A major component of rheological studies is examining the behavior and deformation of flow of materials and deciphers the complex interactions between forces of solid and fluid states that occur during the event (Pierson, 2005). Field evidence suggests no unique rheological measurement can describe an event in its entirety, rather rheology appears to transform with time, location, and internal feedbacks within the flow (Iverson, 2003). Rheology is calculated from numerical models, either from Bingham viscoplastic model (Whipple and Dune, 1992; O'Brien et al., 1993; Iverson, 1997; Sosio et al., 2007) or the Bagnold grain flow model (Takahashi, 1981; Iverson, 1997) using information obtained from field measurements of deposit thickness to estimate shear strength or in a lab with sediment samples whereby a sieve analysis classifies the percentage of fine material (silt and clay) within the samples (Sosio et al.,

2007). Each model calculates rheology within a debris-flow through the relation of internal shear stress and shear strain (Iverson, 1997).

Debris-flow velocity and runout are also important values to quantify as they directly relate to hazard intensity of the event (Hungri, 2005). The velocity of debris-flows varies greatly, however debris-flows are regarded as extreme rapid movements that can reach speeds of up to 20 meters per second, and can extend or runout long distances of 20 kilometers (Takahashi, 1981; Costa, 1984). The velocity of debris-flows is dependent on two main factors: (1) the characteristics of the debris material such as the concentration of sediment or the dispersal of grain sizes; and (2), the topographic characteristics of the debris-flow channel such as width, depth, and slope angle (Takahashi, 1981). The velocity and runout of debris-flows can be measured a number of ways including field observations of the travel distances of older deposits, implementation of fluid mechanics equations such as the super-elevation equation or the runup equation, or by using numerical models to model velocity and the distance traveled (Jakob, 2005; Sosio et al., 2007; Fell et al., 2008). Peak discharge could be argued as the most important variable in the study of debris-flows (Hungri, 2000). Peak discharge relates to the surges found during a debris-flow, and therefore is a measurement of the distinct destructiveness of debris-flows. The peak discharge of a single surge has the capability of being as much as 40 times larger than a severe flood (Hungri, 2000). Calculation of peak discharge can provide vital information on key debris-flow aspects such as maximum flow depth, velocity, momentum, distance of runout, force upon impact, and ability to break through channels and other natural barriers (Hungri, 2000).

Research Methods

The ability to test debris-flow models and the availability of real-time debris-flow data is very limited because of the lists of complications that come with the study of debris-flows

discussed in previous sections. However, researches have started to experiment with ways in which debris-flow simulation and numerical models could be tested through the use of experimental debris-flow laboratory flumes and video footage (Hooke, 1967; Costa and Williams, 1984; Davies, 1990; Iverson, 1997; Reid et al., 1997; Major and Iverson, 1999; Iverson et al., 2010; McCoy et al., 2010). These experiments revealed important information on the behavior and role of debris-flow surges (Davies, 1990) and tested the efficiency of existing quantitative modeling methods (Iverson et al., 2010).

The researchers deployed field monitoring systems in locales experiencing high-frequency debris-flows. For example, in Hurlimann et al. (2003), observation stations were used to gather real-time data during a series of debris-flows. These stations were equipped with video cameras and photography cameras, ultrasonic and radar devices, geophones, and rain gages. The stations provided information on flow behavior and depositional processes, ground vibration intensity, and velocity.

Prior to the 2000s, debris-flow and alluvial fan research was limited to very coarse resolution map data obtained by traditional surveying and GPS methods (Hooke, 1967; Kostaschuk et al., 1986; McCarthy et al., 1997). During this time, identification of small-scale alluvial fan features and parameter measurements such as volume, slope, and gradient was accomplished by means of field surveys, aerial photography, and coarse scale maps (e.g. Coe et al., 1997). These traditional methods were not only time consuming, but were also subjective and always came with a level of uncertainty (Cavalla and Marchi, 2008).

GIS is a tool used to store, manipulate, visualize, interpret, and understand spatial data or physical topographic data commonly in the form of digital elevation models (DEMs). Numerous morphometric measures (i.e. mean slope, angle and height of the fan apex, and length of the fan) have been used to quantify and compare alluvial fans between regions with the use of GIS

(Hashimoto et al., 2008). A number of alluvial fan hazard assessments also use GIS analyses to identify catchments and areas at risk of debris-flows (Yu et al., 2006; Welsh and Davies, 2010).

Recent advances in remote sensing technologies have opened the door to a variety of new methods for analyzing mass wasting events. One of the largest growing remote sensing themes is laser scanning or LiDAR – light detection and ranging. Unlike traditional surveying methods that are time consuming and produce minute data sets, laser scanning is capable of acquiring several million 3D points in a matter of minutes (Gordon et al., 2001). Laser scanning is mainly used to create high-resolution 2.5D digital elevation models (DEMs) from resulting 3D high-density raw point clouds. DEMs are representation of surface topography in a raster grid or in a TIN (triangulated irregular network) format (Jaboyedoff et al., 2012). Since the exponential growth of laser scanning in the last decade, environmental researchers have found many applications of the technology including mapping (e.g. flood inundations or vegetation), monitoring landscape and/or landform deformation (landslides, rockfalls, debris-flows, c.), and monitoring erosion (e.g. coastal and river erosion) (Jaboyedoff et al., 2012).

Modern laser scanning has developed into 2 basic approaches: airborne laser scanning (ALS) and terrestrial laser scanning (TLS). The earliest ALS attempts with an environmental approach occurred in the 1960s to 1980s, and most of the basic principles were verified and accepted in the literature by the late 1990s (Wehr and Lohr, 1999; Baltsavias, 1999; Shan and Toth, 2008; Jaboyedoff et al., 2012). ALS can be implemented either by a helicopter or by an aircraft, with the former method allowing for a higher resolution and the latter method allowing for multi-direction camera orientation. ALS works by emitting the laser from the flight vehicle in a series of swaths (Fig. 2.1). Most ALS sensors have full waveform capability and have the ability of meter to decimeter resolution and a point density of up to 100 points/m² (Jaboyedoff et al., 2012). An ALS determines the x,y,z position of a point by knowing the direction of the laser

beam and by recording the attitude of the sensor (i.e. pitch, roll, and yaw) with an inertial measuring system. An absolute position is then determined through the use of GPS.

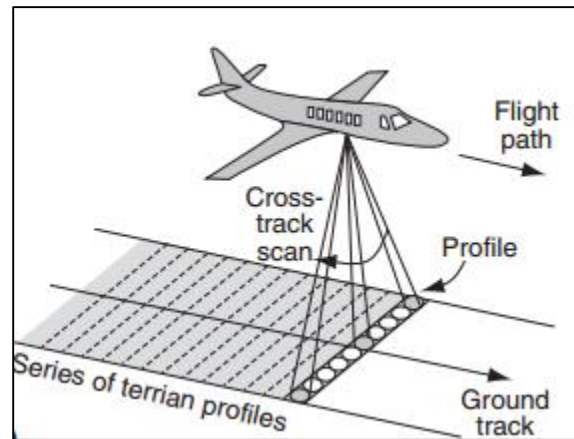


Figure 2.1. Basic operation of an ALS (image adapted from Petrie and Toth, 2008).

Environmental applications of TLS appeared in the late 1990s, much later than ALS, but it did not really gain much recognition until the early 21st century. TLS in the literature, however, has most rapidly grown in the last 5 years or so (Petrie and Toth, 2008; Hiremagalur et al., 2007; Jaboyedoff et al., 2012). TLS is especially useful for obtaining high-resolution bare earth DEMs as it has the capability of centimeter to millimeter resolution and can have a point density of 50 to 10,000 points/m² (Fig. 2.2). While TLS has higher resolution when compared to ALS, TLS is limited in its spatial extent it can cover. ALS is more useful for larger scale landscapes such as a mountain range while TLS is more useful for smaller scale landforms and sub-landform features such as alluvial fans and debris-flow levees, respectively.

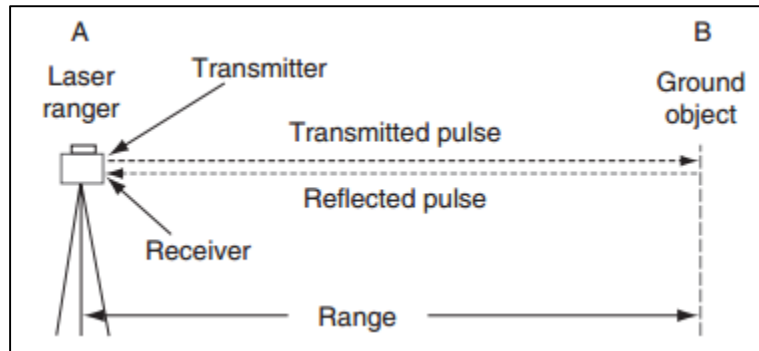


Figure 2.2. Basic operation of a pulse based TLS (image adapted from Petrie and Toth, 2008).

While applications of TLS and ALS are still developing in mass wasting studies, there are still a number of studies in the debris-flow literature that are developing new approaches and testing new methodologies. ALS has been used to identify various specific morphologies such as surface roughness and slope curvature (Staley et al., 2006; Cavalli and Marchi, 2008), on alluvial fans for hydraulic analyses (Catani et al., 2003), for characterizing surface roughness (Volker et al., 2007; Frankel and Dolan, 2007), and for extracting fine-scale debris-flow features (Wasklewicz et al., 2008). TLS has been used to evaluate rock slope instabilities (Abellan et al., 2014), detect surface change in rugged topography (Schurch et al., 2011b), study post-fire debris-flow initiation (Schmidt et al., 2011; Staley et al., 2014), study debris-flow channelization, (Wasklewicz and Hattanji, 2009; Wasklewicz and Staley, 2010), and delineate controls of debris-flow erosion and deposition on alluvial fans (Schurch et al., 2011a; Scheinert et al., 2012).

The main advantages of laser scanning methods are: an ability to acquire high-resolution realistic 3D topographic data, the ease of setting up, high-speed data acquisition, and a recent trend in affordability. On the other hand, it does come with some limitations such as its shadowing effect, and its post-processing requirements such as registration and vegetation filtering that are hindered by the immensity of the dataset and can come with a level of complication and time-consumption.

Debris-flow and Alluvial Fan Hazards

Residing on an alluvial fan comes with a level of risk to flooding and debris-flows. A need exists to conduct an investigation of the possible consequences of debris-flows in areas of alluvial fan development (Welsh and Davies, 2010). An added risk to debris-flow occurrences on alluvial fans is they are often disregarded as a potential threat. This results from three items: (1) debris-flows as a geomorphological phenomenon are not well understood by the general public; (2) they tend to occur intermittently over time-scales longer than the 100-year return interval used in flood hazard assessments; and (3), because of 1 and 2, and because they function so differently from other hazards such as flooding, the effects of debris-flows are often overlooked (Welsh and Davies, 2010). Within the hazards literature, debris-flows are characterized as short-lived hazards. They are often lethal, disruptive and expensive to restore from with costs to victims often exceeding millions of dollars annually (Tobin and Montz, 1997). For example, in December of 2003, a common rainstorm (2-year recurrence interval) initiated 68 debris-flows near suburban communities in California, washing away 30 trailer homes, trapping 52 people, and killing 16 (Santi et al., 2011).

Clarification of Hazard Terminology

A natural hazard is the threat or probability of an environmental event with the potential to negatively impact people (Tobin and Montz, 1997; Hurlimann et al., 2008). The level of risk and vulnerability of a natural hazard occurring is examined and documented in a hazard analysis. A debris-flow hazard analysis should include a combination of location, probability of occurrence within a given temporal scale (from frequency calculations), and magnitude and/or intensity (Jakob, 2005; Fell et al., 2008; Hurlimann et al., 2008). But, what do all of these terms mean in the context of natural hazards? This is a common question addressed within the literature where there is discussion regarding the importance of explicitly defining hazard terms

(Cutter, 1996; Fell et al., 2008). The two terms most specific to this study are risk and vulnerability.

Risk is the probability that exposure to a hazardous event will lead to negative consequences to wellbeing or physical property (Cutter, 1996; Fell et al., 2008; Tobin and Montz, 1997). For example, people who live on the coast of North Carolina are at risk to hurricanes because the probability of a hurricane occurring in this region is high. Many natural hazard studies are moving from a hazard-based approach (focused on return periods) to more of a risk based approach (Jakob et al., 2012). Risk can be measured a number of ways depending on the variables used such as fatalities, injuries, damage to property, economic disruption, or a combination of any. (Fell et al., 2008, Aronica et al., 2012, Jakob et al., 2012). Risk is often represented quantitatively by calculating the frequency of incidence to estimate probability, for example a 100-year flood would have a 1% chance of occurring (Cutter, 1996).

Vulnerability, related to risk, is a very important concept in the field of natural hazards. Vulnerability is the extent of harm to residents, loss of material items and activities, or the lack of ability to respond because of social circumstances during extreme natural events (Cutter, 1996; Fell et al., 2008; Santi et al. 2011; Jakob et al., 2012). Cutter (1996) distinguishes between two main perspectives of vulnerability within the hazards literature. The first is understanding vulnerability through explaining its social causes. In this perspective, the amount of vulnerability is determined by three factors: economic resources; political and social control; and social class. The second perspective assesses vulnerability according to the geographic juxtaposition of people to a hazard. In this perspective, vulnerability is determined by creating a model of the potential to be exposed to a hazard (Cutter, 1996). This is the more useful understanding of vulnerability because it encompasses all hazard vulnerabilities. A society cannot experience a hazard unless there are people present to be affected by that hazard. While, socio-economic and

political factors do play a major role in hazard vulnerabilities, there has to be an intersection of an event and a population for hazard vulnerability to be present.

Debris-flow Hazard Research

There are many different proposed methodologies for conducting a debris-flow hazard analysis. These methods vary regionally and nationally, and reflect the specific environments and needs of each particular locality. With the exception of Austria, Switzerland, and Japan, there are few statewide or nationally accepted guidelines for quantifying and mapping debris-flow hazard zones (Jakob, 2005). While some states in North America have developed a standard for conducting a debris-flow hazard analysis, there is no nationally accepted procedure. A debris-flow hazard analysis is a multidisciplinary approach that requires fieldwork, computer processing, and a level of discernment. The purpose of a debris-flow hazard analysis is to describe and quantify how the risk of debris-flows influences the vulnerability of alluvial fan hazards (Youberg, 2010). The spatial pattern of debris-flow deposition on alluvial fans is one of the most critical factors in the understanding of the potential hazards of debris-flow processes (Staley et al., 2006; Santi et al., 2011). This can now be accurately quantified with the use of GIS and 2D computer modeling, which, according to Jakob (2005), should always be implemented to aid in both modeling of debris-flows and estimation of hazardousness.

While debris-flow hazard recognition and assessment in North America is still in its beginning stages, there is agreement in the literature of the steps required to conduct a debris-flow hazard assessment (Jakob, 2005). There are 6 overall steps in a hazard analysis (Jakob, 2005), including (1) recognizing the presence of a debris-flow hazard; (2) calculation of debris-flow probability; (3) calculation of debris-flow magnitude; (4) developing frequency-magnitude relationships; (5) understanding magnitude and intensity design issues; and (6), represent the quantified results with maps.

The first and most important step of any debris-flow hazard analysis is the identification of a debris-flow threat (Harris and Pearthree, 2002; Giraud, 2005; Jakob, 2005; Youberg, 2010; Welsh and Davies, 2010). This is initially achieved through observation in the field and/or from high-resolution aerial photographs. Key debris-flow characteristics identified via field observations include large amount of deposited sediment on an alluvial fan, levees, snouts, abundance of well-rounded boulders, and buried vegetation. Measuring and mapping these deposits provide further fundamental information on travel distance, relative age, and a minimum count of past flow events (Giraud, 2005).

Identifying areas potentially prone to a debris-flow can also be accomplished through the use of the Melton ratio. This is typically used to select basins prone to hydrogeomorphic hazards and to differentiate between flood prone basins and debris-flow basins (Melton, 1957; Jackson et al., 1987; Bovis and Jakob, 1999; De Scally et al., 2001; Wilford et al., 2004; Welsh and Davies, 2010). The Melton ratio is defined as the slope of the drainage basin divided by the square root of the drainage basin area.

The next steps (2-5) in a debris-flow hazard analysis include important information regarding debris-flow probability, magnitude, intensity, and frequency. Debris-flow probability is dependent on the availability of eroded sediment, the frequency of hydroclimatic events that exceed thresholds, and ages of past flows using relative or absolute dating methods (Jakob, 2005). Debris-flow magnitude is dependent on debris-flow volume, peak discharge, and area of inundation (Coe et al., 1997; Marchi and Vincenzo, 2004; Webb et al., 2008b). Intensity is characterized by 3 parameters: velocity, depth, and deposit thickness. Debris-flow velocity influences the force at impact and the runout distance, while flow depth and deposit thickness assesses the vulnerability of buildings and efficiency of mitigation structures respectively (Jakob, 2005).

2D Modeling and Hazard Mapping

2D debris-flow modeling is the most widely used method for concluding a debris-flow hazard analysis and developing hazard maps (Jakob, 2005; Fell et al., 2008, Hurlimann et al., 2008; Aronica et al., 2012). Two-dimensional models take into account the topography and debris-flow volume and depth, which provide valuable information to examine spatial variability and volume distributions on alluvial fans. The resulting data can be used to provide an accurate calculation of damages to buildings located on the fan surface. A variety of 2D debris-flow modeling software has been used within the literature including LAHARZ (Schilling, 1998; Hurlimann et al., 2008; Magirl et al., 2010) RAMMS (Bertoldi et al., 2012; Christen et al., 2012; Hussin et al., 2012), and FLO-2D (O'Brien et al., 1993, 2011; Sosio et al., 2007). However, FLO-2D is considered the best option for a debris-flow hazard analysis in metropolitan Phoenix, AZ because of its ability to take into account flow path obstructions such as buildings, homes, walls, etc. and because the software and its protocols are accepted and used by the Maricopa County Flood Control District. FLO-2D is a 2D dynamic model used to predict events such as flooding, mudflows, and debris-flows. The model is an offshoot of the diffusive Hydrodynamic Model (DHM) and implements DEMs and specific input parameters to simulate flood hydraulics, estimate velocity and depth, predict inundation area, and calculate flow termination (O'Brien et al., 1993; Iverson, 2003). FLO-2D can successfully model flow over complex landscapes and has the ability to evaluate street flow allowing it to simulate urban flooding on developed fans by taking flow path obstructions (buildings) into account (O'Brien et al., 1993). Debris-flow modeling using inflow hydrographs combined with a sediment concentration component and by calculating yield stress, viscosity, and granular dispersive stresses permit a good approximation of debris-flows (Youberg, 2010). The final output of FLO-2D, and the results of any debris-flow hazard analysis, is the generation of hazard maps based on calculated

debris-flow runout, depths, velocities, and intensities. A debris-flow hazard map is defined either as a spatial representation of zones of equal intensity of potential debris-flows (Jakob, 2005) or as a combination of an exposure map with frequency calculations of likely debris-flow events in terms of different factors (i.e. type of initiation, level of magnitude/volume, intensity, or variation in volume and velocity with distance) (Fell et al., 2008).

FLO-2D has been used in numerous studies to effectively model floods, identify debris-flow hazard areas, and estimate flow intensity for risk calculation (O'Brien and Julien, 1988; Hubl and Steinwendtner, 2001; Garcia et al., 2003; Rickenmann et al., 2006; Armento et al., 2008; Hurlimann et al. 2008; Hsu et al., 2010; Lin et al., 2011; Bertoldi et al., 2012; Sodnik et al., 2012; Gomes et al., 2013). FLO-2D has also been used to provide models and predictions of debris-flow and flooding events across Arizona and specifically in Maricopa County (Fuller, 2008; 2009). However, it should be noted that some studies have found FLO-2D tends to overestimate the runout length of coarse-grained granular debris-flows because of yield strength assumptions (Sosio et al., 2007; Wu et al., 2013). Regardless, FLO-2D is still used in many different areas and implemented in many government guidelines for evaluating regional debris-flow hazards (Giraud, 2005; AMEC Earth and Environmental, Inc, 2010; Youberg, 2010). This study is unique in that it uses a known historic debris-flow event to calibrate models employed to investigate potential risks in densely developed areas of the MPA. The results raise awareness in the local area of the potential conditions leading to debris-flows of concern to the local population.

Within the literature, the results of the 2D debris-flow models are implemented to generate different types of hazard zone maps to provide support for the debris-flow hazard analysis (Giraud, 2005; Bertoldi et al., 2012). First, an exposure map is constructed using the area of inundation to zone areas of susceptibility (Jakob, 2005; Fell et al., 2008; Aronica et al.,

2012). The exposure map represents the area and spatial distribution of potential debris-flow events and then can be used to develop a hazard map (Fell et al., 2008; Aronica et al., 2012). A debris-flow hazard map is defined either as a spatial representation of zones of equal intensity of potential debris-flows (Jakob, 2005) or as a combination of an exposure map with frequency calculations of likely debris-flows in terms of different factors (i.e. type of initiation, level of magnitude/volume, intensity, or variation in volume and velocity with distance) (Fell et al., 2008). Finally an exposure map and a hazard map can be combined to create a map that represents risk. A risk map is used to describe the temporal and spatial probability of occurrence as well as the vulnerability by accounting for the property and people at risk (Fell et al., 2008; Aronica et al., 2012).

Quantifying Building Vulnerability

The development of debris-flow hazard maps provides vital information on debris-flow exposure, intensity, frequency, magnitude and volume, and risk and vulnerability. The combination of this information allows for the quantification and qualification of building vulnerability, a common calculation used as the ultimate result of a debris-flow hazard analysis (Fuchs et al., 2007; Bell and Glade, 2004; Akbas et al., 2009; Jakob et al., 2012). To review, vulnerability is the expected amount of economic loss as a result of a natural hazard whereas risk is the combination of the probability of a hazard, items at risk (structures), and its consequences (vulnerability) (Bell and Glade, 2004; Akbas et al., 2009).

Quantification of debris-flow building damage is a fairly new concept within the literature, and has been executed in a variety of ways. Earlier research by Borter (1999) suggested debris-flow intensity (flow velocity and depositional height) should be used to calculate vulnerability. Borter (1999) developed a stepwise vulnerability function that were later shown to underestimate vulnerability with depths higher than 1.8 m and overestimated when

depths were lower than 1.8m (Akbas et al., 2009). A qualitative understanding of building vulnerability has been suggested in the literature where average vulnerability was based on qualitative intensity values of low, medium, and high that correspond to deposition heights (Fell and Hartford, 1997; Bell and Glade, 2004). While this method is useful, it is clearly subjective and dependent on the specific construction technique of the area. These previous methods (Borter, 1999; Fell and Hartford, 1997) were tested on light timber frame construction, which resulted in an overestimation of vulnerability when applied to more robust brick and concrete construction. Fuchs et al. (2007) developed a function to quantitatively denote vulnerability of stronger brick and concrete construction. In Fuchs et al. (2007) and Totschnig et al. (2011), vulnerability was defined in terms of loss versus intensity, where intensity corresponded to height at deposition. Vulnerability was then quantified based on loss potentials in terms of insurance loss functions. While these studies are a good first step, there are disadvantages in disregarding flow velocity and in the way loss is quantified as lack of necessary data is often hard to come by (Jakob et al., 2012).

There is agreement in the literature (Akbas et al., 2009; Jakob et al., 2012) on the best practice for establishing building vulnerability. This approach requires the compilation of a larger more varied dataset with the combination of debris-flow intensity in terms of height and velocity, and a corresponding quantitative description of building damage ranked in a series of damage classes. Jakob et al. (2012) used 66 case studies and tested key variables (flow depth at impact, velocity at impact, peak discharge, total volume, and extent of damage to a structure) to determine the best indicator of building vulnerability. This study found a combination of flow depth and maximum velocity led to the most consistent results leading to a debris-flow intensity index ($I_{DF} = dv^2$). A range of I_{DF} 's that correspond to 1 of 4 damage classes, each with its own qualitative description (Table 2.1 and 2.2). For example, an I_{DF} that ranged from 0-1 would have

a high correlation to damage class one (some sedimentation), and I_{DF} that ranged from 1-10 would correlate the most with damage class two (some structural damage). Any I_{DF} value that exceeds 1,000 would have a 100% chance of damage class four which would be complete destruction.

Damage Class	Description of Damage
Some Sedimentation (1)	Sediment-laden water ingresses building's main floor or basement; requires renovation; up to 25% insured loss
Some Structural Damage (2)	Some supporting elements damaged and could be repaired with major effort; 25–75% insured loss
Major Structural Damage (3)	Damage to crucial building-supporting piles, pillars and walls will likely require complete building reconstruction; 75% insured loss
Complete Destruction (4)	Structure is completely destroyed and/or physically transported from original location; 100% insured loss

Table 2.1. Damage Classes with corresponding qualitative description and percent of insured loss for each (Jakob et al., 2012).

Damage Class	Probability of each damage class occurring do to a specific I_{Df} range				
Some Sedimentation (1)	70%	22%	0%	0%	0%
Some Structural Damage (2)	30%	50%	37%	5%	0%
Major Structural Damage (3)	0%	22%	38%	28%	0%
Comple Destruction (4)	0%	6%	25%	67%	100%
I_{DF}	0-1	1-10 ¹	10 ¹ -10 ²	10 ² -10 ³	>10 ³

Table 2.2. The percent probability of damage occurring for a specified debris-flow intensity (I_{DF}) (Jakob et al., 2012).

This particular method is the best method to date as it makes use of a large study group, it defines vulnerability in terms of both flow height and velocity, and it accounts for uncertainty by

using a range of I_{DF} values. However, it is impossible to predict the exact building damage from debris-flow impacts. There are predictability issues in the dynamic and static behavior of debris-flows, ambiguities in flow depth and velocity calculations, and the condition, structure, and material make of any particular building has indeterminate behavioral responses to debris-flow impacts. These concerns highlight a simple empirical method is most useful to define building vulnerability as a result of debris-flow impacts (Jakob et al., 2012).

CHAPTER 3: STUDY AREA

Metropolitan Phoenix AZ (MPA)

Metropolitan Phoenix Arizona (MPA) consists of scattered mountain ranges where small but steep catchments generate debris-flows and alluvial fans in the piedmont of the ranges. Many of the mountains are now subject to urban expansion and the alluvial fans that abut the steep slopes are becoming areas of residential development (Dorn, 2011). Debris-flows in this area are supply limited and occur during major rainstorms (Jakob, 2005). They initiate when colluvium (debris) located in small (<20,000 m²) spoon-shaped catchment is rapidly saturated by rainfall. The slopes are unstable because they are typically very steep (>30°), with little vegetation, and an extensive amount of exposed bedrock which allows overland flow from rain to move rapidly into the small catchments and transform the colluvium into a debris-flow (Dorn, 2011). Once a debris-flow has occurred, a future occurrence is dependent on the time it takes for sediment recharge, suitable antecedent moisture conditions, and an incidence of another rainfall event or landslide event that could potentially convert into a debris-flow (Jakob, 2005; Youberg, 2010).

Arizona is subject to wet intervals and large rainstorms in response to moist subtropical air masses (Fig. 3.1A). Floods from rainstorms in Arizona typically occur in the fall, winter, and spring seasons as a result of frontal and/or low-pressure systems or by moisture advection from dissipating tropical cyclones (Griffiths et al., 2009). However, the summer monsoon season brings over half of the annual precipitation in Arizona (Fig. 3.1B). Monsoonal activity is heightened by waves of moist air flowing from the Gulf of California. Rainstorms that occur during this season can bring extreme amounts of rain over several days producing 400 to 1,200-year rainfall events. (Pearthree and Youberg, 2006).

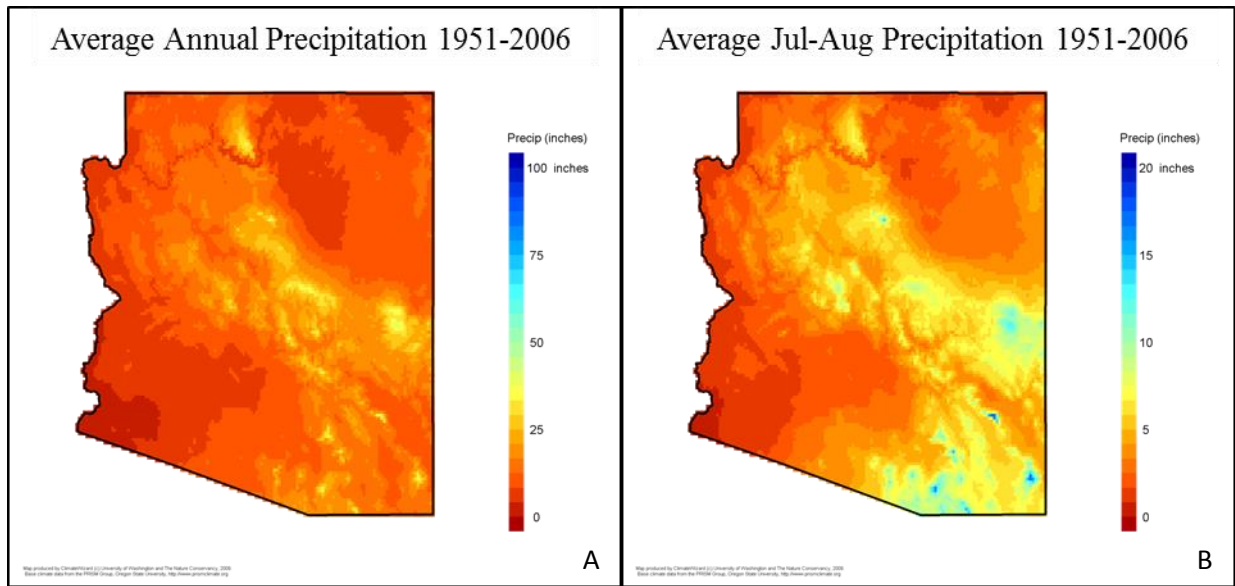


Figure 3.1. Maps of AZ representing average annual precipitation (A) and average monsoonal precipitation (B) for the past ~57 years (Flood Control District of Maricopa County, 2013).

The large summer monsoon rainstorms are especially effective in producing floods and triggering multiple debris-flows across Arizona. Over the past few decades, debris-flows have been recognized in the literature as a significant hazard to the mountainous regions of Arizona (Wohl and Pearthree, 1991; Melis et al., 1997; Griffiths et al., 2004; Pearthree, 2004; Pearthree, and Youberg, 2006; Pearthree et al., 2007). For example, evidence from geologic mapping of alluvial fans at the Santa Catalina Mountains, located north-east of Tucson, indicates that debris-flows in the area have a recurrence interval of ~1,000 years (Youberg et al., 2008). In Maricopa County, the recurrence interval for debris-flows is likely higher as a result of the drier environment and smaller elevations (Youberg, 2010), which is one of the reasons debris-flows tend to be overlooked as hazards in the area (Dorn, 2010). However, there has been a recent increase in rainfall-induced debris-flows in Arizona because of a number of low frequency, high magnitude rainstorms and an increase in wildfires (Pearthree and Youberg, 2006; Magirl et al., 2007; Griffiths et al., 2009; Youberg, 2010; Dorn, 2011). The onset of these events has led to a

common theme in the literature: the need for a new assessment of debris-flow hazards in Arizona (Pearthree and Youberg, 2006; Pearthree et al., 2007; Dorn, 2010; 2011) and the objective of this study is to specifically address this need.

MPA is an ideal location for the assessment of debris-flow hazards as it provides a prime example of urban sprawl onto alluvial fans (Helm, 2003). Phoenix, AZ is located in the Basin and Range physiographic province of southern Arizona. Widespread faulting occurred ~5-15 million years ago and resulted in uplifting of long mountain ranges and basins of portions of central, southern, and western Arizona. This topography has been evolving to the present day Basin and Range Province of Arizona. The mountains typically stretch out in a northwest-southeast direction and are constructed younger (Proterozoic) igneous, metamorphic, and sedimentary rocks (Stefanov and Green, 2013). Weathering of rock in desert areas such as southern Arizona is a result of a combination of mechanical and chemical weathering. Typical forms of mechanical weathering in these environments include: wind erosion; salt weathering; freeze thaw cycles; wet dry cycles; or weakening because of pressure release after exposure at the surface from deep burial. Examples of chemical weathering processes include: hydration; hydrolysis; dissolution from carbonic acid; oxidation; and biological activity such as lichens and algae (Stefanov and Green, 2013). Entrainment and transport of the weathered sediment is accomplished gravity-driven processes, raindrop impacts, overland flow, and aeolian processes. These processes are also important to soil formation and maintenance. Soils are critical to water retention and agriculture in this region. The most common types of soil in Phoenix are Aridisols and Entisols. Aridisols are soils found in hot arid regions while Entisols are a young type of soil that does not yet have extensive soil horizon development (Stefanov and Green, 2013).

Two sites are selected for the current study. Elephant Mountain is an undeveloped location, which has experienced a recent (2010) debris-flow. This debris-flow can be mapped

with a combination of aerial photography, digital elevation models, and field observations. Precipitation leading to the debris-flow was recorded at a local rain gauge. Shaw Butte is a developed site where field observations and past research (Dorn 2010; 2011) indicate a strong potential debris-flow risk (Fig. 3.2). Both of the chosen sites are located in Maricopa County, AZ, and Shaw Butte is specifically located in Metropolitan Phoenix Arizona. Site selection was limited to geographically similar sites, had known historical debris-flows, and appropriate conditions that allowed for fieldwork, ALS, and TLS.

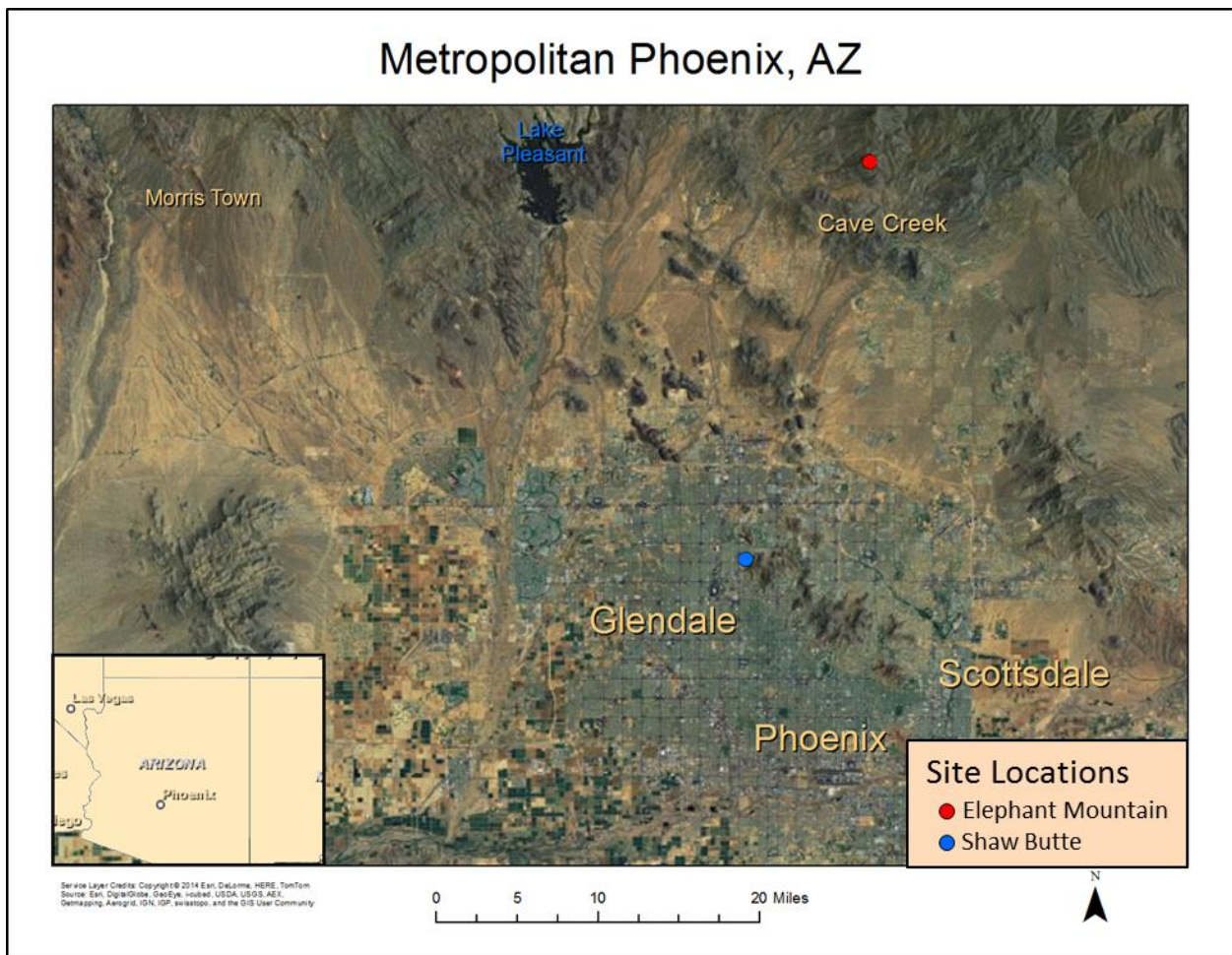


Figure 3.2. Map of MPA with the undeveloped model calibration site at Elephant Mountain in red and the developed hazard analysis site at Shaw Butte in blue.

Elephant Mountain

The study site at Elephant Mountain (Fig. 3.2, 3.3, and 3.4) is located near Cave Creek at the northern fringe of metropolitan Phoenix, AZ. While this area is not yet considered developed, urbanization is increasing exponentially as the area experiences accelerated population growth. Geologically, Elephant Mountain is composed of middle tertiary volcanic rocks with older domes and sequences of andesite, trachyandesite, and trachyte rocks and it has a tertiary bed that dips to the south-west and layered with tuff and embedded basaltic rocks (Leighty et al.,1997).

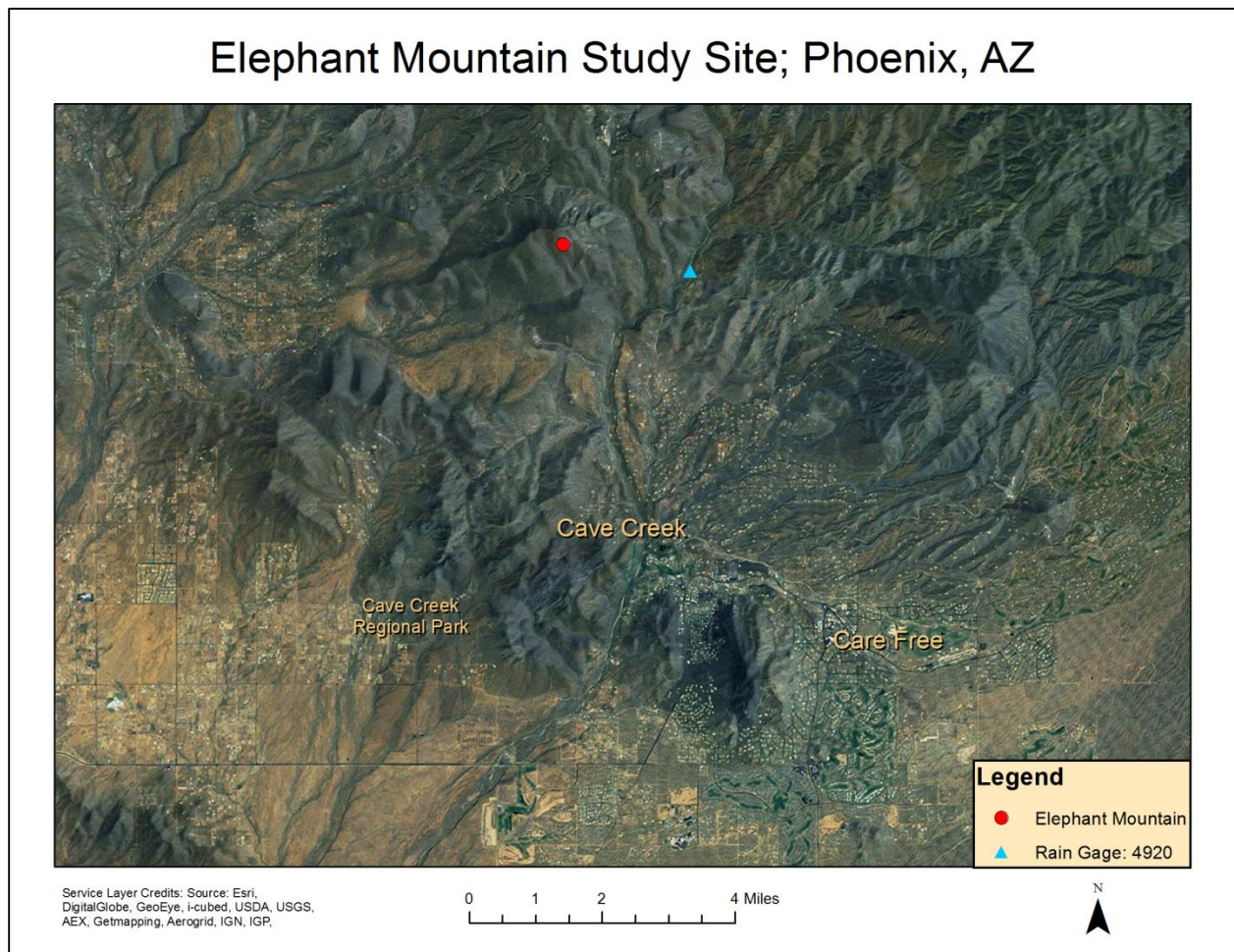


Figure 3.3. Map of the undeveloped model calibration site at Elephant Mountain (circle) and its closest rain gage (triangle) that was used for rainfall data.

Elephant Mountain is the site of a recent debris-flow that traveled out of its bedrock feeder channel and deposited ~500 meters away from initiation (Fig. 3.4) (Dorn, 2010). This latest debris-flow occurred January 18-22 of 2010, and marked the first substantial debris-flow to be historically identified in the area (Dorn, 2010; 2011). This debris-flow was initiated by a series of rainstorms over several days. According to local rain gauge data, the total amount of measured precipitation equaled 158 mm, with a total of 105.41 mm of accumulation occurring in a 24hr period. Fortunately, this event happened far enough away from urbanization that no damage to development occurred. However, if an event like this happened near a developed area, the consequences would be detrimental to structures that were situated at the base of the debris-flow channel (Dorn, 2011). The recent event and existing knowledge on the debris-flow are the reasons why this site was chosen.

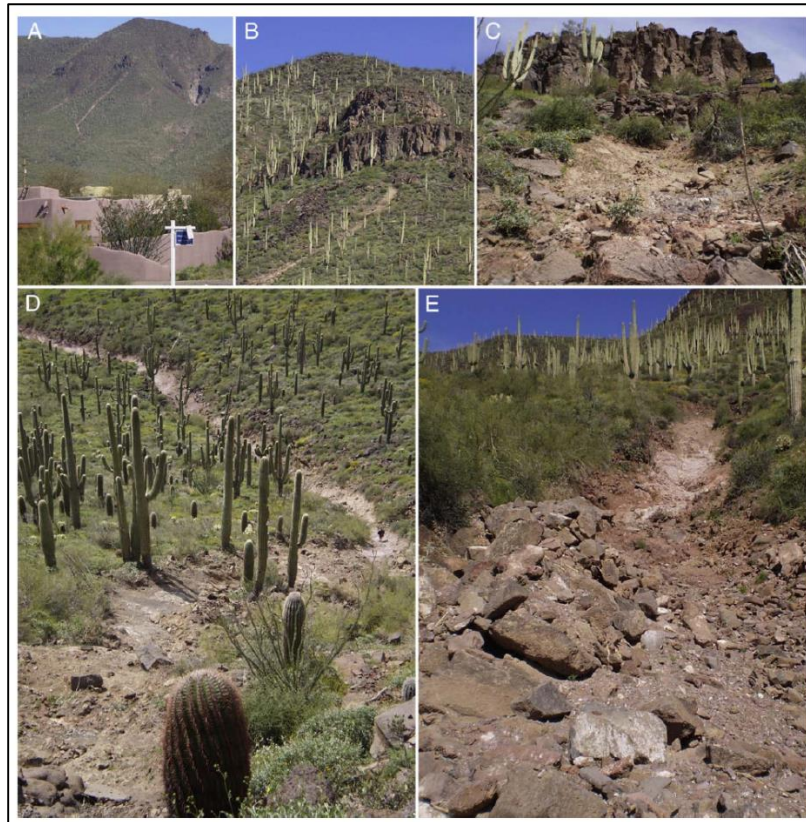


Figure 3.4. Images of the Elephant mountain debris-flow site that occurred in 2010 (images adapted from Dorn, 2010).

Shaw Butte

Shaw Butte (Fig. 3.2, 3.5, and 3.6) is located in the area of North Mountain in north central Phoenix, AZ near the northwestern end of the Phoenix Mountains. The Phoenix Mountains extend for ~8 miles and consist of a general range with a series of isolated peaks. These mountains are characterized as an uplifted fault block that has a northwest orientation (Johnson et al., 2003). Proterozoic metamorphic rocks dominate the Phoenix Mountains, while Shaw Butte specifically is dominated by Proterozoic granodiorite and greenstone, the oldest of the units in the mountain range. The granodiorite is overlain by two basalt flows that range in age from ~20 million years old to ~13-16 million years old (Leighty, 1997).

Shaw Butte Study Site; Phoenix, AZ

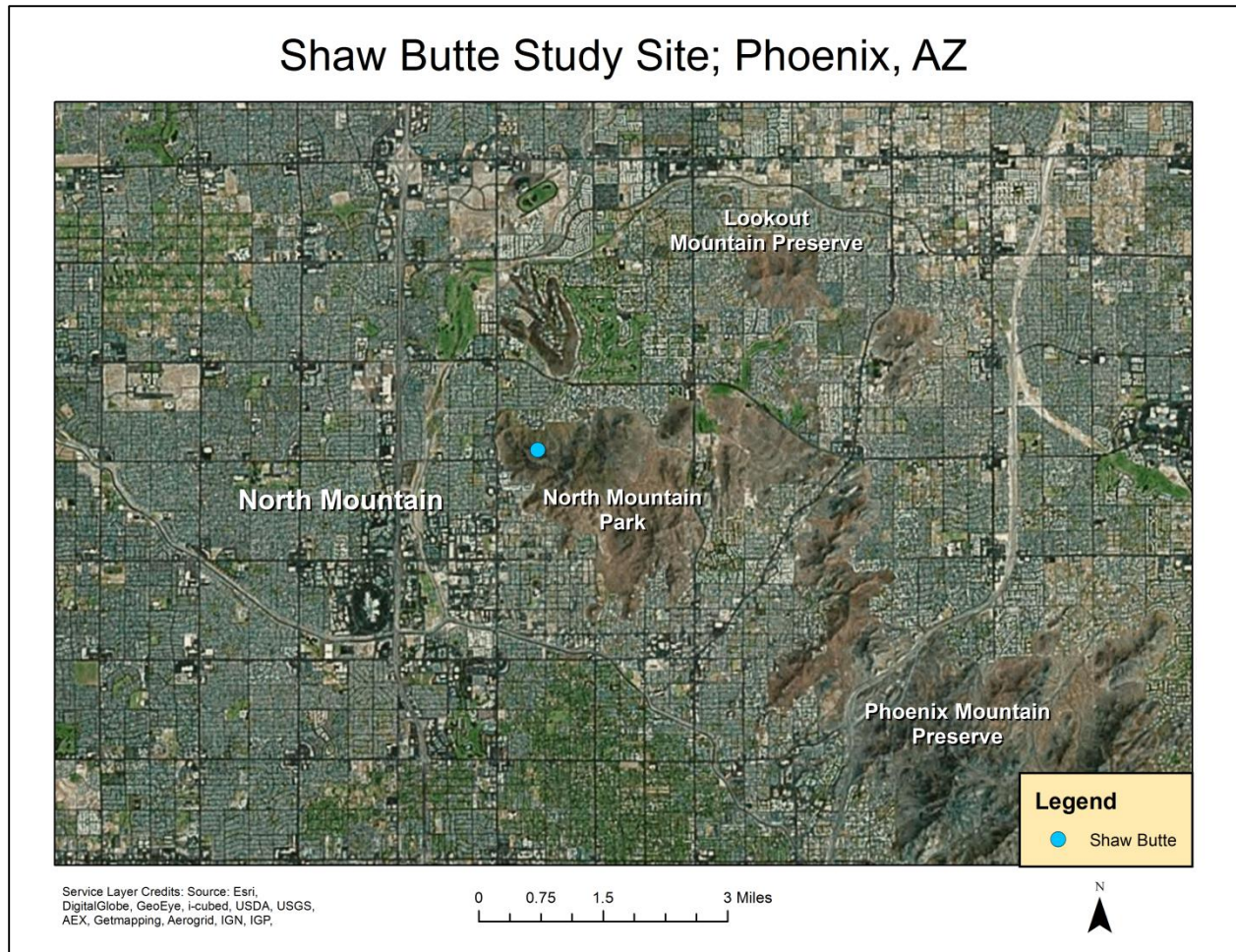


Figure 3.5. Map of the developed hazard analysis site at Shaw Butte on North Mountain.

There are approximately 29 debris-flow catchments in the area covering about 22,000 m² of space and reaching an elevation of about 177 m (Dorn, 2011). For this study, one debris-flow site was chosen from this area (Figure 3.5 and 3.6). Varnish microlamination dating has indicated that there have been at least 4 events in the past at this particular site and the last event occurred in the historical past between 350-650 years ago, with a recurrence interval of 6,000 years (Dorn, 2011).

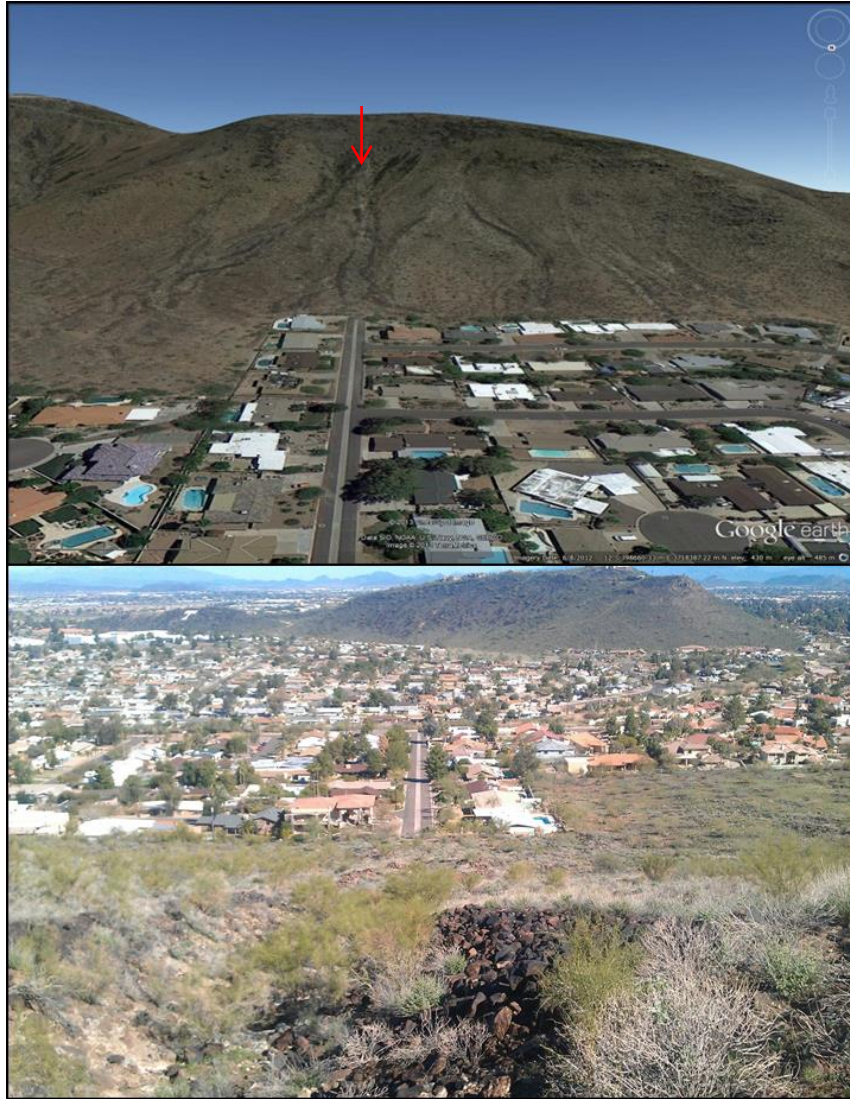


Figure 3.6. Images of the developed site at Shaw Butte on North Mountain, one looking south towards the mountain and debris-flow levees (top) and one looking north towards the potentially at risk neighborhood from the top of the right levee (bottom).

This site was chosen because it has physical similarities to the Elephant Mountain site, previous research conducted at the site (Dorn, 2011), and because of its close proximity to a large neighborhood, allowing for a debris-flow hazard analysis. Physical similarities between the Shaw Butte and Elephant Mountain sites include a spoon shaped catchment, steep unstable slopes, and exposed bedrock, all of which are conducive for debris-flow generation (Fig. 3.7).

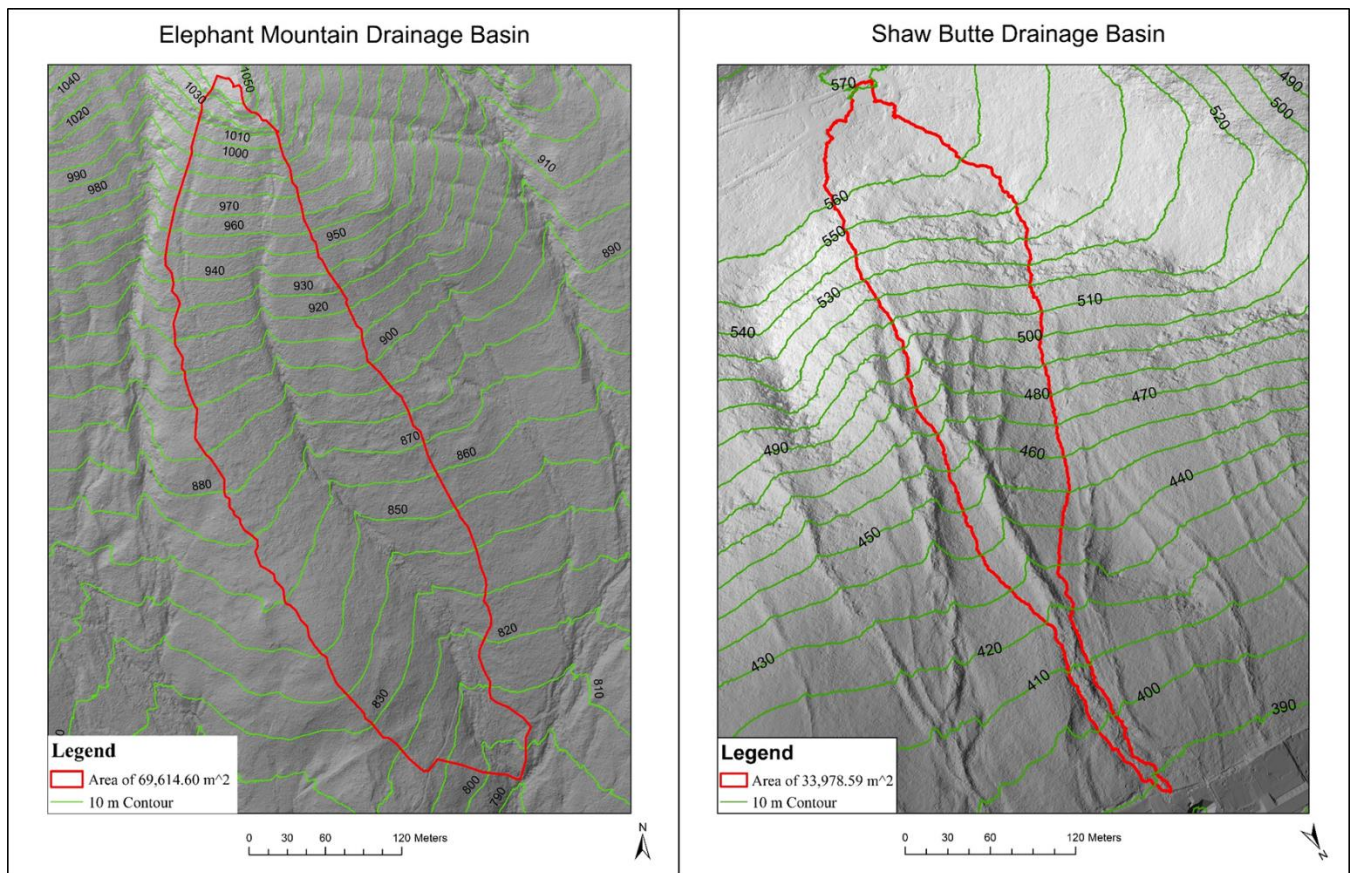


Figure 3.7. Slope map of the drainage basin at the Elephant Mountain study site (right) and Shaw Butte study site.

The main difference between the two sites is the area of the drainage basin. The drainage basin at Elephant Mountain has a total area of 69,614.60 m² while Shaw Butte’s drainage basin has a total area of 33,978.59 m². Another distinction is the shape of the drainage basin. While both basins appear to exhibit the classic spoon shaped catchment, the Elephant Mountain basin tends to maintain this shape all the way to its fan apex whereas the Shaw Butte basin tends to narrow towards the fan apex. However, the length and the slope of each drainage basin is very similar. The total lengths of the Elephant Mountain and Shaw Butte drainage basins are 601.50 m and 549.28 m, respectively.

CHAPTER 4: METHODOLOGY

Jakob (2005) has outlined the steps to accomplishing debris-flow hazard analysis. Dorn (2010, 2011) accomplished the first of these steps in Phoenix, AZ by identifying debris-flow hazards and analyzing event frequency. Dorn (2011) randomly sampled 9 sites in the Phoenix area and determined the ages of 34 debris-flows using varnish microlamination and lead-profile dating techniques. Four sites generated debris-flows in the 20th century and another four sites experienced events in the last 350 years (Dorn, 2011). The minimum occurrence rates for the 9 sites ranged from 1,600-6,000 years. While these low frequency rates seem to indicate a lower risk that a debris-flow will occur in an individual's lifetime, these findings only represent an approximate value of debris-flow frequency because of the approach used to acquire these data. The exact number of debris-flows over time cannot be exactly accounted for because there is always a possibility that evidence of past flows could have been wiped away by more recent flows or evidence could have been covered up either by natural or anthropogenic means (Dorn, 2011; Welsh and Davies, 2010). Despite the high return interval of debris-flow frequency, the next phase in the process is to assess the debris-flow magnitude and the associated potential risks in developed areas of Phoenix.

The 2010 debris-flow at Elephant Mountain serves as an example of what could be expected from a debris-flow in a populated MPA neighborhood under similar climatic conditions. The calculated and modeled specifications of this debris-flow are used and applied to a more populated area in MPA to produce a hazard assessment of the resulting impacts if this were to occur in a populated area. Shaw Butte was selected as a geographically similar drainage to the Elephant Mountain site to ensure comparable debris-flow results under similar topographic, sedimentologic, and climatic conditions. The underlying premise is to use initial

field measurements, high-resolution DEM data, and historical rainfall data to run a series of 2D debris-flow models within the built-environments present along the bajada draining the northern portion of Shaw Butte. The 2d models allow for an assessment of vulnerability of housing structures located at Shaw Butte.

Summary of Methods

First, there was a need to obtain the necessary data in order to run the 2D debris-flow models. This information included field work and a sediment analysis, terrestrial laser scanning (TLS) and volumetric calculations, and airborne laser scanning (ALS) and digital elevation model (DEM) generation. The compilation of this data permit the development of a calibrated model at the undeveloped 2010 debris-flow site at Elephant Mountain. Once this model was calibrated it was applied to the developed site at Shaw Butte under four separate scenarios all differing in terms of rainfall magnitude. A calibrated model, developed from the recent debris-flow event of 2010 was needed because it provides an unbiased approach that maintains consistency and accuracy.

The field work and sediment analysis was needed to provide evidence that these events are in fact debris-flows. This information also gives insight into the internal characteristics of the flow while providing sediment concentration by volume statistics, an important parameter needed within the 2D modeling software. TLS was conducted at the Elephant mountain site to allow for accurate volume calculations, another important input parameter for the 2D modeling. The ALS data was used to develop high resolution DEMs that were used as the topographic base in which the models could be generated on. Finally, a building vulnerability analysis was conducted at the Shaw Butte site within each model scenario to provide a qualitative and quantitative definition of the level of debris-flow vulnerability at Shaw Butte.

Field Work and Sediment Analysis

A preliminary field expedition during the spring of 2013 was conducted to select debris-flow/alluvial fan sites, gain a field perspective of the sites, obtain sediment samples, and make AxBxC particle size measurements. AxBxC particle measuring is a method of quantifying the size of rocks. This was done in order to provide an idea of the size ranges of the existing particles at both sites that would contribute to the body of the debris-flows. Measurements were made along the top of the levees as well as within the matrix of the levees. The particle size measurements from the top of the levees were made up of large boulder to cobble sized particles while the measurements from within the levees were made up of intermediate to coarse sized particles.

For the undeveloped site at Elephant Mountain, 96 AxBxC particle size measurements were made every one-meter along the top of the right levee (88 meters) looking downslope. A total of 51 AxBxC particle size measurements were also made within the matrix of the levee from a section of the upper channel. For the developed site at Shaw Butte, AxBxC particle size measurements were made every one-meter along the top of both the right and left debris-flow levees. The left levee's total length measured about 104 meters, however there was a gap of about 18 meters a little over half way down the levee so 94 particle size measurements were taken over a total of about 86 meters. The total length of the right levee measured 31 meters with a total of 30 particle size measurements. A total of 48 AxBxC particle size measurements were also made within the matrix of the left levee.

Sediment Laboratory Analysis

Three sediment samples were taken at Elephant Mountain, one within the catchment area, one within the levee of the upper channel, and one from the matrix materials within the levee near the apex of the debris-flow channel. A total of 5 sediment samples were taken from the

Shaw Butte site. Three sediment samples were collected from the catchment area and two sediment samples were collected from the matrix of the levees.

A wet sieving pipette analysis was conducted on three separate portions of each sediment sample to provide an average sediment concentration value. A wet sieving pipette analysis is based on weight measurements and settling rates of fine particles. It works by first separating the fine particles (silt and clay) from the larger particles (sand and gravel). The fine particles are inserted into a tall graduated cylinder and mixed with desalinated water. The solution sits for a specific period of time until a sample from the top can be extracted and measured. The time to wait between mixing and extraction is based on predetermined settling rates of these fine particles. The results of the sediment analysis allow for categorization of the flow rheology based on the percentage of fine material within the sediment samples. The fraction of silt and clay particles is the most important control on the mobility of the flow because these fine particles play a critical role in the flow's ability to retain water and maintain cohesion (Whipple and Dunne, 1992). Therefore, the rheology is vital to this study and will provide further insights into the debris-flow dynamics on the fan surface (Iverson, 2003).

Terrestrial Laser Scanning (TLS) and Volumetric Calculations

A Leica C10 Laser Scanner was used to survey the Elephant Mountain site. The C10 is a medium range scanner (~300 m) that employs laser time-of-flight to obtain xyz data of the surface. The C10 has a complete range of motion allowing it to scan at a field-of-view of 360° by 270°. A typical TLS survey involves scanning from multiple positions to cover an entire feature and to fill any void spaces created by any number of variables (i.e. a 270 degree limited vertical view of the scanner due to the tripod, topographic complexity that creates data shadows from the single-return instrument, etc.). All of the surveys are connected together through the use of high-definition targets, which create a common Cartesian coordinate system and allow error to be

controlled within and between scans through registration of the targets. A total of 38 TLS surveys were conducted at the Elephant Mountain study site starting below the catchment area, along the debris-flow from the bottom of the bedrock channel to the area of deposition from the event that occurred in 2010.

Debris-flow magnitudes can be determined from volume calculations and area of inundation (Jakob, 2005). Volumetric calculations were made at the base of the feature where evidence of the 2010 debris-flow was present. Leica Geosystems Cyclone software v. 8.x was utilized to develop volume calculations from the TLS point clouds. A 3D mesh was generated from the bare earth point cloud and a reference plane was created at the base of the most recent debris-flow. All sediment above this reference plane was measured to determine the total volume of the recent debris-flow deposits. The volume measurement is used to accurately establish the outflow hydrography in the 2D debris-flow model.

Airborne Laser Scanning (ALS) Data Collection

Airborne Laser Scanning was conducted at both sites in 2013 by McKim and Creed, Inc., an engineering and surveying company based in Raleigh, NC. A Riegl VQ-480 laser scanning system and a 26mp Visual Intel Camera integrated with an iOne IMSTM sensor, all mounted to the bottom of a Bell LongRanger 206L-1 helicopter were used to develop topographic and aerial imagery data (Fig. 14). The VQ-480 laser scanner has the ability of capturing over 50 points per square meter, depending on the altitude and speed of the aircraft. This remote sensing integration allows McKim and Creed, Inc. to create extremely accurate large-scale point clouds and obtain high-resolution orthographic and oblique imagery (Vincent et al., 2013). The resulting point clouds were then vegetation filtered and converted into high resolution DEMs that serve as the base for the 2D debris-flow models.

FLO-2D Modeling

FLO-2D is a two-dimensional mathematical flood-routing model used to simulate debris-flows over complex topography. FLO-2D was chosen for this study as it is widely used, tested, and accepted in the literature. FLO-2D was first implemented at Elephant Mountain in order to create a calibrated model that could be applied to the developed site at Shaw Butte for a hazard assessment. Calibration of the model was achieved through trial and error of input parameter modifications. Parameters were altered until the simulated debris-flow and the actual debris-flow of 2010 were in accordance based on runout distance, depositional area, and volume, which was adjusted based on the sediment concentration by volume (Cv) parameter. The calibrated model was then applied to the developed alluvial fan site at Shaw Butte where a series of scenarios were applied that differed in rainfall magnitude (Table 4.1). All scenarios maintained consistency because the application of the calibrated model, the antecedent moisture conditions were set to 90%, and the total rainfall was restricted to a 24 hour time period at a 1 hour interval.

Shaw Butte Modeling Scenarios

Four separate scenarios all differing in rainfall magnitude were each combined with the calibrated model and applied to the developed site at Shaw Butte (Table 4.1).

Scenario ID	Event Type	Rainfall Event	Total Rainfall amount (mm)
1	Historical Debris-flow Event	2010 Elephant Mountain Event	105.41
2	Low Average Event (AVG1)	Average Rainfall (7/01/2014)	52.07
3	High Average Event (AVG2)	Average Rainfall (2/15/2003)	67.56
4	Maximum Historical Rain Event	Max Rainfall in 24hrs (9/25/1997)	305.29

Table 4.1. Outline of each model scenario applied to the Shaw Butte site at North Mountain based on differences in rainfall.

The first model scenario conducted was the exact rainfall conditions that occurred at Elephant Mountain during the 2010 debris-flow (Fig. 4.1) to show what would happen to the neighboring community if the same conditions occurred at Shaw Butte. This scenario had a total rainfall of 105.41 mm in a 24 hour period which, according to the National Weather Service, has a reoccurrence interval of about 25 years (NOAA’s National Weather Service, 2014).

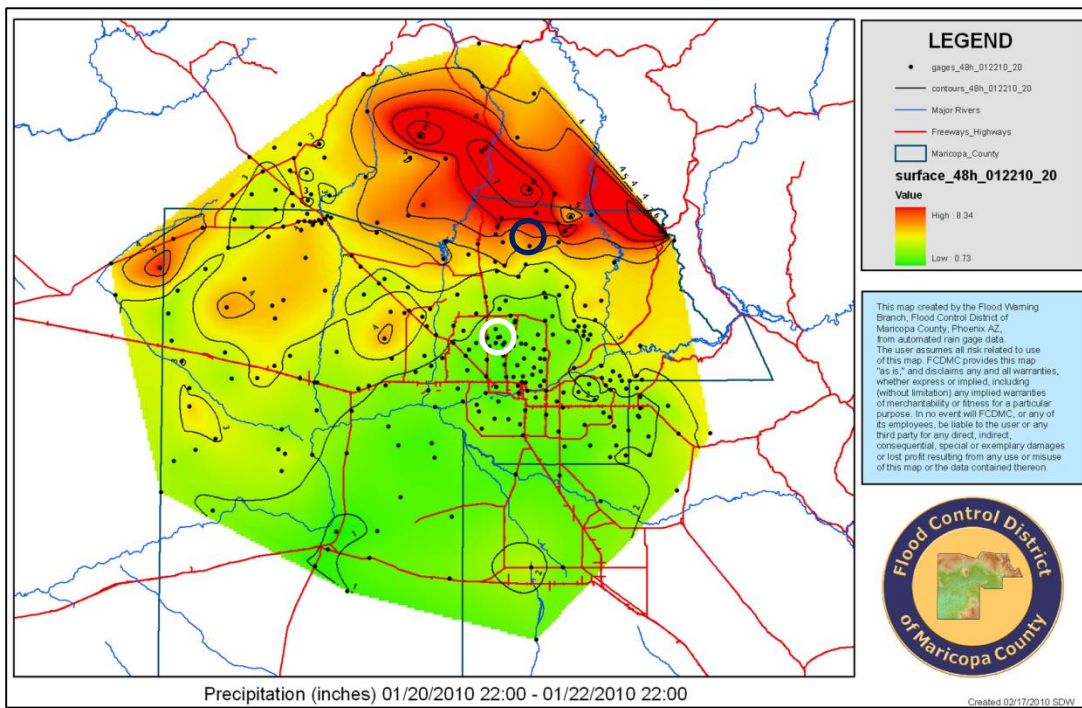


Figure 4.1. 2010 debris-flow inducing rainstorm at Elephant Mountain; with the Elephant Mountain gage located in the yellows and reds of the northeastern section and Shaw Butte located just south of Elephant Mountain in the yellow and lighter greens (Flood Control district of Maricopa County’s Alert System Data Report Generator, 2013).

Scenarios 2-4 were chosen based on average 24 hour rainfall data within the historical record provided by the Flood Control district of Maricopa County’s Alert System Data Report Generator (2013). The second and third scenarios are used to represent a range of average seasonally high magnitude rainfall events (Fig. 4.2) with scenario two representing recorded rainfall totals on the lower end of the average and scenario three representing the recorded rainfall totals on higher end of the average. Scenario 2 included a total of 52.07 mm of

precipitation that occurred in July of 2014 during the summer monsoon season while the scenario 3 included a total of 67.56 mm of precipitation and occurred in February of 2003. Rainfall data for both of these events was obtained from the rain gage at the Shaw Butte study site (gage 4850).

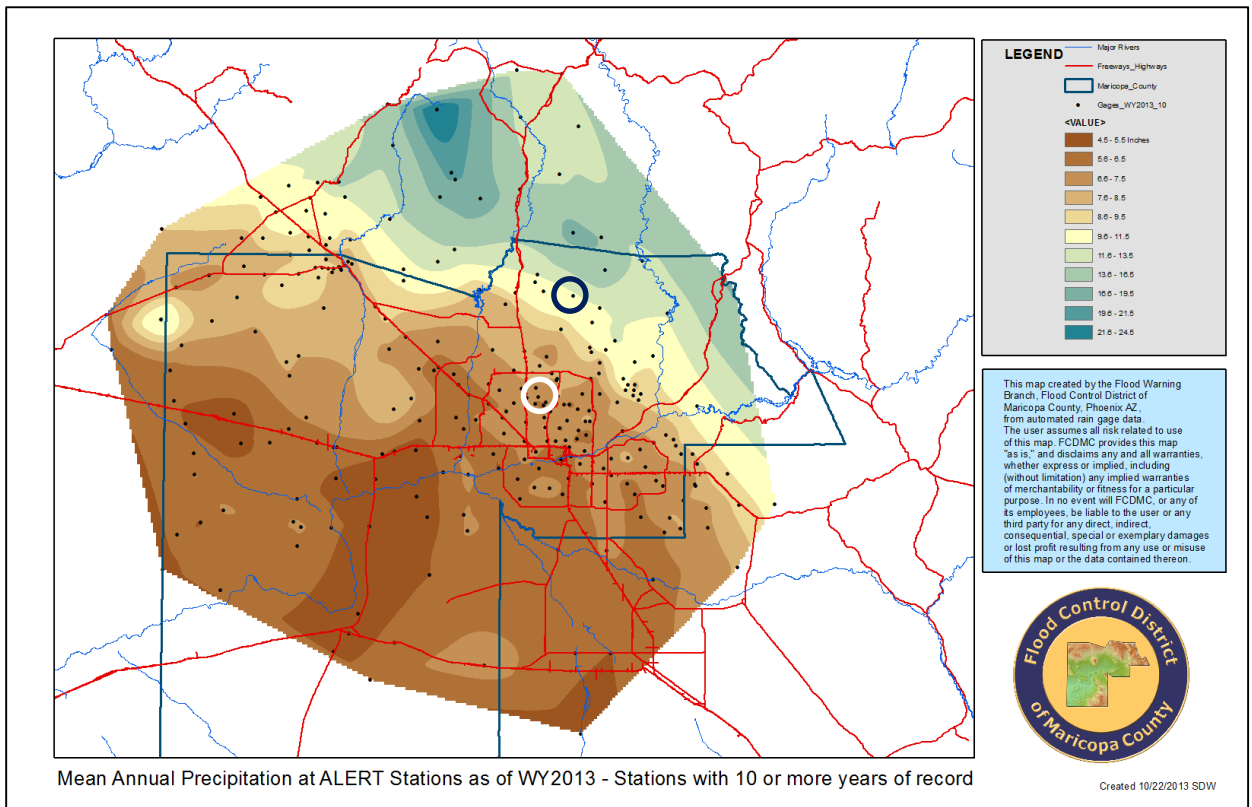


Figure 4.2. Mean Annual Precipitation recorded from gage stations with 10 or more years on record; with the Elephant Mountain gage located in the yellows and greens of the northeastern section and Shaw Butte located just south of Elephant Mountain in the lighter browns (Flood Control District of Maricopa County’s Alert System Data Report Generator, 2013).

A final simulation (Scenario four) is designed to represent the extreme rainstorms that occur in the MPA area (Fig. 4.3). A rainstorm from September 25, 1997 is used to represent extreme rainfall conditions. The particular rainstorm used for scenario four occurred on September 25, 1997, and is the maximum rainfall event ever recorded within a 24 hour period in MPA. This rainstorm represents the highest rainfall ever recorded within a 24-hour period in the MPA. This particular rainstorm was a result of Tropical Storm Nora, which brought intense

rainfall over the northwest portion of Maricopa County on September 25th and 26th. This storm event originally formed on September 16th as a hurricane on the Pacific coast of southern Mexico near Acapulco and eventually migrated north crossing over the Baja California peninsula where it continued north-northwest into the U.S. near the CA/AZ border. According to (Flood Control district of Maricopa County (2013), the calculated 24 hour, 100 year rainfall amount in northwest Maricopa County is about 106.7 mm which was exceeded at 6 different rain gage locations in the area. The rain gage that received the highest rainfall totals during this time, and therefore the gage used for this scenario, was gage 5185 at Harquahala Mountain which recorded a total of 305.29 mm of rain in a 24 hour period.

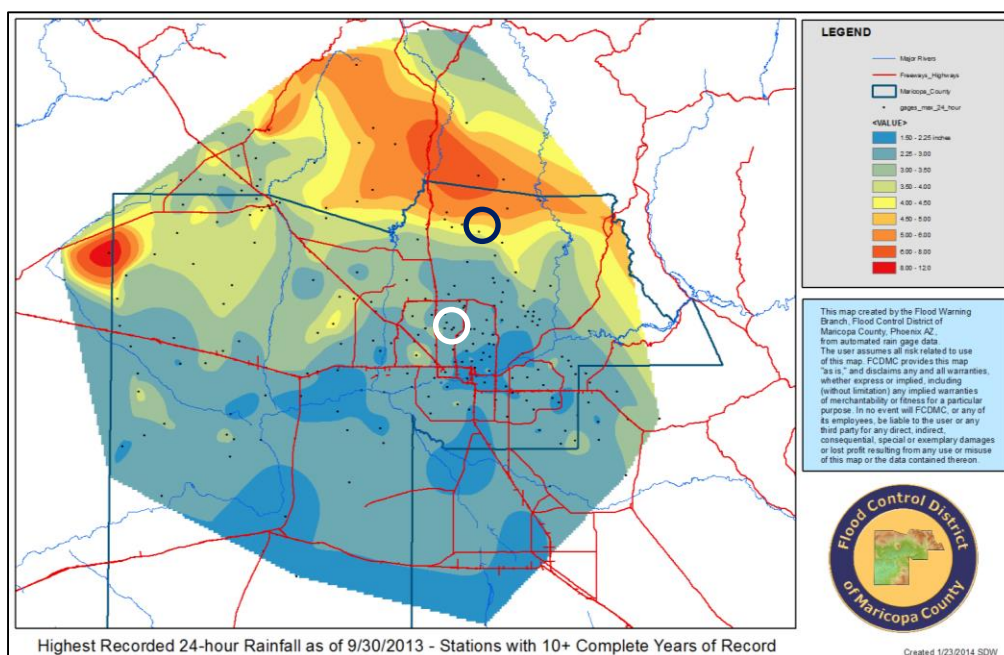
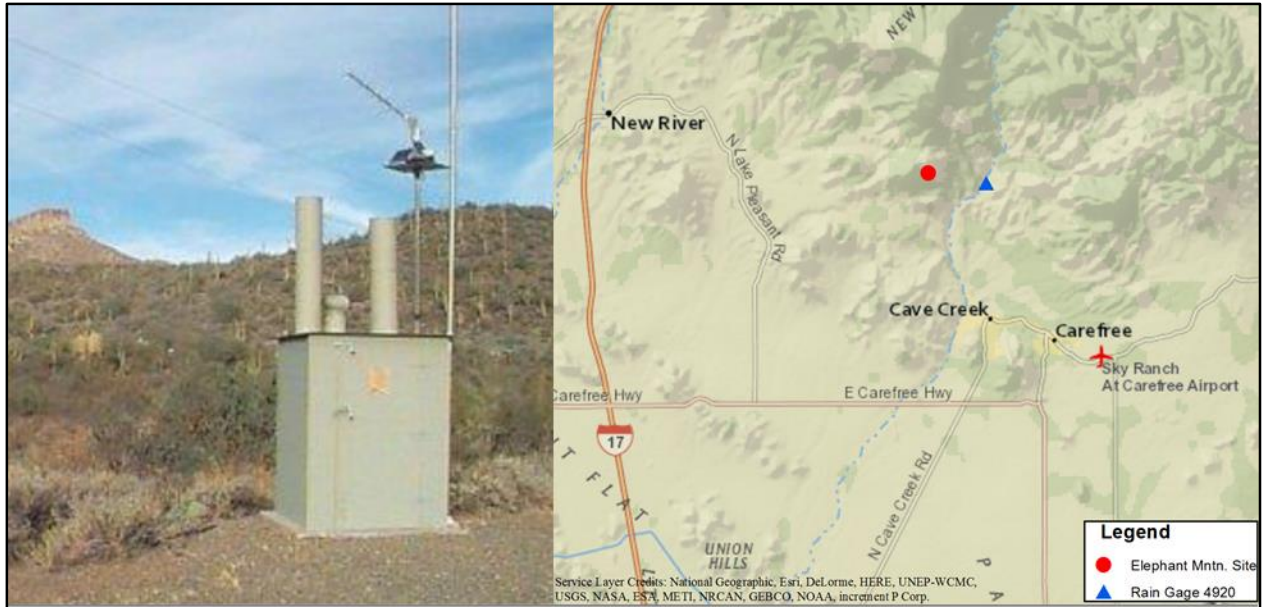


Figure 4.3. 24 hour rainstorm extremes from gage stations with 10 or more years on record; with Elephant Mountain gage located in the yellows and reds of the northeastern section and Shaw Butte located just south of Elephant Mountain in the lighter blues and greens (Flood Control District of Maricopa County’s Alert System Data Report Generator, 2013).

The steps taken to perform the modeling were conducted according to the FLO-2D manual (O’Brien, 2011). The first step in the FLO-2D modeling process is formatting and importing the necessary data. First, the DEMs created from the ALS data were aggregated in

ArcMAP and resampled into a 1.5 m ASCII grid file. This step is done in order to maintain a balance between the DEM resolution and model runtime. DEM resolution must be fine enough to maintain the necessary level of topographic detail, but also large enough to fit into the capacity of the model itself in a time efficient manner. The next step was to import a clipped version of the drainage basin DEM data into FLO-2D, along with the corresponding imagery that was collected during the ALS process. Within FLO-2D, there is a Grid function that allows the imported data to be converted into a format useable by the model. The grid function takes the imported DEM and converts it into a series of uniform grid cells that are each individually used to apply the model equations. FLO-2D requires model boundary conditions to be defined through the computational area tool and through the delineation of inflow and outflow nodes. The computational area can have a significant impact on model runtime as it defines the boundary within which the model simulations are executed. The inflow node was set at the upper-most cell in the drainage basin and assigned a hydrograph, while a series of outflow nodes were set at the fan apex. Hydraulic roughness and flow resistance was simulated with a Manning's n shapefile that assigned a Manning's n value to each grid cell within the computational area. The n values ranged from 0.02 to 0.06 and were classified according to the techniques described in Barnes (1967), Arcement and Schneider (1989), and Coon (1998) for the varied features and vegetation along the channel within the drainage basin.

The rainfall runoff tool was applied to input rainfall data and create a rainfall hydrograph. Real-time rainfall data for the 2010 storm at Elephant Mountain was obtained from the precipitation gage 4920: Cave Creek at Spur Cross Rd. (Fig. 4.4) provided by the Flood Control district of Maricopa County's Alert System Data Report Generator (2013).



Average Monthly Rainfall at Elephant Mountain Rain Gage 4920 at Cave Creek

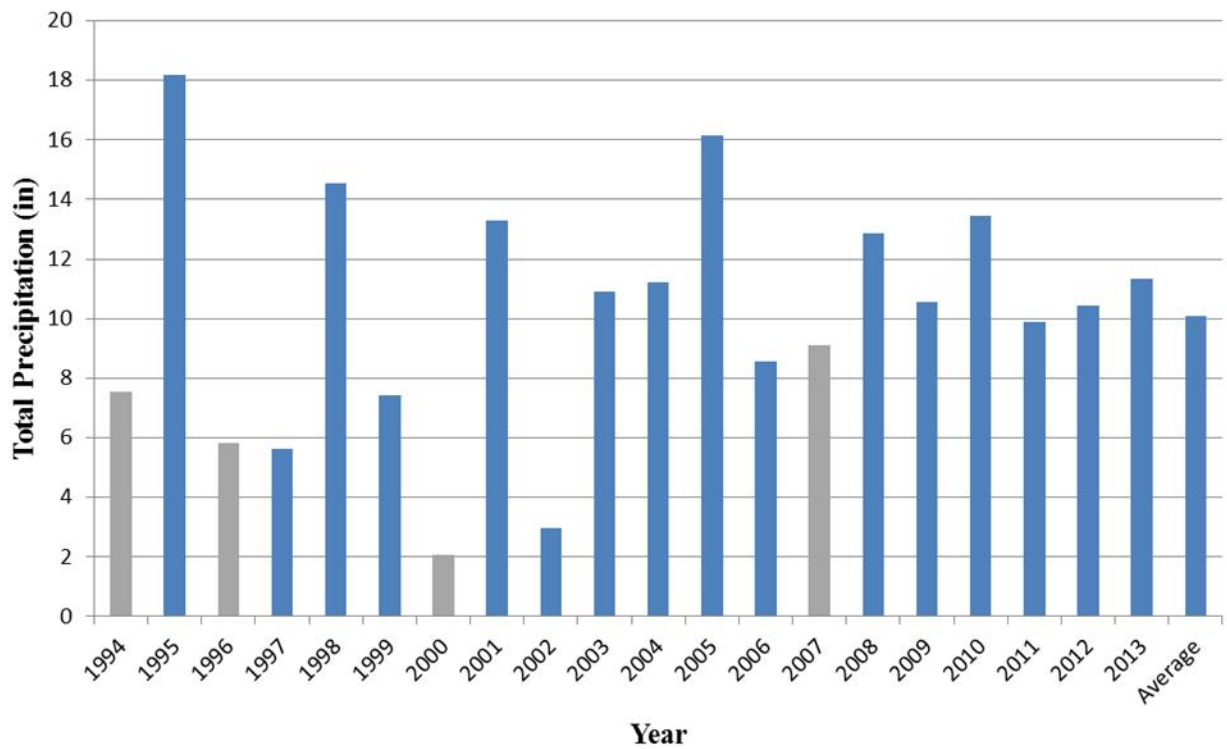


Figure 4.4. Top left: image of rain gage 4920 at cave creek; top right: map of rain gage 4920; bottom: Average monthly rainfall for the past 2 decades at this gage, years in grey represent an incomplete dataset due to gage malfunction. Data provided by the Flood Control District of Maricopa County (2013).

Infiltration parameters were defined in the model with land use and soil shape files. The land use and soil shape files were acquired from the United States Geological Survey (2014) and the United States Department of Agriculture (USDA) Natural Resource Conservation Service (NRCS) Web Soil Survey (2013) respectively. Land use for Elephant Mountain is defined as ‘shrub-brushland rangeland’ while the soil type is defined by NRCS as 45% Lehmans with 30% rock outcrop complex. The undeveloped mountainous area at Shaw Butte has a soil type of ‘RS’, which changes at the barrier of development into ‘EbD’. According to NRCS, ‘RS’ soil type is defined as very gravelly loam material on top of cemented material and bedrock with a 65% rock outcrop and a 20% cherioni complex. ‘EbD’ is defined as 100% gravelly loam with moderate alkaline and layers of very cobbly sandy clay loam. Soil type is important in the FLO-2D modeling process as it provides needed information on the yield stress coefficient and the viscosity coefficient (Bertoldi, 2012).

Finally, the debris-flow modeling was achieved with a debris-flow hydrograph. The debris-flow hydrograph was created through the combination of the rainfall hydrograph and the calculated volumes, which are contingent on the sediment concentration values (C_v). The sediment concentration values were assigned according to a maximum C_v of 0.6, a value provided by the FLO-2D manual (O’Brien, 2011), and the shape of the rainfall hydrograph given that observations in peak discharge are associated with higher sediment concentrations. A series of maps were created displaying the key variables: maximum depth, maximum velocity, debris-flow intensity, and intensity scaled to Jakob et al.’s (2012) building vulnerability index.

Building Vulnerability Index

Vulnerability in the current study is defined as the extent of damage that occurs to a home based on the combination of flow depth and velocity of a debris-flow event. Vulnerability will be described in both a qualitative and quantitative approach following the process outlined by Jakob

et al. (2012). According to Jakob et al. (2012), it is very difficult to definitively estimate vulnerability in terms of human casualties, as they are usually a result of secondary factors such as building collapse. In general, vulnerability is also difficult to ascertain because of the complexity in predicting debris-flow behavior and therefore, the nature and extent of building damage (Jakob et al, 2012). Additionally, quantifying vulnerability in terms of monetary losses, introduces further complications, as these losses are conditional based on the economic status of a given locality. Therefore, there was a need to generate a simple model that could be applicable to various regions.

To fill this need, Jakob et al. (2012) developed a simple debris-flow vulnerability model. This model was derived from sixty-eight worldwide peer reviewed case studies with events that ranged from large debris-flows that flattened entire villages to smaller events that just caused some sedimentation damage to homes. The dynamic forces within a debris-flow are controlled by two key variables: flow depth and flow velocity. A number of equations using depth and velocity were tested and plotted against the actual documented cases and one in particular was found to have the most consistent correlation with building damage, establishing the Building damage intensity index (I_{DF}). Building damage intensity index (I_{DF}) is the maximum flow depth (d) multiplied by the square of the maximum flow velocity (v) ($I_{DF}=dv^2$). The I_{DF} correlates with impact force and therefore serves as an accurate representation of building damage.

To use this vulnerability model, maximum velocity and depth must be recorded at the building location to calculate the I_{DF} of that particular building. Then, a damage probability matrix (Table 4.2 and 4.3), constructed from the results in Jakob et al. (2012), can be used to estimate the amount of damage a structure will encounter based on its associated I_{DF} calculation. For example, a debris-flow impact force on a building with an I_{DF} of 50 will have a 6% chance of Complete Destruction (IV), a 22% chance of Major Structural Damage (III), a 50% chance of

Some Structural Damage (II), and a 22% chance of Some Sedimentation (I). Each damage class also has an associated percentage of insured loss (Table 4.3). For this study, this calculated percent will be combined with the total assessed value of each home affected to give a rough estimate of monetary losses.

Damage Class	Probability of each damage class occurring due to a specific I_{DF} range				
	Some Sedimentation (I)	70%	22%	0%	0%
Some Structural Damage (II)	30%	50%	37%	5%	0%
Major Structural Damage (III)	0%	22%	38%	28%	0%
Complete Destruction (IV)	0%	6%	25%	67%	100%
I_{DF}	0-1	1-10 ¹	10 ¹ -10 ²	10 ² -10 ³	>10 ³

Table 4.2. The percent probability of damage occurring for a specified debris-flow intensity (I_{DF}) (Jakob et al., 2012).

Damage Class	Description of Damage
Some Sedimentation (I)	Sediment-laden water ingresses building's main floor or basement; requires renovation; up to 25% insured loss
Some Structural Damage (II)	Some supporting elements damaged and could be repaired with major effort; 25–75% insured loss
Major Structural Damage (III)	Damage to crucial building-supporting piles, pillars and walls will likely require complete building reconstruction; 75% insured loss
Complete Destruction (IV)	Structure is completely destroyed and/or physically transported from original location; 100% insured loss

Table 4.3. Damage Classes with corresponding qualitative description and percent of insured loss for each (Jakob et al., 2012).

CHAPTER 5: RESULTS

Results from Initial Data Acquisition

The most important variables needed for the modeling process was information on sedimentology obtained from the field measurements and sediment analysis, volumetric calculations obtained from the TLS data, and high resolution DEMs from the ALS data. The AxBxC particle measurements made from the existing levees in the field provided an idea of the sizes of particles that could contribute to the flow body. The particle size measurements from the top of the levees were made up of large boulder to cobble sized particles (Fig. 5.1 and 5.3). The particle size measurements from within the levees were made up of intermediate to coarse sized particles (Fig. 5.2 and 5.4). The cobble size measurements from Elephant Mountain had a maximum AxBxC value of 2,000,000 cm³ while the maximum AxBxC value for Shaw Butte was smaller at 300,000 cm³. The intermediate to coarse particle size measurements made within the levee at Elephant Mountain had a maximum value of about 600 cm³ while Shaw Butte had a larger maximum value of 1,800 cm³.

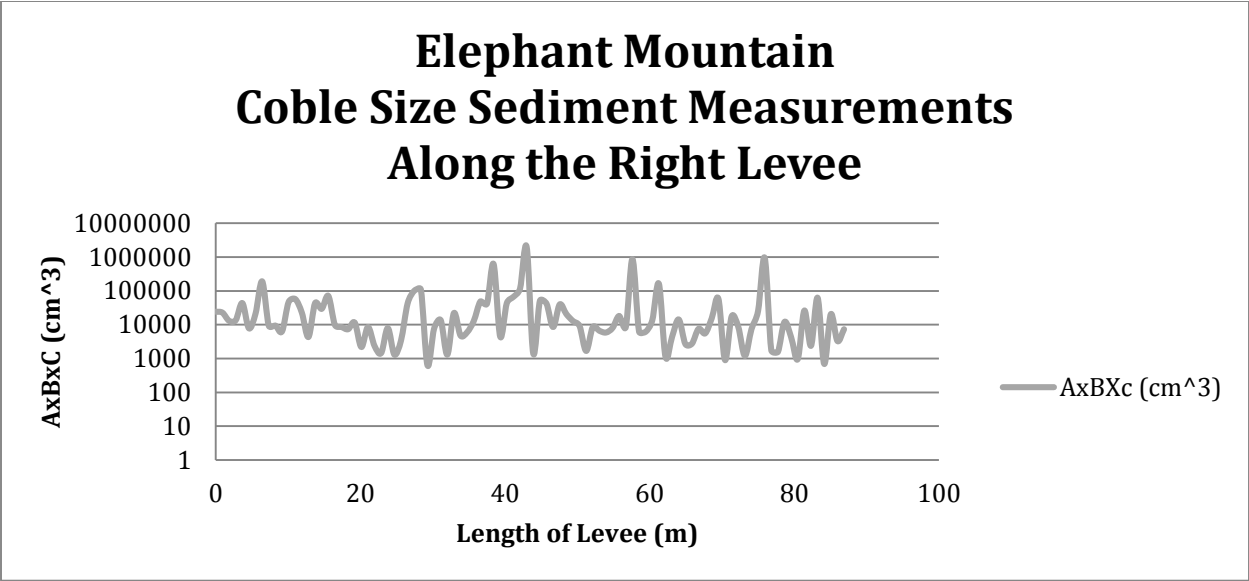


Figure 5.1. Graph of a total of 96 AxBxC particle size measurements made every one-meter along the top of the right levee looking downslope for a total of 88 meters at the undeveloped site at Elephant Mountain.

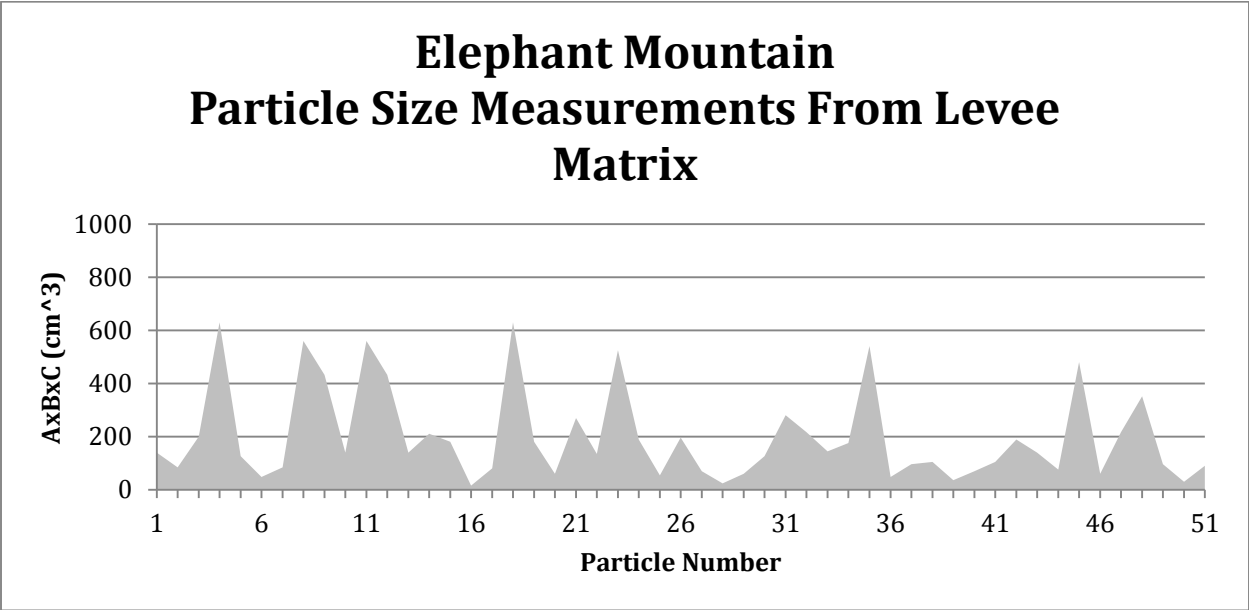


Figure 5.2. Graph of a total of 51 AxBxC particle size measurements made within the matrix of the levee from a section of the upper channel at the undeveloped site at Elephant Mountain.

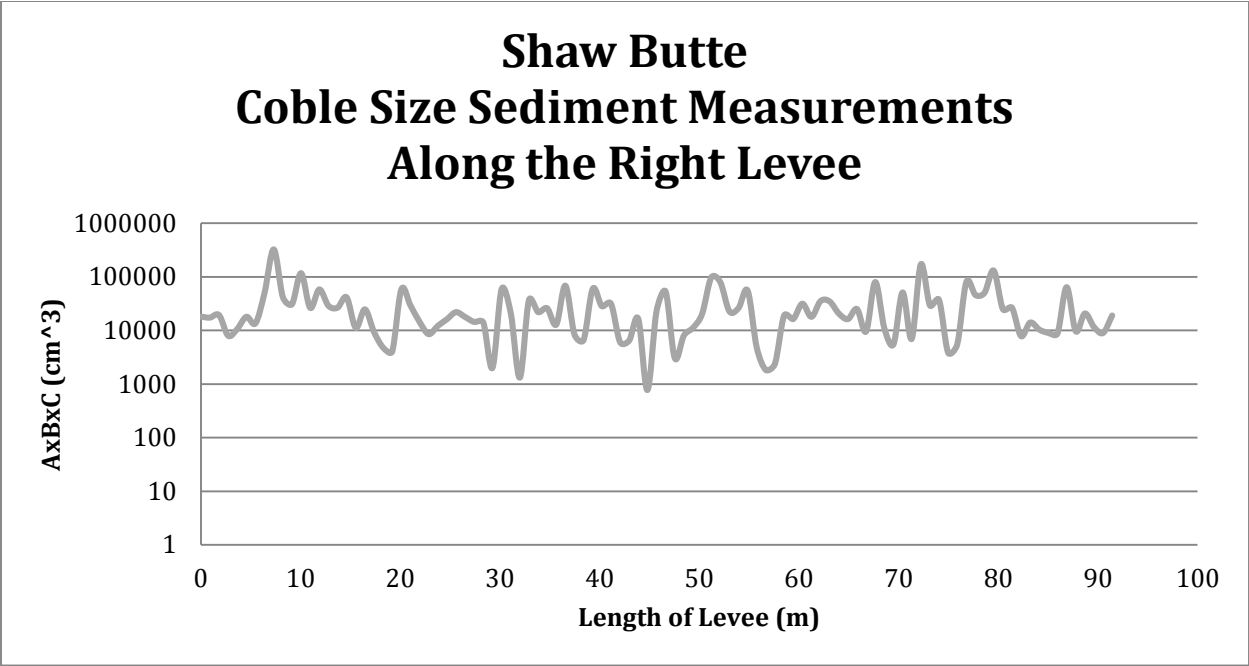


Figure 5.3. Graph of 100 AxBxC particle size measurements made every one-meter along the top of the right debris-flow levee at the developed site at Shaw Butte.

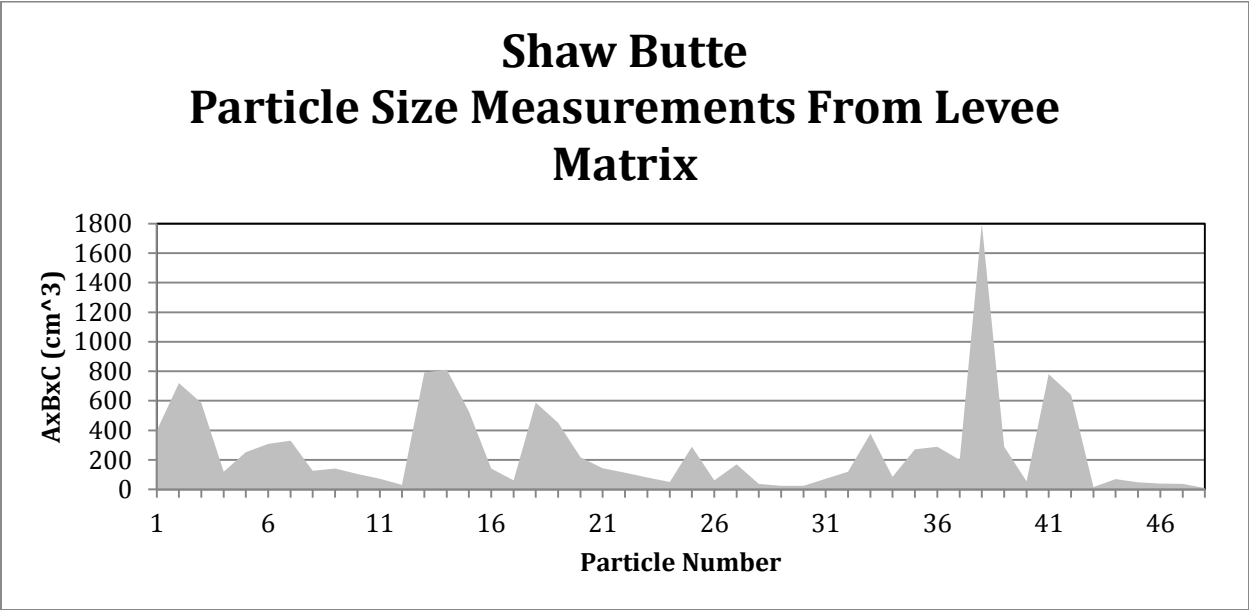


Figure 5.4. Graph of 48 AxBxC particle size measurements made within the matrix of the left levee.

Field observations of the fine grained sediment samples taken from various sections at both sites dominantly consist of silt to sand sized particles with some gravel sized particles scattered throughout. These samples were analyzed a step further with the wet sieving pipette analysis (Table 5.1). The results from this analysis correspond to the field observations providing evidence of high concentrations of silt and clay. The Elephant Mountain sediment samples are characterized by an average of 53.03% of sand, 19.79% of clay and 27.17% of silt. The Shaw Butte sediment samples are characterized by an average of 47.96% of sand, 18.17% of clay, and 33.89% of silt. Therefore, the sediment at Shaw Butte is characterized by a higher concentration of a silty-clay mixture when compared to the sediment that is present at Elephant Mountain. This is important as it provides information that the 2D models need in order to accurately illustrate the internal mechanisms of the flow.

Elephant Mountain Sediment Samples			
	% Sand	% Clay	% Silt
Catchment	48.83	19.15	31.03
Levee Matrix	64.45	17.64	17.91
Upper Channel	44.82	22.60	32.58
Average	53.03	19.79	27.17
Shaw Butte Sediment Samples			
Levee Matrix 1	34.89	19.18	45.93
Levee Matrix 2	41.89	20.25	37.86
Catchment 1	49.06	18.61	32.33
Catchment 2	63.47	15.73	20.80
Catchment 3	60.04	15.48	24.47
Average	47.96	18.17	33.89

Table 5.1. Table of the results of the laboratory sediment analysis. High percentages of fine particles such as silt and clay provide evidence of debris-flow activity.

TLS and ALS were needed in order to make accurate volumetric calculations and generate high resolution DEMs, respectively. Out of the 38 total scan setups, there was a total registration error of 0.003 m. The amount of ground hits in the resulting point cloud were

hindered due to the extensive amount of vegetation. The volumetric measurements made from the resulting bare earth mesh, totaled to 2,147.26 m³ of volume. The resolution of these DEMs were scaled to a 1.5 m resolution to maintain a balance between model runtime and accuracy, as a higher resolution results in a higher model runtime.

FLO-2D Modeling

Calibrated Model at Elephant Mountain

A calibrated model at Elephant Mountain was needed in order to provide a base model that could be used at the Shaw Butte site. The 24 hour rainfall data for Elephant Mountain on January 21, 2010 was inputted into the FLO-2D model to generate a rainfall runoff hydrograph (Fig. 5.1). This rainstorm resulted in a total of 105.41 mm of rain. The rainfall hydrograph was combined with the maximum C_v value of 0.6 to create a debris-flow hydrograph (Fig. 5.1). The input of this information allowed for the generation of the modeled debris-flow.

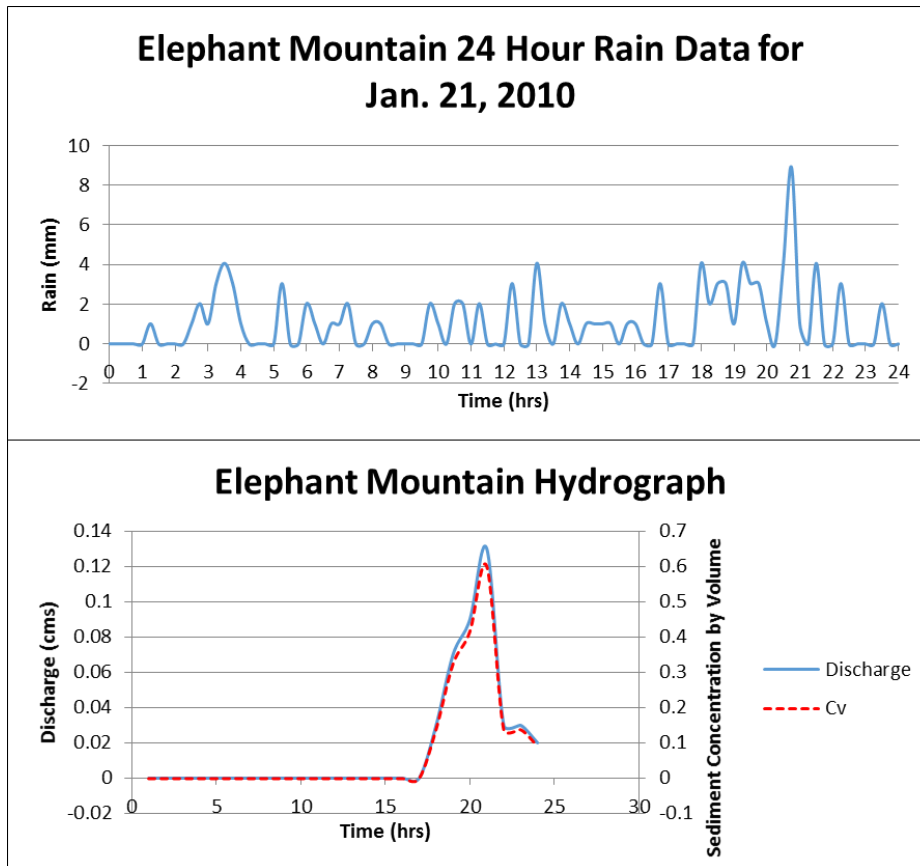


Figure 5.5. Rainfall event that led to the debris-flow at Elephant Mountain in 2010. Resulted in a total of 105.41 mm of precipitation (top). The combination of rainfall, Cv values, and topographic data develops the debris-flow hydrograph (bottom).

Once all of the necessary information was applied to the FLO-2D model at the Elephant Mountain site (Table 5.1 and Fig. 5.5), the key variables were adjusted until the results replicated the evidence found in the field. The final calibrated FLO-2D model resulted in a total discharge volume of 2,317.3 m³ and a maximum area of inundation of 5,764.5 m² (Fig. 5.6). The maximum depth resulted in 3.8 m and concentrated directly below the fan apex and within the existing channel (Fig. 5.6). The maximum velocity resulted in 1.1 m/s with the highest velocities concentrated within the existing debris-flow channel (Fig. 5.6). When looking at the entire feature, the highest depths are dominantly located towards the top of the flow and begin to decrease as elevation decreases. Lower velocities are located toward the top of the flow and

increase as elevation increases. The combination of the maximum flow depths and maximum velocities resulted in a maximum debris-flow intensity of 2.99, with the highest values again being concentrated in the debris-flow channels (Fig. 5.6). Because the maximum I_{DF} was only at a value of 3, the event did not exceed damage class I, which is described as some flooding and some sedimentation. The areas that are in blue and green strictly represent water flow, therefore, the debris-flow is only located in areas designated by red and yellow colors.

Once the calibrated model was developed at the Elephant Mountain site, the same model was used to apply four separate rainfall scenarios to the developed site at Shaw Butte on North Mountain.

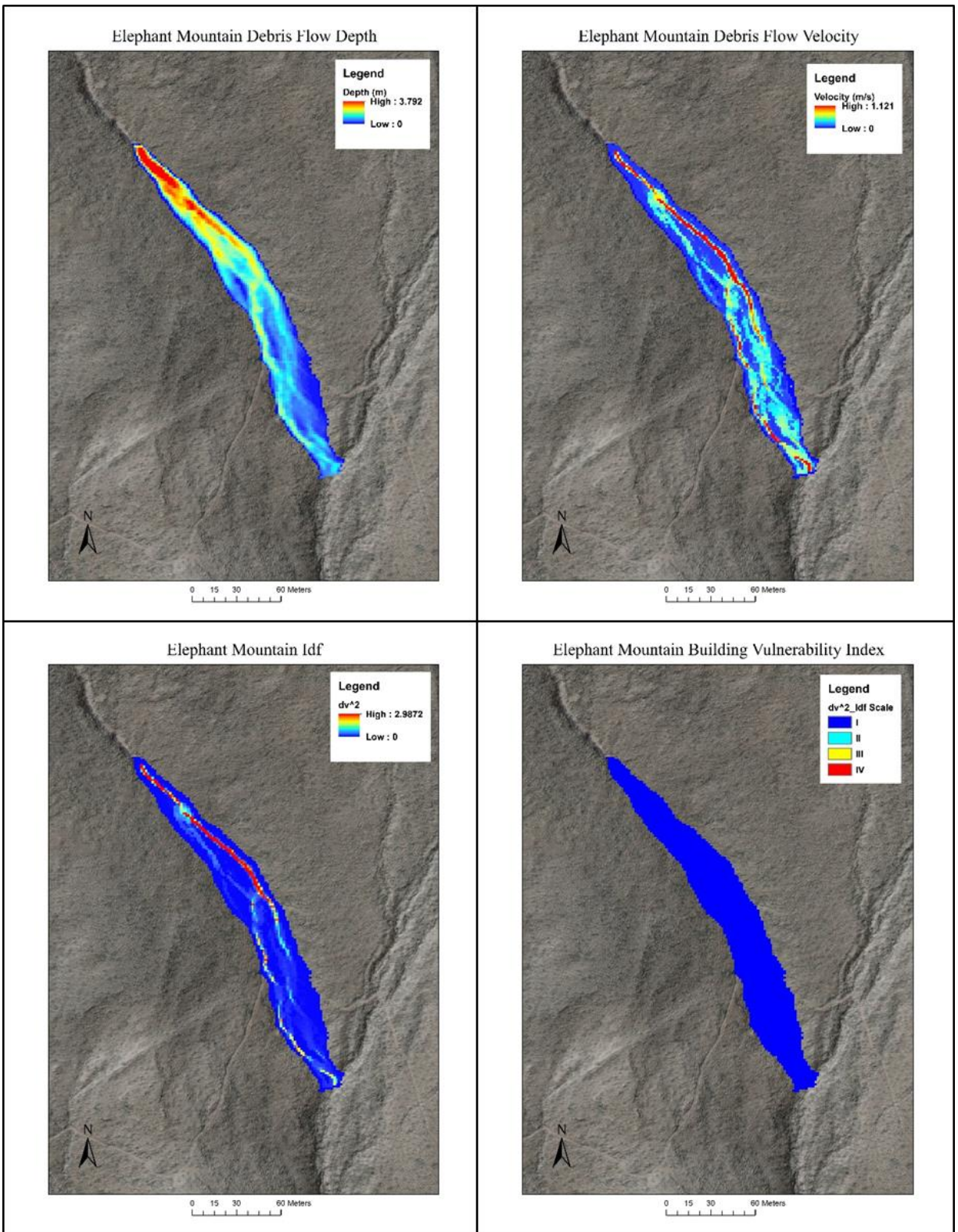


Figure 5.6. Shows the mapped FLO-2D results of the 2010 debris-flow at Elephant Mountain including flow depth (top left), flow velocity (top right), raw intensity values (I_{Df}) (bottom left), and intensity in terms of the building vulnerability index (bottom right).

Scenario 1: Historical Debris-flow Recorded at Elephant Mountain

The first scenario used the exact same simulation calibrated at the Elephant Mountain site, using the same rainfall event that led to the historical debris-flow in late January of 2010. However, the resulting discharge and therefore hydrograph output is different because of the contrasting topography of Shaw Butte (Fig. 5.7).

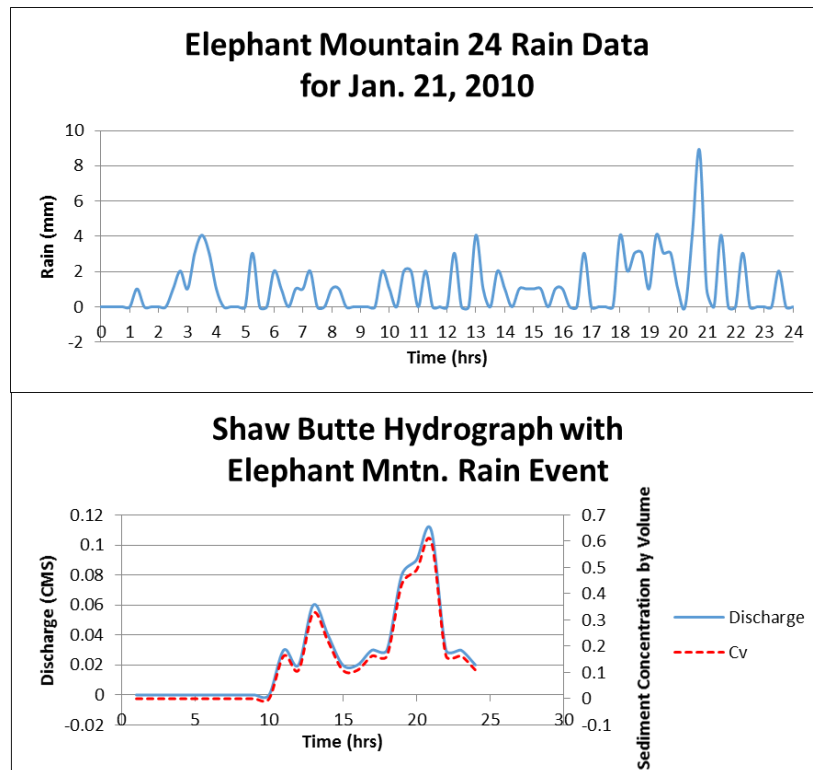


Figure 5.7. Rainfall event that led to the debris-flow at Elephant Mountain in 2010. Resulted in a total of 105.41 mm of precipitation (top). The combination of rainfall, Cv values, and topographic data develops the debris-flow hydrograph (bottom).

Scenario 1, at Shaw Butte, resulted in a total discharge volume of 3416.24 m³ and a maximum area of inundation of 21561.75 m² (Fig. 5.8). The maximum depth resulted in 3.4 m and concentrated directly below the fan apex and within the existing channel (Fig. 5.8). The maximum velocity resulted in 2.5 m/s with the highest velocities concentrated within the existing debris-flow channel (Fig. 5.8). The combination of the maximum flow depths and maximum

velocities resulted in a maximum debris-flow intensity of 14.9, with the highest values being concentrated in the debris-flow channel and at the base of the flow where final deposition occurs (Fig. 5.8). Because the maximum debris-flow intensity reached a value of ~15, the event was mostly characterized by damage class I (some flooding and sedimentation) with some spots of damage class II (some structural damage). The areas that are in blue and green (value of ~0) strictly represent water flow, therefore, the actual debris-flow is only located in areas designated by red and yellow colors (Fig. 5.8).

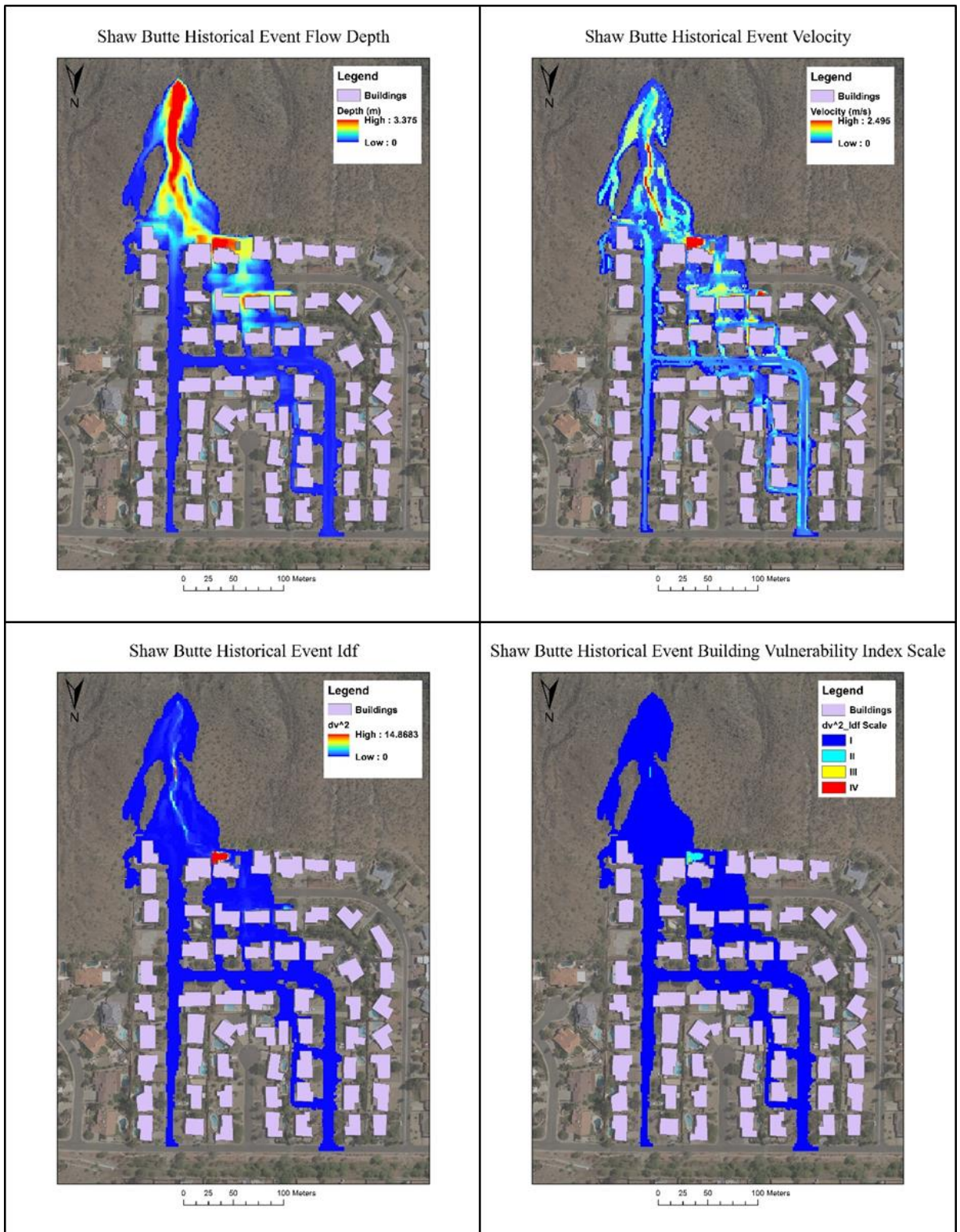


Figure 5.8. Shows the mapped FLO-2D results at the Shaw Butte site with application of the rain event of 2010 at Elephant Mountain. The results include flow depth (top left), flow velocity (top right), raw intensity values (bottom left), and intensity in terms of the building vulnerability index (bottom right).

When looking at the patterns of the entire event, the maximum flow depths are concentrated at the fan apex, within the existing channel, and at the first and second rows of homes toward the northwest. The maximum velocities are also concentrated within the existing channel and first three rows of homes to the northwest. The highest debris-flow intensities occur along the channel and is especially concentrated at the home located at the northern most end of the flow where the developed area and the undeveloped area meet (165 m north of the fan apex). The majority of the area of inundation for this event is categorized as a level one damage class that causes flooding and some sedimentation damage. This event also includes a damage class level two in the channel at the fan apex as well as at the northern most end of the channel where the flow meets the first row of homes. This particular area also indicates a chance of damage class level three in between the first two homes on the first row. Damage class two is characterized by some structural damage while damage class three is characterized by major structural damage. From this event, 22 homes are affected, most of which have flooding issues and some sedimentation (class I). One home however is hit with a combination of some structural damage (class II) and major structural damage (class III) on its eastern side (Table 5.2).

Scenario		Total Number of Homes Affected	Number of homes affected by damage class	Damage Class	Damage Description	Insured Loss
1	Historical Debris Flow Event	22	21	I	Some Sedimentation	up to 25%
			0.75	II	Some Structural Damage	25-75%
			0.25	III	Major Structural Damage	75%
2	Average 1 Rain Event	22	22	I	Some Sedimentation	up to 25%
			0	II	Some Structural Damage	25-75%
			0	III	Major Structural Damage	75%
3	Average 2 Rain Event	27	26	I	Some Sedimentation	up to 25%
			1	II	Some Structural Damage	25-75%
			0	III	Major Structural Damage	75%
4	Max Historical Rain Event	44	40	I	Some Sedimentation	up to 25%
			3	II	Some Structural Damage	25-75%
			1	III	Major Structural Damage	75%

Table 5.2. Number of homes affected and their corresponding damage class description and percent of insured loss for all four scenarios.

Scenario 2: Lower Average Event (AVG1)

The second scenario represents a lower average summer monsoonal rain event in MPA. The rainfall totaled 52.07 mm over a 24-hour period of time (Fig. 5.9). This rainstorm differs from the others in that there is one large peak of high intensity rainfall in a short period of time rather than a continuous storm with various intensities. This rainstorm produced a total discharge volume of 1,558.41 m³ and a maximum area of inundation of 26,313.75 m² (Fig. 5.10).

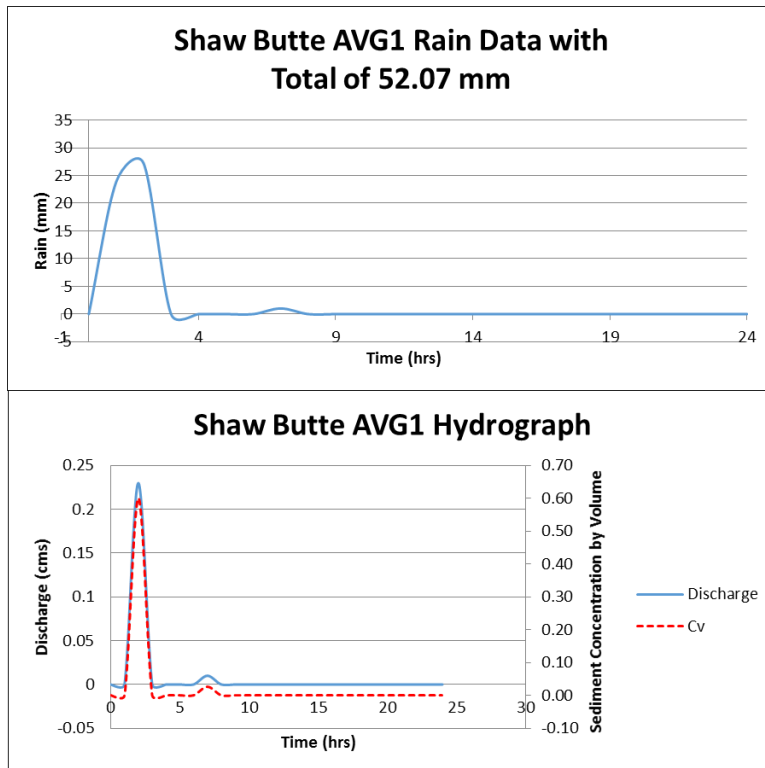


Figure 5.9. The lower average (avg1) rainfall event that resulted in a total of 52.07 mm of precipitation (top). The combination of rainfall, Cv values, and topographic data develops the initially peaked debris-flow hydrograph (bottom).

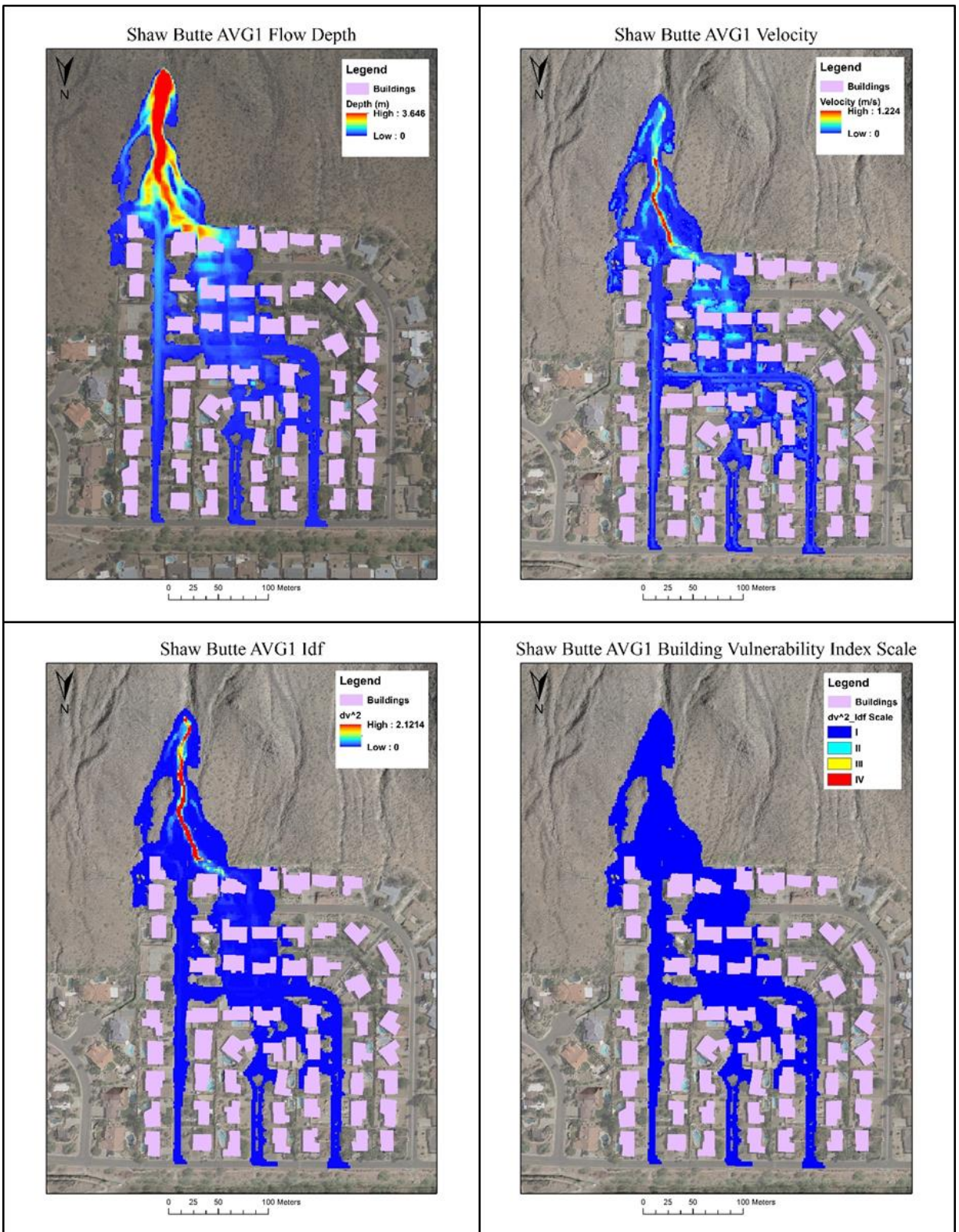


Figure 5.10. Shows the mapped FLO-2D results at the Shaw Butte site with application of the lower average rain event (avg1). The results include flow depth (top left), flow velocity (top right), raw intensity values (bottom left), and intensity in terms of the building vulnerability index (bottom right).

This modeled scenario produced similar results to scenario one, however the highest flow depths and velocities are more distinctly confined to the existing channel, flowing to the west and in between the second and third homes of the first row (Fig. 5.10). The maximum depth was 3.6 m (Fig. 5.10) while the maximum velocity resulted in 1.2 m/s (Fig. 5.10). These results led to a maximum debris-flow intensity (I_{Df}) of 2.1 concentrated at the fan apex and within the preserved debris-flow channel. Despite showing similar flow patterns to scenario 1, there was only a class one of damage within the area of inundation. The 53 mm difference in precipitation between the 2010 rainfall data and the rainstorm in Scenario 2 likely resulted in the lesser impacts on the infrastructure at the site. Because the maximum I_{Df} was only at a value of 2, the event did not exceed damage class I, which is described as some flooding and some sedimentation. The areas that are in blue and green strictly represent water flow, therefore, the debris-flow is only located in areas designated by red and yellow colors. From this event, a total of 22 homes are affected by both flooding and some sedimentation damage (Table 5.2).

Scenario 3: Higher Average Event (AVG2)

The third scenario represents a higher average rainfall in MPA that resulted in a total of 67.56 mm of precipitation in a 24-hour period. These types of rainstorms are characterized by a steady lower intensity rainfall followed by two distinct peaks of rainfall intensity that occurred in about a 10-hour period of time. When combined with a maximum C_v value of 0.6, the resulting debris-flow hydrograph crests toward the end of the 24-hour period (Fig. 5.11). A total discharge volume of 2,720.71 m³ and a maximum area of inundation of 29,756.25 m² resulted from this debris-flow simulation (Fig. 5.12).

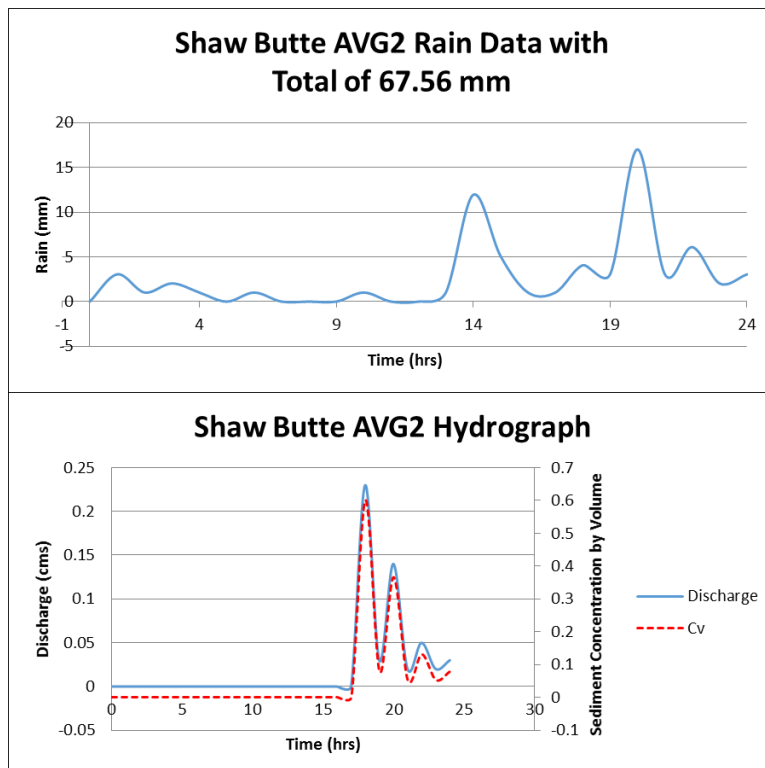


Figure 5.11. The Higher Average (avg2) rainfall event that resulted in a total of 67.56 mm of precipitation (top). The combination of rainfall, Cv values, and topographic data develops the peaked debris-flow hydrograph (bottom).

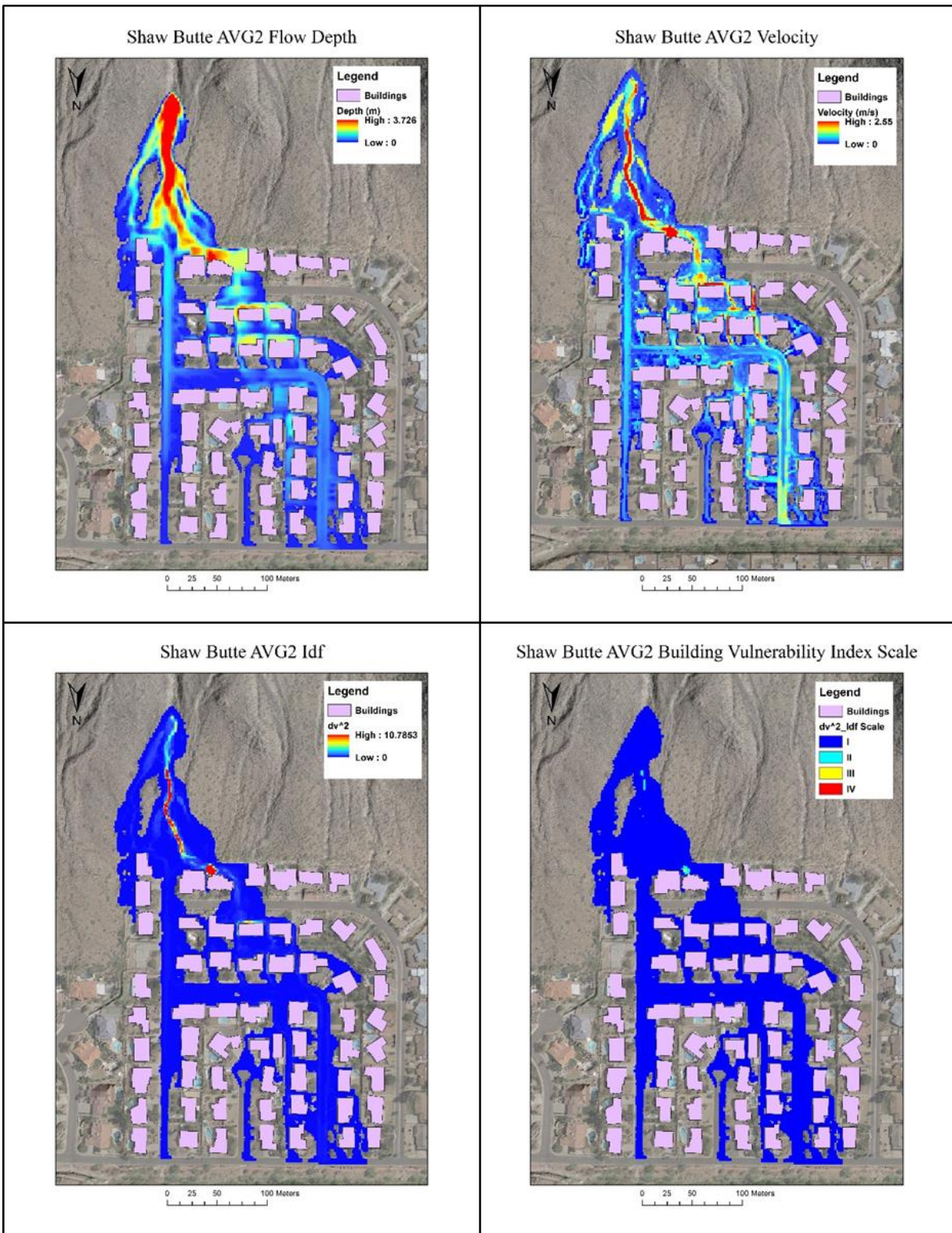


Figure 5.12. Shows the mapped FLO-2D results at the Shaw Butte site with application of the higher average rain event (avg2). The results include flow depth (top left), flow velocity (top right), raw intensity values (bottom left), and intensity in terms of the building vulnerability index (bottom right).

This modeled scenario produced similar results when compared to scenarios 1 and 2, in terms of maximum flow depths and velocities. However, the maximum depth and velocity values are more distinctly confined to the debris-flow channel, flowing west and in between the second and third homes of the most southern row (Fig. 5.12). The model output for scenario 3 resulted in a maximum flow depth of 3.7 m, a maximum velocity of 2.6 m/s, and a maximum debris-flow intensity of 10.8 (Fig. 5.12), results that are most similar to scenario 1. When looking at the entire feature, the highest depths are dominantly located within the channel and at the base of the flow where final deposition occurs at the line of development. Higher velocities are also located within the confinements of the debris-flow channel. The areas that are in blue and green strictly represent water flow, therefore, the debris-flow is only located in areas designated by red and yellow colors (Fig. 5.12). Because the maximum debris-flow intensity only reached 10.8, the area of inundation mostly consisted of damage class one with some damage class two within the channel half way between the fan apex and the line of development, and a small section of damage class two at the eastern edge of the second home on the first row. This event resulted in a total of 27 affected homes mostly damaged by flooding and some sedimentation. More homes were affected by this debris-flow because it traveled further northwest into the neighborhood. One of the homes, the same one in scenario one, was affected by a combination of damage class one and two leading to some structural damage (II) and major structural damage (III) (Table 5.2).

Scenario 4: Maximum Historical Rainfall

Scenario 4 represents a debris-flow hydrograph driven by the highest total precipitation on record and is chosen to simulate an extreme case scenario. Precipitation is consistent with a high intensity, long duration rainstorm with multiple peaks in rainfall magnitude that resulted in a total of 305.29 mm of rain in a 24-hour period of time (Fig. 5.13). The precipitation continued much longer but for the purposes of consistency within the study it was cut off at the 24-hour

mark. Scenario 4 resulted in a total discharge volume of 14,945.59 m³ and a maximum area of inundation of 50,202 m² (Fig. 5.14).

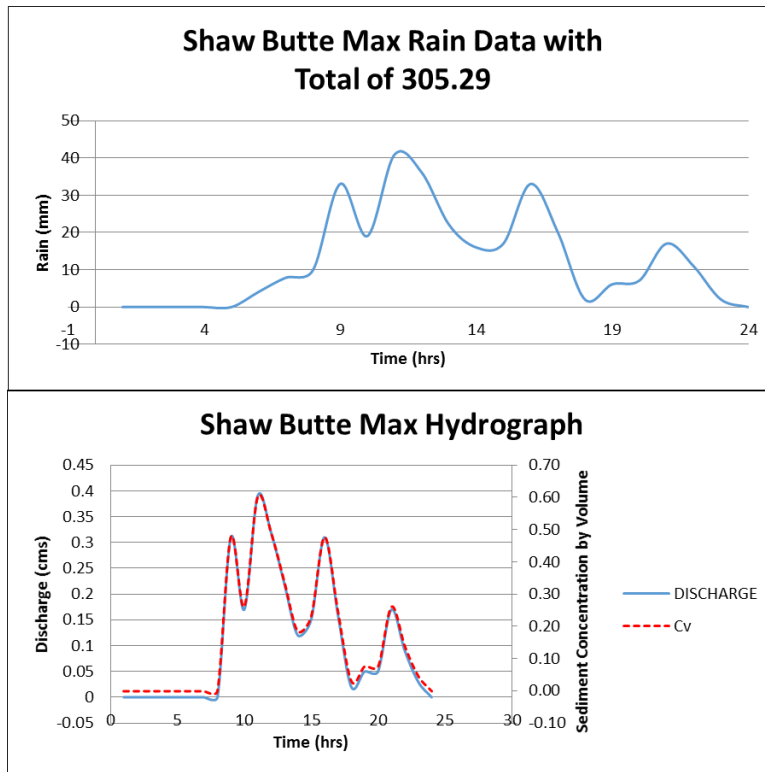


Figure 5.13. The maximum recorded historical rainfall event that resulted in a total of 205.29 mm of precipitation (top). The combination of rainfall, Cv values, and topographic data develops the resulting debris-flow hydrograph (bottom).

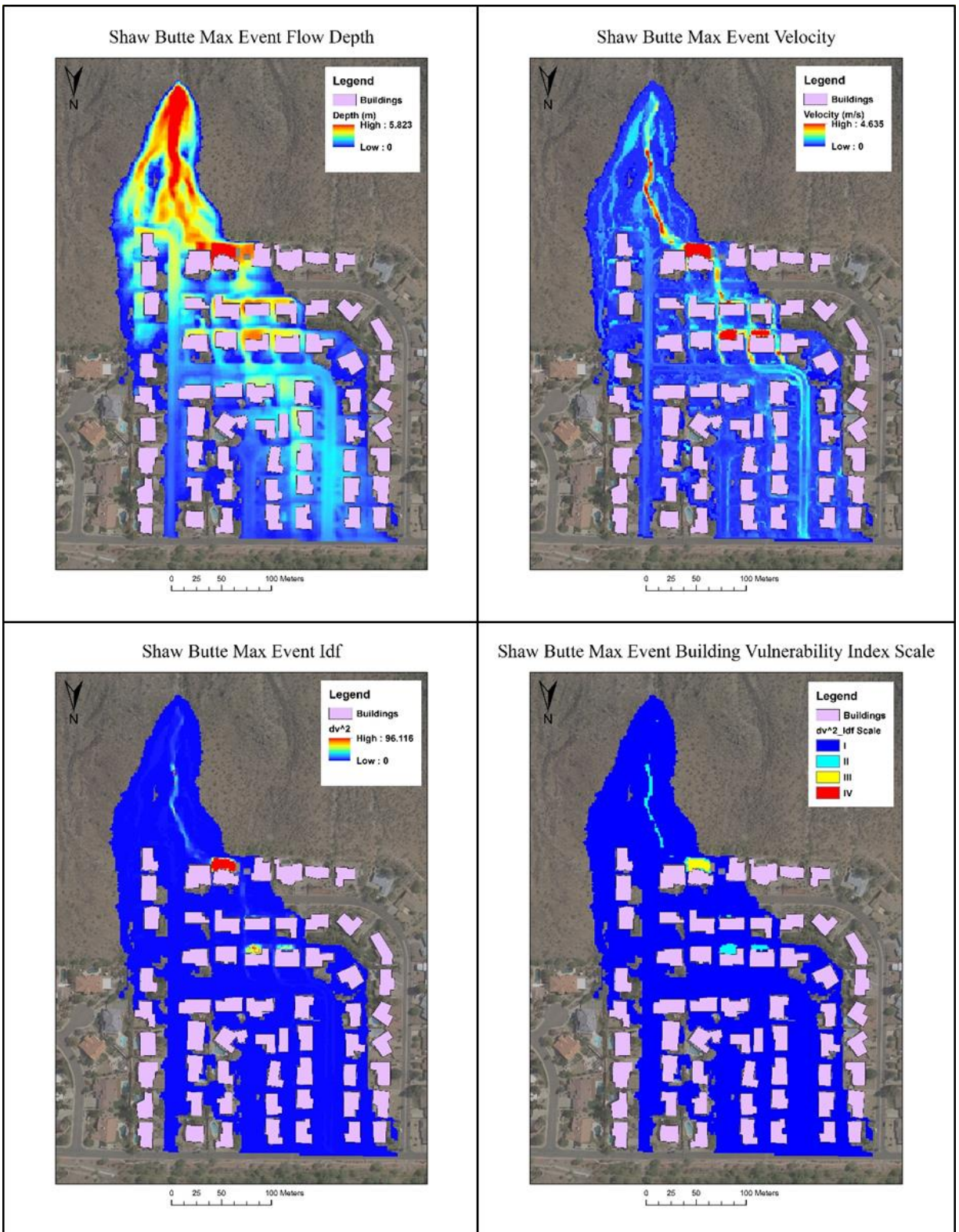


Figure 5.14. Shows the mapped FLO-2D results at the Shaw Butte site with application of the maximum historical rain event. The results include flow depth (top left), flow velocity (top right), raw intensity values (bottom left), and intensity in terms of the building vulnerability index (bottom right).

The 205.29 mm that resulted from this maximum rainstorm event lead to a maximum flow depth of 5.8 m, a maximum velocity of 4.6 m/s, and a maximum debris-flow intensity of 96.1 (Fig. 5.14). The highest depths were concentrated within the debris-flow channel and in the area below the fan apex. Depths began to decrease about 112 m below the fan apex until the flow reached the line of development and came into contact with the first row of homes (165 m north-northwest from the fan apex). Velocity does not reach its maximum until about 72 m below the fan apex where it continues downslope within the debris-flow channel and into the first row of homes. The areas that are in blue and green strictly represent water flow, therefore, the debris-flow is only located in areas designated by red and yellow colors (Fig. 5.14). The debris-flow measured to about 117 m at its largest width which occurred directly below the fan apex and it exhibited a maximum runout distance of about 364 m. A total of 44 homes were damaged within the area of inundation which included damage classes one through three due to the maximum debris-flow intensity reaching a value of 96.1 (Table 5.2). The majority of the area of inundation is characterized by damage class one causing some flooding and some sedimentation damage. Damage class two was located within the channel and at homes on the first, second, and third rows causing some structural damage. Damage class three was also present and caused major structural damage at the second home on the first row.

CHAPTER 6: DISCUSSION

Debris-flow initiation is dependent on volume of loose sediment, slope angle, and water availability from rainfall (Welsh and Davies, 2010). The likelihood of debris-flow initiation is increased by steeper slopes, exposed bedrock, which increases the velocity of runoff and flow of debris, high antecedent moisture conditions, and sustained and/or extreme rainfall (Giraud, 2005; Youberg, 2010). Field evidence suggests that debris-flows in MPA typically form from a combination of extreme seasonal rainfall and colluvial failure by which a rock fall or landslide transforms into a debris-flow (Iverson et al., 1997; Dorn, 2011).

Field work and sediment analysis

Features created from debris-flows such as levees provide information on two major aspects: (1) Since levees form in parallel pairs, they act to confine the flow volume (Blair and McPherson, 2009), and (2) levees can be used to reveal the history and characteristics of past flows (Youberg, 2010; Dorn, 2011). The particle size measurements from the top of the levees are made up of large boulder to cobble sized particles. The particle size measurements from within the levees were made up of intermediate to coarse size particles. The results from the AxBxC particle measurements show that the levees at Shaw Butte have more variability in particle sizes with a smaller maximum boulder size (320,000 cm³). The levees at Elephant Mountain are characterized by a more homogenous range of boulder sizes but with sharp peaks in the maximum (2,000,000 cm³).

These results also indicate the levees at Elephant Mountain tend to have a more homogenous size range with a maximum of 600 cm³ whereas Shaw Butte is a bit more heterogeneous with a much higher maximum of 1,800 cm³. Therefore, Shaw Butte has somewhat smaller boulders than Elephant Mountain, but the internal matrix of the levees at Shaw Butte are characterized by a larger amount of intermediate size particles. Debris-flows have the ability to

move these larger particles because of their high concentrations of clay which helps to maintain cohesive, dispersive, and buoyant forces, and support the debris-flow particles as a whole.

The sediment samples taken from both sites dominantly consisted of silt to sand sized particles with some gravel sized particles scattered throughout.

The key initial results of this study include the laboratory sediment analysis, which is an important method used within the literature to characterize the debris-flow rheology (Sosio et al., 2007). Within this analysis, multiple sediment samples were taken at both sites and tested for percentages of fine particles such as sand, silt, and clay. The high levels of silt and clay serve as evidence of past debris-flows and of the potential of future debris-flows. A clayey matrix has two major impacts on debris-flow behavior: one, it inhibits the settling of larger coarse particles; and two, it can prevent the body of the flow to mix together allowing the material to maintain cohesion and preventing conversion into a hyperconcentrated flow (Scott et. al., 1995; Blair and McPherson, 2009). When comparing the Shaw Butte results with the Elephant Mountain results, the percentage of clay was comparable however, Shaw Butte had a higher percentage of silt versus what was found at Elephant Mountain. This is an important finding because of the critical role that these fine particles play in the mobility of debris-flows (Whipple and Dunne, 1992). The sediment analysis provides needed information on the internal characteristics of the flow rheology and required data for the sediment concentration by volume (C_v) variable.

2D Debris Flow Modeling

2D debris-flow modeling is the most widely used method for concluding a debris-flow hazard analysis and developing hazard maps (Jakob, 2005; Fell et al., 2008, Hurlimann et al., 2008; Aronica et al., 2012). Two-dimensional models take into account the topography and debris-flow volume and depth, which provide valuable information to examine spatial variability and volume distributions on alluvial fans. FLO-2D is a desirable model to use for this study as it

can successfully model flow over complex landscapes and has the ability to evaluate street flow allowing it to simulate urban flooding on developed fans by taking flow path obstructions (buildings) into account (O'Brien et al., 1993).

Model Calibration

The results also included a successful replication of the 2010 debris-flow that occurred at Elephant Mountain. The model produced a maximum depth of 3.8 m, a maximum velocity of 1.1 m/s, and a maximum debris-flow intensity of 2.99 concentrated directly below the fan apex and within the channel. If there were structures built within the area of inundation, the most dangerous area to build would be at the fan apex and within the debris-flow channel, which is a result that corresponds to what Dorn (2011) concluded. Structures built within the area of inundation would generally have a damage class of one which, according to Jakob et al. (2012) would result in some sedimentation and flooding damage.

The model calibration was accomplished through the use of existing rainfall data provided by the Flood Control District of Maricopa County (2013), a high resolution DEM created from ALS, Cv value of 0.6 determined from the sediment analysis, infiltration parameters based on soil and land use data, and manning's n values (roughness). Factors such as flow depth and velocity is dependent on the characteristics of the debris material such as the topographic characteristics of the debris-flow channel such as width, depth, and slope angle and the concentration of sediment or the dispersal of grain sizes (Takahashi, 1981). Therefore the model was calibrated thorough the manipulation of the sediment concentration by volume variable. This value was adjusted until the model output resembled the debris-flow evidence in the field, on the high resolution DEM, and from the TLS volumetric calculations. The access to this information was pivotal to this study as it provided a starting point in generating the calibrated debris-flow model that could be applied to alternative sites within the MPA area.

Shaw Butte Model Scenarios

With the use of the calibrated model, four model scenarios, varying in precipitation totals, were developed and applied to Shaw Butte on North Mountain. This study site served as a developed location that could not only allow for the testing of the calibrated model, but also to conduct a vulnerability hazard analysis on the neighboring homes of the area. The first simulation used the same exact model scenario that occurred at Elephant Mountain in 2010. This model included a total of 105.43 mm of rain within a 24-hour period. The sediment concentration by volume hydrograph for the first scenario is contrasting to the Elephant Mountain site due to the distinct topographic differences in the un-natural topography of the developed alluvial fan. The hydrograph at Elephant Mountain resulted in a single peaked discharge whereas the hydrograph at Shaw Butte resulted in a multi-peaked discharge. This could be because the model considers that the topography at Shaw Butte is more conducive for the development of debris-flow surges when compared to the topography at Elephant Mountain. Both models resulted in similar maximum depth values where the Elephant Mountain site had a maximum depth of 3.8 m and the Shaw Butte site had a maximum depth value of 3.4 m. The two sites, however, do differ in maximum velocity values. The Elephant Mountain site had a maximum velocity of 1.1 m/s while Shaw Butte had a maximum velocity of 2.5 m/s. These differences likely result from the fact that Shaw Butte has a more consistently steep slope angle (Fig. 3.7) as well as lack of channel confinement when compared to Elephant Mountain. The higher velocities of Elephant Mountain are strictly found within the confines of the existing debris-flow channel, which could lead to an increased likelihood of flow buildup and impediment. On the other hand, the Shaw Butte site does not confine the flow nearly as much and the existing un-natural topography includes impervious surfaces that serve as venues by which the flow can potentially accelerate.

The results section also includes a range of average events that occur at the Shaw Butte site of North Mountain. It was important to pick a range of events that varied in magnitude and intensity because (1), the selection of rainfall data was coming from actual real time rainfall events and therefore there was no single event that encapsulated an exact average; and, (2) the two scenarios not only differ in rainfall magnitude but they also differ in discharge. The first average event (Scenario 2) is used to represent a lower magnitude average summer monsoonal rainstorm and was developed using a total of 52.07 mm of precipitation. All of rainfall occurred abruptly in the first ~5-hours of the 24-hour period, resulting in an initially peaked hydrograph. The second average scenario (Scenario 3), had a total of 67.56 mm of mostly continuous rainfall with a series of peaks towards the end of the 24 hour period. Both scenarios had the bulk of the flow concentrated at the fan apex and down the existing channel where it exited towards the northwest and into the developed neighborhood. Both scenarios had similar flow depths with the lower average event having 3.6 m of maximum depth and the higher average event having 3.7 m of maximum depth. Again, the differences occur in the maximum velocity outputs. The lower average precipitation scenario resulted in a maximum velocity of 1.2 m while the higher average precipitation scenario resulted in a maximum velocity of 2.6 m. For the lower average precipitation scenario, the body of the debris-flow nearly encroached on the developed areas, whereas the bulk of the higher average precipitation scenario inundated the built environment and ran out a longer distance.

Finally, the last scenario that was tested was a maximum historic storm that had the highest total precipitation ever recorded in the MPA area. The area of inundation and the location of the maximum flow depths and maximum velocities follow the same patterns as the first three scenarios however; the maximum depth and velocity values are obviously much greater. The maximum depth was 5.8 m, 2-3 meters greater than the other three scenarios. The maximum

velocity was 4.6 m/s, which is also 2-3 m/s greater than the previous scenarios. This discrepancy is obviously due to the extreme increase rainfall magnitude, showing a relation between rainfall magnitude and area of inundation of higher debris-flow intensities.

The compilation of these results indicates two major characteristics. The first is that where there is a greater magnitude of rainfall there is an increased likelihood of not only debris-flow inundation but also debris-flow intensity and area of inundation. A debris-flow threshold varies with topography, lithology, and most importantly rain intensity and magnitude (Baum and Godt, 2010). The necessary threshold of rain intensity must be exceeded for a debris-flow to ensue (Caine, 1980). Also, these results corroborate with the case that was made by Dorn (2010; 2011) where the highest threat of vulnerability is located at the fan apex and directly below the fan apex. In all of the mapped results, the areas with the highest debris-flow depth, velocities, and therefore intensities were located at the fan apex and in the area below the apex. In addition, the results show that the complexity of the topography below the fan apex plays a major role in the direction of flow and therefore the topographic area of impact. For instance, upon first glance at the Shaw Butte site, it appears that the worse of the flow would be parallel to the debris-flow channel and down the adjacent street. But, after running the debris-flow models, the topography is as such that the flow is directed towards the northwest rather than directly north. It is even more interesting to see how the layout of the urban development also plays a role in the distribution of the flow and therefore the area of inundation. The flow direction, magnitude, and inundation under natural conditions (debris-flows across the alluvial fan) would potentially play a major role in urban planning in the event of building in areas susceptible to debris-flows. However, this was beyond the scope of my thesis.

Building Vulnerability Index

Residing on an alluvial fan comes with a level of vulnerability to flooding and debris-flows. A need exists to conduct an investigation of the possible consequences of debris-flows in areas of alluvial fan development (Welsh and Davies, 2010). Debris-flows can have a significant effect on the surface topography of the alluvial fan. As a result, debris-flow characteristics such as run-out, inundation, trajectory, and magnitude of future flows are greatly affected on an event-to-event basis. The addition of urban development onto alluvial fans further complicates the interaction of these processes and converts this phenomenon from a natural event to a dangerous hazard (Pelletier et al., 2005). Therefore the interpretation and mapping of spatial patterns of debris-flows plays a critical role in the understanding of the potential hazards of debris-flow processes (Staley et al., 2006; Santi et al., 2011).

The ultimate objective of this study was to use the results of the models to interpret and map the spatial patterns of debris flows in order to conduct a building vulnerability analysis. Vulnerability for this study is defined in terms of building damage based on Jakob et al.'s (2012) debris-flow intensity equation (dv^2) and Building Vulnerability Index. Table 7 displays a compilation of all of the homes affected by each debris-flow scenario at Shaw Butte along with the corresponding damage class, description, and percent of insured loss.

Scenario		Total Number of Homes Affected	Number of homes affected by damage class	Damage Class	Damage Description	Insured Loss
1	Historical Debris Flow Event	22	21	I	Some Sedimentation	up to 25%
			0.75	II	Some Structural Damage	25-75%
			0.25	III	Major Structural Damage	75%
2	Average 1 Rain Event	22	22	I	Some Sedimentation	up to 25%
			0	II	Some Structural Damage	25-75%
			0	III	Major Structural Damage	75%
3	Average 2 Rain Event	27	26	I	Some Sedimentation	up to 25%
			1	II	Some Structural Damage	25-75%
			0	III	Major Structural Damage	75%
4	Max Historical Rain Event	44	40	I	Some Sedimentation	up to 25%
			3	II	Some Structural Damage	25-75%
			1	III	Major Structural Damage	75%

Table 6.1. Number of homes affected and their corresponding damage class description and percent of insured loss for all four scenarios.

For scenario one, the 2010 rainstorm that led to the debris-flow at Elephant Mountain, there was a maximum area of inundation of 21561.75 m² affecting a total of 22 homes. Many of the homes, affected only by damage class one, would have experienced minor flooding and some sedimentation damage that would have resulted in claims of with up to 25% of insured loss. The home located on the first row, second from the left, however, was affected by both damage class two and three, which causes some structural damage and major structural damage respectively with 25-75% of insured loss.

For Scenario 2, the lower, average rainfall resulted in total of 22 homes receiving some impact from the debris-flow surges and tailwater associated with the surges. The homes experienced damages mainly associated with damage class one, which is some flooding and some sedimentation damage. Scenario 3 (higher average rainfall) resulted in a total of 27 homes being inundated by the debris-flow surges and tailwater associated with the surges. Of the 27 homes, 26 were affected by damage class one (some flooding and some sedimentation damage), and the same home that was hit in scenario three was again hit by a damage class two causing some structural damage and a 25%-75% of insured loss.

Finally, the maximum precipitation of record, Scenario 4, had the largest area of inundation and affected the greatest number of homes. A total of 44 homes were damaged, 40 of which received a damage class one (some flooding and some sedimentation damage and up to 25% in insured losses), 3 homes received a damage class two (some structural damage and a range of 25%-75% in insured losses), and 1 home was affected by damage class three (major structural damage and 75% of insured loss).

Among all four scenarios there is a repetitive pattern in terms of building damage. The homes closest to the fan apex and homes subsequently towards the northwest are the most vulnerable to debris-flow impacts. Debris-flows, much like rivers, take the path of least resistance. It could be concluded that if the fan at Shaw Butte was still in its natural state, one would likely see a traditional depositional fan-like pattern; however, since the topography of the fan has been urbanized and therefore altered, the resulting debris-flow patterns reflect those changes. Another pattern is, the fact that as rainfall magnitude increases so does area of inundation, therefore homes closest to the fan apex are the most at risk, with risk decreasing exponentially the further out a home is. However, this only applies to the area where the bulk of the flow traverses. The pattern of flow tends to flow in a northerly direction directly from the fan apex, and then right at the line of development the topography is as such that it causes the flow to jut toward the west. This causes damage to homes further back on the western side of the neighborhood versus the homes on the eastern side, therefore highlighting the importance of the role that topographic complexity can play on debris-flow mobilization.

Limitations of the research

One of the major enigmatic components of this research is rainfall and its distribution across the landscape. For this study, the approach to rainfall was to use data that was historically accurate and spatially applicable to the study area. There is no way to know for sure the future of

the climatic patterns of the area. However, there is some agreement within the climate change literature that the future climate will be characterized by rainstorms intensification associated with regional variations in dry and wet sequences. Future climate change simulations hypothesize an escalation in seasonal irregularity of extremes (Houghton et al., 2001). The combination of little knowledge of future climatic patterns and the theorized trend towards climatic extremes only heightens the risk of these developed areas that have evidence of potential debris-flows.

Strengths and Weaknesses of FLO-2D

FLO-2D can accurately simulate flood hydraulics, estimate velocity and depth, predict area of inundation, and calculate termination of the flow. FLO-2D is a favorable model to use for this study because of its accuracies, its reputation within the literature, its ability to adapt to complex topography, and accurately simulate debris-flows on developed alluvial fans by taking flow path obstructions (buildings, homes, etc.) into account. Another added benefit is that this particular modeling software was developed in southwest United States – the same environment as the study sites chosen for this research. However, FLO-2D does come with some limitations. FLO-2D does tend to overestimate the runout length of coarse-grained granular debris-flows because of the existing yield strength assumptions (Sosio et al., 2007; Wu et al., 2013). Issues also arise within the sediment concentration by volume parameterization. The sediment concentration by volume (C_v) parameter is the concentration of sediment versus water within a debris-flow. The FLO-2D reference manual (O'Brien, 2011) specifies the correct C_v value to use in specific cases. However, the model is based on hyperconcentrated flows so it tends to under predict the total concentration by volume. This is because the C_v values are only representing the matrix materials rather than the combination of the matrix materials and the more coarse bouldery debris.

CHAPTER 7: CONCLUSIONS

This study has aimed at developing and testing a method for modeling potential debris-flows in areas of the MPA where the natural alluvial fan surface has been altered by urban expansion and development. This new method expands on the existing literature by providing a more accurate field representation of the potential of debris-flows in MPA by corroborating the models with an actual historical debris-flow with the aid of ALS, TLS, and sediment analysis. This method includes using FLO-2D to develop a calibrated debris-flow model on an existing recent debris-flow site and applying this model to a developed area that is potentially vulnerable to debris-flows based on field evidence of past events.

This research uses existing debris-flow hazard analysis methods (Jakob, 2005; Jakob et al., 2012) while simultaneously providing a hazard assessment for the area of Shaw Butte in North Mountain MPA and concludes with a vulnerability analysis and debris-flow hazard vulnerability maps. This research addresses the following questions:

1. Is a historically documented non-urban debris flow capable of inundating and damaging buildings on the alluvial fan at Shaw Butte in MPA?
2. What is the potential for building damage under modeled scenarios under average and extreme rainfall conditions?

The results not only provide evidence to conclude that a peak rainstorm is capable of producing a debris-flow at Shaw Butte but it also provides evidence that the area could potentially be vulnerable to debris-flows even under average monsoonal rainstorms. The results also show that the area's most vulnerable to a debris-flow impact are directly below the fan apex, within the existing debris-flow channel, and along the flow trajectory that is linked to the alluvial fan topography. The results also suggest that the urbanization of alluvial fans could in fact have an effect on the pattern of flow versus what would occur under natural conditions. More

research, however would need to be conducted in order to specify what these differences, if any, would be.

These results are important in that they can provide communities and hazard management agencies with decision-making data and mitigation information based upon the degree of risk and therefore vulnerability associated with different debris-flow magnitudes. However, alluvial fans that have already been developed are a challenging and delicate social and political matter. Structural features such as levees or debris basins can be employed however these means are usually expensive and, in the long run, unreliable (Welsh and Davies, 2011). The most advantageous option is to identify hazardous fans to begin with and prevent development on them. This approach may be difficult in MPA as debris-flows are not yet considered a hazard in the area, however, with more research and an increase in awareness, the area may be able to move in this direction and decrease the amount of urbanization on alluvial fans.

Future Research

While this study adds to the literature by providing a unique method to debris-flow modeling as well as corroborating results within existing studies (Dorn, 2010; 2011), there is definitely room to expand and improve. One concept would be to run the same Shaw Butte scenarios but on a DEM surface that has the urbanization removed. Debris-flow models at this site with the development removed would allow for a comparison of flow patterns between developed topography and undeveloped topography. It would also give insight into the practices of future development patterns in the case of building on existing natural alluvial fans.

Another concept would be to develop a bracket of variations (an ensemble, as done in other environmental and climatic modeling) of debris-flow model results using multiple modeling software's such as FLO-2D, RAMMS, and LAHARZ. The current methods provide a good starting point and approximation of the potential hazards of debris-flows in the Shaw

Butte area, however; having multiple modeled outcomes would provide a range of results that could contribute a more accurate description of the potential impacts.

Broader Impacts and Geographical Context

The issue of urban expansion onto potentially hazardous yet highly scenic alluvial fans is not restricted to the MPA area; this is also a broader issue in the southwestern United States especially in major cities such as Las Vegas, Tucson, AZ, San Francisco, Los Angeles, and Salt Lake City. The scale of the general problem of urban expansion onto alluvial fans can also be expanded into a worldwide issue, but with differing socio-economic issues. In the southwest United States, these potentially dangerous areas are sites of attraction to the higher income population for their resources and desired views. However, in less developed areas such as South and Central America, India, and parts of China, the socio-economic situation is reversed. These are regions where the impoverished and less fortunate are forced to move onto potentially dangerous areas such as alluvial fans. Many of the dwellings in these areas are not the sturdy masonry structures found in the MPA for instance, they are typically characterized as overly crowded shantytowns with makeshift unstable dwellings.

With that in mind, the perspective of this study was to take a worldwide broad issue and focus it on a specific area to provide added knowledge and documentation of the relationship between urban expansion and debris-flow hazards. This holistic approach is geared to the modern idea of the anthropocene. The argument of this perspective is that the environment cannot be considered devoid of anthropogenic forces and therefore, the prediction of earth surface changes is contingent on the understanding of the interactions between human and geomorphic processes. While the magnitude of vulnerability and the geomorphology of debris-flows vary in space and time, the risk of these events is worldwide and is therefore important to hazard research.

REFERENCES

- Abellán, A., Oppikofer, T., Jaboyedoff, M., Rosser, N. J., Lim, M., & Lato, M. J. (2014). Terrestrial laser scanning of rock slope instabilities. *Earth Surface Processes and Landforms*, 39(1), 80-97.
- Akbas, S. O., Blahut, J., & Sterlacchini, S. (2009). Critical assessment of existing physical vulnerability estimation approaches for debris-flows. *Landslide processes: from geomorphological mapping to dynamic modelling*. CERG Editions, Strasbourg, 229-233.
- AMEC Earth and Environmental, Inc.; Wright Water Engineers, Inc.; and Wenk and Associates. (2010). City of aspen Urban Runoff management Plan. A guide to stormwater management in the city of Aspen. Web: 25 March. 2013 <
<http://www.aspenpitkin.com/Departments/Engineering/Stormwater/Development-Construction/>
- Arcement Jr, G. J., & Schneider, V. R. (1989). Guide for Selecting Manning's Roughness Coefficients for Natural Channels and Flood Plains United States Geological Survey Water-supply Paper 2339. pubs. usgs. gov/wsp/2339/report. pdf.
- Armento, M., Genevois, R., and Tecca, P., 2008, Comparison of numerical models of two debris flows in the Cortina d' Ampezzo area, Dolomites, Italy: *Landslides*, v. 5, no. 1, p. 143-150.
- Aronica, G. T., Biondi, G., Brigandì, G., Cascone, E., Lanza, S., and Randazzo, G. (2012). Assessment and mapping of debris-flow risk in a small catchment in eastern Sicily through integrated numerical simulations and GIS. *Physics and Chemistry of the Earth, Parts A/B/C*.
- Baltsavias, E.P. (1999). Airbone laser scanning: basic relations and formulas. *ISPRS J Photogramm Remote Sens* 54:199–214.
- Barnes, H. H. (1967). Roughness characteristics of natural channels: U.S. Geological Survey Water-Supply Paper 1849, pp. 213.
- Bell, R., and Glade, T. (2004). Quantitative risk analysis for landslides—Examples from BÍldudalur, NW-Iceland. *Natural Hazards and Earth System Science*, 4(1), 117-131.
- Bertoldi, G., D'Agostino, V., and McArdell, B. W. (2012). An integrated method for debris-flow hazard mapping using 2D runout models. *Interpraevent*.

- Blackwelder, E. (1928). Mudflow as a Geologic Agent in Semiarid Mountains (with discussion by Joseph T. Singewald, jr.). *Geological Society of America Bulletin*, 39(2), 465-483.
- Blair, T., and McPherson, J. (2009). Processes and forms of alluvial fans. In: Parsons, A., and Abrahams, A. (eds) *Geomorphology of desert environments*. New York: Springer, pp. 413-467.
- Borter, P. (1999). Risikoanalyse bei gravitativen Naturgefahren, Bundesamt für Umwelt. Wald und Landschaft, Bern, p 1999.
- Bovis, M. J. and Jakob, M. (1999). The role of debris supply conditions in predicting debris-flow activity. *Earth Surface Processes and Landforms*, 24: 1039–54.
- Catani, F., Farina, P., Moretti, S. and Nico, G. (2003). *Spaceborne radar interferometry: a promising tool for hydrological analysis in mountain alluvial fan environments, erosion prediction in ungagged basins: integrating methods and techniques*. Sapporo: IAHS Publication No., pp. 241-248.
- Cavalli, M. and Marchi, L. (2008). Characterization of the surface morphology of an alpine alluvial fan using airborne LiDAR. *Natural Hazards and Earth System Sciences*, 8: 323-333.
- Christen, M., Bühler, Y., Bartelt, P., Leine, R., Glover, J., Schweizer, A., ... & Volkwein, A. (2012). Integral hazard management using a unified software environment. In Proceedings of 12th Congress Interprevent (pp. 77-86).
- City of Phoenix. (2009). Zoning ordinance of the City of Phoenix, Arizona. Codified through Ordinance No. G-5391, adopted June 17, 2009, effective August 1, 2009. Supplement No. 16, Update 1. <http://www.municode.com/Resources/gateway.asp?pid=13534&sid=3> (last accessed 8 September 2009).
- Coe, J., Glancy, P., and Whitney, J. (1997). Volumetric analysis and hydrologic characterization of a modern debris-flow near Yucca Mountain Nevada. *Geomorphology*, 20: 11-28.
- Coon, W. F., Estimation of roughness coefficients for natural stream channels with vegetated banks, U.S. Geol. Survey Water Supply Pap., 2441, 133 pp., 1998.
- Costa, J. E. (1984). Physical Geomorphology of Debris-flows. In: Costa, J. E. and Fleisher, P. J. (eds) *Developments and applications of geomorphology*. Berlin: Springer-Verlag, pp. 268-317.

- Costa, J. E. and Williams, G. P. 1984. Debris-flow dynamics (videotape). United States Geological Survey Open File Report 84-606.
- Cutter, S. (1996). Vulnerability to environmental hazards. *Progress in Human Geography*, 20(4), 529-539.
- Davies, T. R. H. (1990). Debris-flow surges-experimental simulation. *New Zealand Journal of Hydrology*, 29, 18-46.
- De Scally, F.A., Slaymaker, O. and Owens, I.F. (2001). "Morphometric controls and basin response in the Cascade Mountains". *Geografiska Annaler*, 83A (3):117-130
- de Scally, F.A. and Owens, I.F. (2004). "Morphometric controls and geomorphic response on fans in the Southern Alps, New Zealand". *Earth surface processes and landforms*, 29: 311-322.
- Desloges, J. R., and Gardner, J. S. (1984). Process and discharge estimation in ephemeral channels, Canadian Rocky Mountains. *Canadian Journal of Earth Sciences*, 21(9), 1050-1060.
- Dorn, R. I. (2009). Desert rock coatings. In *Geomorphology of Desert Environments* (pp. 153-186). Springer Netherlands.
- Dorn, R. I. (2010). Debris-flows From Small Catchments of the Ma Ha Tuak Range, Metropolitan Phoenix, Arizona. *Geomorphology*, 120(3-4), 339-352.
- Dorn, R. I. (2011). Do Debris-flows Pose a Hazard to Mountain-Front Property in Metropolitan Phoenix, Arizona? *The Professional Geographer*, 64(2), 197-210.
- Fell, R., Corominas, J., Bonnard, C., Cascini, L., Leroi, E., & Savage, W. Z. (2008). Guidelines for landslide susceptibility, hazard and risk zoning for land use planning. *Engineering Geology*, 102(3-4), 85-98.
- Fell R. and Hartford, D. (1997). Landslide risk management. In: Cruden D, Fell R (eds) *Landslide risk assessment*. Balkema, Rotterdam, pp 51-109.
- Flood Control district of Maricopa County. (2013). *Rainfall and Weather*. Retrieved from <http://www.fcd.maricopa.gov/Rainfall/rainfall.aspx>.

- Frankel, K. and Dolan, J. (2007). Characterizing arid region alluvial fan roughness with airborne laser swath mapping digital topographic data. *Journal of Geophysical Research*, 112, pp. F02025.
- Fuller, JE Hydrology & Geomorphology, Inc. (2008). Technical Documentation Notebook for White Tank Mountain Fans 1 & 2 Alluvial Fan Floodplain Delineation Study. Report submitted to the Flood Control District of Maricopa County.
- Fuchs, S., Heiss, K., & Hübl, J. (2007). Towards an empirical vulnerability function for use in debris-flow risk assessment. *Natural Hazards and Earth System Science*, 7(5), 495-506.
- Fuller, JE Hydrology & Geomorphology, Inc. (2009). FLO2D modeling performed for FCD2008C007 – Piedmont Flood Hazard Assessment Manual Evaluation. Unpublished data submitted to the Flood Control District of Maricopa County.
- Gabet, E.J., and Mudd, S.M. (2006). The mobilization of debris-flows from shallow landslides. *Geomorphology* 74: 207-218.
- Garcia, R., López, J.L., Noya, M., Bello, M.E., Bello, M.T., González, N., Paredes, G., Vivas, M.I., and O'Brien, J.S. (2003). Hazard mapping for debris-flow events in the alluvial fans of northern Venezuela. 3rd International Conference on Debris-Flow Hazards Mitigation: Mechanics, Prediction, and Assessment: Davos, Switzerland, American Society of Civil Engineers, v. 1, p. 589-599.
- Giraud, R.E. (2005). Guidelines for the geologic evaluation of debris-flow hazards on alluvial fans in Utah. *Utah Geological Survey*, Miscellaneous Publication 05-6.
- Gomes, R. A. T., Guimarães, R. F., de Carvalho, J., Abílio, O., Fernandes, N. F., & do Amaral Júnior, E. V. (2013). Combining spatial models for shallow landslides and debris-flows prediction. *Remote Sensing*, 5(5), 2219-2237.
- Gordon, S., Lichti, D., Stewart, M. (2001). Application of a high-resolution, ground-based laser scanner for deformation measurements. In: Proceedings of the 10th international FIG symposium on deformation measurements, Orange, California, USA, 19–22 March 2001, pp 23–32.
- Griffiths, P. G., Webb, R. H., & Melis, T. S. (2004). Frequency and initiation of debris-flows in Grand Canyon, Arizona. *Journal of Geophysical Research: Earth Surface* (2003–2012), 109(F4).

- Griffiths, P. G., Magirl, C. S., Webb, R. H., Pytlak, E., Troch, P. A. and Lyon, S. W. (2009). Spatial distribution and frequency of precipitation during an extreme event: July 2006 mesoscale convective complexes and floods in southeastern Arizona. *Water Resources Research*, 45, pp. W07419.
- Harris, R. C. and Pearthree, P. A. (2002). A home buyer's guide to geological hazards in Arizona. *Arizona Geological Survey Down-To-Earth*, 13: 1–36.
- Hashimoto, A., Oguchi, T., Hayakawa, Y., Lin, Z., and Wasklewicz, T. (2008). GIS analysis of depositional slope change at alluvial-fan toes in Japan and the American Southwest. *Geomorphology*, 100: 120-130.
- Helm, C. R. (2003). Leapfrogging, urban sprawl, and growth management: Phoenix, 1950–2000. *American Journal of Economics and Sociology*, 60, 245–283.
- Hiremagalur, J., Yen, K.S., Akin, K., Bui, T., Lasky, T.A., and Ravani, B. (2007). Creating standards and specifications for the use of laser scanning in CalTrans projects. Technical report no F/CA/RI/2006/46, California Department of Transportation, US (www.ahmct.ucdavis.edu/images/AHMCT_LidarFinalReport.pdf).
- Hooke, R. (1967). Processes on arid-region alluvial fans. *Journal of Geology*, 75: 438-460.
- Houghton, J.T., Ding, Y., Griggs, D.J., Noguera, M., Van Der Linden, P.J., Dai, X., Maskell, K., and Johnson, C.A. (2001). *Climate change 2001: the scientific basis*. Vol. 881. Cambridge: Cambridge university press.
- Hsu, S. M., Chiou, L. B., Lin, G. F., Chao, C. H., Wen, H. Y., & Ku, C. Y. (2010). Applications of simulation technique on debris-flow hazard zone delineation: a case study in Hualien County, Taiwan. *Natural Hazards & Earth System Sciences*, 10(3).
- Hübl, J., & Steinwendtner, H. (2001). Two-dimensional simulation of two viscous debris-flows in Austria. *Physics and Chemistry of the Earth, Part C: Solar, Terrestrial & Planetary Science*, 26(9), 639-644.
- Hungr, O. (2000). Analysis of debris-flow surges using the theory of uniformly progressive flow. *Earth Surface Processes and Landforms*, 25: 483-495.
- Hungr, O. (2005). Classification and Terminology. In: Jakob, M. and Hungr, O. *Debris-flow hazards and related phenomena*. Berlin, Heidelberg: Springer, pp. 9-21.

- Hurlimann, M., Rickenmann, D., and Graf, C. (2003). Field and monitoring data of debris-flow events in the Swiss Alps. *Canadian Geotechnical Journal*, 40:161-175.
- Hürlimann, M., Rickenmann, D., Medina, V., and Bateman, A. (2008). Evaluation of approaches to calculate debris-flow parameters for hazard assessment. *Engineering Geology*, 102(3), 152-163.
- Hussin, H. Y., Luna, B. Q., Van Westen, C. J., Christen, M., Malet, J. P., & van Asch, T. W. (2012, April). Assessing the debris flow run-out frequency of a catchment in the French Alps using a parameterization analysis with the RAMMS numerical run-out model. In *EGU General Assembly Conference Abstracts* (Vol. 14, p. 12593).
- Iverson, R. M. (1997). The physics of debris-flows. *Reviews of Geophysics*, 35(3), 245-296.
- Iverson, R. M., Reid, M., and LaHusen, R. (1997). Debris-flow mobilization from landslides. *Annual Review of Earth and Planetary Sciences*, 25: 85-138.
- Iverson, R. M. (2003). The debris-flow rheology myth. In *Debris-flow Mechanics and Mitigation Conference*, Mills Press, Davos, pp. 303-314.
- Iverson, R. M., Logan, M., LaHusen, R. and Berti, M. (2010). The perfect debris-flow? Aggregated results from 28 large-scale experiments. *Journal of Geophysical Research*, 115, pp. F03005.
- Jaboyedoff, M., Oppikofer, T., Abellán, A., Derron, M. H., Loye, A., Metzger, R., & Pedrazzini, A. (2012). Use of LIDAR in landslide investigations: a review. *Natural hazards*, 61(1), 5-28.
- Jackson, L. E., Kostaschuk, R. A., and Macdonald, G. M. (1987). Identification of debris-flow hazard on alluvial fans in the Canadian Rocky Mountains. *Reviews in Engineering Geology*, 7, 115-124.
- Jakob, M. and Hungr, O. (2005). Introduction. In: Jakob, M. and Hungr, O. *Debris-flow hazards and related phenomena*. Berlin, Heidelberg: Springer, pp. 1-7.
- Jakob, M. (2005). Debris-flow hazard analysis. In: Jakob, M. and Hungr, O. *Debris-flow hazards and related phenomena*. Berlin, Heidelberg: Springer, pp. 411-443.
- Jakob, M., Stein, D., and Ulmi, M. (2012). Vulnerability of buildings to debris-flow impact. *Natural hazards* (Dordrecht), 60(2), 241-261.

- Johnson, J.K., Reynolds, S.J., and Jones, D.A. (2003). Geologic map of the Phoenix Mountains, Central Arizona. Arizona Geological Survey Digital Geologic Map 28.
- Kostaschuk, R. A., MacDonald, G. M., & Putnam, P. E. (1986). Depositional process and alluvial fan-drainage basin morphometric relationships near Banff, Alberta, Canada. *Earth Surface Processes and Landforms*, 11(5), 471-484.
- Larsen, M.C., Wieczorek, G.F., Eaton, L.S., Morgan, B.A., and Torres-Sierra, H. (2001). Natural hazards on alluvial fans: the debris-flow and flash-flood disaster of northern Venezuela, December 1999. *EOS, Transactions - American Geophysical Union* 82 (47), 572–573.
- Leighty, R.S., Skotnicki, S.J., and Pearthree, P.A. (1997). Geologic map of the Cave Creek quadrangle, Maricopa County, Arizona. Arizona Geological Survey open file report 97-1.
- Lin, J., Yang, M., Lin, B., and Lin, P. (2011). Risk Assessment of debris-flows in Songhe Stream, Taiwan. *Engineering Geology*, 123: 100-112.
- Magirl, C. S., Webb, R. H., Schaffner, M., Lyon, S. W., Griffiths, P. G., Shoemaker, C., and Unkrich, C. L. (2007). Impact of recent extreme Arizona storms. *EOS*, 88: 191–93.
- Magirl, C. S., Griffiths, P. G., and Webb, R. H. (2010). Analyzing debris-flows with the statistically calibrated empirical model LAHARZ in southeastern Arizona, USA. *Geomorphology*, 119(1–2), 111-124.
- Major, J. and Iverson, R. (1999). Debris-flow deposition: effects of pore-fluid pressure and friction concentrated at flow margins. *Geological Society of America Bulletin*, 111: 1424-1434.
- Marcato, G., Bossi, G., Rivelli, F., & Borgatti, L. (2012). Debris flood hazard documentation and mitigation on the Tilcara alluvial fan (Quebrada de Humahuaca, Jujuy province, North-West Argentina). *Natural Hazards Earth System Science*, 12: 1873-1882.
- McCarthy, T. S., et al. (1997). The gradient of the Okavango fan, Botswana, and its sedimentological and tectonic implications. *Journal of African Earth Sciences*, 24(1), 65-78.
- McCoy, S. et al. (2010). Evolution of a natural debris-flow: in situ measurements of flow dynamics, video imagery, and terrestrial laser scanning. *Geology*, 38: 735-738.
- Melis, T. S. (1997). Geomorphology of debris-flows and alluvial fans in Grand Canyon National Park and their influence on the Colorado River below Glen Canyon Dam, Arizona.

- Melton, M.A. (1965). The geomorphic and paleoclimatic significance of alluvial deposits in southern Arizona. *Journal of Geology*, 73: 1-38
- NOAA's National Weather Service Hydrometeorological Design Studies Center Precipitation Frequency Data Server. (2014). Retrieved from:
http://hdsc.nws.noaa.gov/hdsc/pfds/pfds_map_cont.html?bkmrk=az
- O'Brien, J. S., & Julien, P. Y. (1988). Laboratory analysis of mudflow properties. *Journal of hydraulic engineering*, 114(8), 877-887.
- O'Brien, J., Julien, P., and Fullerton, W. (1993). Two-Dimensional water flood and mudflow simulation. *Journal of Hydraulic Engineering*, 119(2), 244-261.
- O'Brien, J. (2011). FLO-2D Reference manual, version 2009.
- Pearthree, P.A., 2004, Fire and sediment deposition: *Arizona Geology*, 34, no. 3, 1-2.
- Pearthree, P. A. and Youberg, A. 2006. Recent debris-flows and floods in southern Arizona. *Arizona Geology*, 36(3), 1-6.
- Pearthree, P. A., Youberg, A. and Cook, C. P. (2007). Debris-flows; an underappreciated flood hazard in southern Arizona. *Geological Society of America Abstracts with Program*, 39(5), 11.
- Pelletier, J., et al. (2005). An integrated approach to alluvial fan flood hazard assessment with numerical modeling, field mapping, and remote sensing. *GSA bulletin*, 117(9-10), 1167-1180.
- Petrie, G. and Toth, C.K. (2008). I. Introduction to laser ranging, profiling and scanning, II. Airborne and spaceborne laser profiles and scanners, III. Terrestrial laser scanners (chapters 1 to 3). In: Shan J, Toth CK (eds) *Topographic laser ranging and scanning: principles and processing*, CRC Press, Taylor & Francis.
- Pierson, T. (2005). Hyperconcentrated flow – transitional process between water flow and debris flow. In: Jakob, M. and Hungr, O. *Debris-flow hazards and related phenomena*. Berlin, Heidelberg: Springer, pp. 159-196.
- Prochaska, A.B., Santi, P.M., Higgins, J.D., and Cannon, S.H. (2008b). Debris-flow runout predictions based on the average channel slope (ACS). *Engineering Geology*, 98: 29-40.

- Reid, M. E., LaHusen, R. G., & Iverson, R. M. (1997). Debris-flow initiation experiments using diverse hydrologic triggers. *Debris-Flow Hazards Mitigation: Mechanics, Prediction and Assessment*, 1-11.
- Reid, M.E., Briwn, D.L., LaHusen, R.G., Roering, J.J., de la Fuente, J., and Ellen, S.D. (2003). Debris-flow initiation from large, slow-moving landslides. *Debris-Flow Hazards Mitigation: Mechanics, Prediction, and Assessment*. pp. 155-166
- Rickenmann, D., Laigle, D. M. B. W., McArdell, B. W., & Hübl, J. (2006). Comparison of 2D debris-flow simulation models with field events. *Computational Geosciences*, 10(2), 241-264.
- Santi, P.M., Hewitt, K., Vandine, D.F., and Cruz, E.B. (2011). Debris-flow impact, vulnerability, and response. *Natural Hazards*, 56:371-402.
- Scheinert, C., Wasklewicz, T., and Staley, D. (2012). Alluvial fan dynamics - revisiting the field. *Geography Compass*, 6(12), 752-775.
- Schilling, S. P. (1998). *LAHARZ: GIS programs for automated mapping of lahar-inundation hazard zones*. US Department of the Interior, US Geological Survey.
- Schmidt, K. M., Hanshaw, M. N., Howle, J. F., Kean, J. W., Staley, D. M., Stock, J. D., & Bawden, G. W. (2011, June). Hydrologic conditions and terrestrial laser scanning of post-fire debris-flows in the San Gabriel Mountains, CA, USA. In *Proceedings of the Fifth International Conference on Debris-flow Hazards Mitigation/Mechanics, Prediction, and Assessment*, Padua, Italy (pp. 583-593).
- Schurch, P., Densmore, A. L., Rosser, N. J. and McArdell, B. W. (2011)a. A novel debris-flow fan evolution model based on debris-flow monitoring and LiDAR topography. In: Genevois, R., Hamilton, D. L. and Prestininzi, A. (eds) *Fifth International Conference on Debris-Flow Hazards Mitigation – Mitigation, Mechanics, Prediction and Assessment; Padua, Italy 14–17 June 2011*, Padua: Casa Editrice Universita` La Sapienza, pp. 263–272.
- Schurch, P., Densmore, A.L., Rosser, N.J., and McArdell, B.W. (2011)b. Dynamic controls on erosion and deposition on debris-flow fans. *Geology*, 39(9), 827-830.
- Shan, J. and Toth, K. (2008). *Topographic laser ranging and scanning: principles and processing*. CRC Press, Taylor & Francis Group, LLC, UK.

- Sodnik, J., Podobnikar, T., and Mikoš, M. (2012). Using lidar data for debris-flow modelling. In: Proceedings of the 12th Congress INTERPRAEVENT, 23–26 April, 2012, Grenoble, France. pp 573–583.
- Sosio, R., Crosta, G. B., & Frattini, P. (2007). Field observations, rheological testing and numerical modelling of a debris-flow event. *Earth Surface Processes and Landforms*, 32(2), 290-306.
- Sosio, R., Crosta, G.B. (2009). Rheology of concentrated granular suspensions and possible implications for debris-flow modeling. *Water Resources Research* 45: W03412.
- Staley, D.M., Wasklewicz, T.A., and Blaszczynsky, J.S. (2006). Surficial patterns of debris-flow deposition on alluvial fans in Death Valley, CA using airborne laser swath mapping data. *Geomorphology*, 74: 152-163.
- Staley, D. M., Wasklewicz, T. A., & Kean, J. W. (2014). Characterizing the primary material sources and dominant erosional processes for post-fire debris-flow initiation in a headwater basin using multi-temporal terrestrial laser scanning data. *Geomorphology*, 214, 324-338.
- Stefanov, W.L., and Green, D. (2013). Geology and soils in deserts of the southwestern United States. In: Malloy, R., Brock, J., Floyd, A., Livingston, M., & Webb, R. H. (Eds.). *Design with the Desert: Conservation and Sustainable Development*. CRC Press, pp. 37-57.
- Takahashi, T. (1981). Debris-flow. *Annual Review of Fluid Mechanics*, 13(1), 57-77.
- Tobin, G.A and Montz, B.E. (1997). *Natural Hazards: Explanation and Integration*. Guilford Press. pp. 281-319.
- USDA Natural Resources Conservation Services, (2013, Dec.). *Web Soil Survey*. Retrieved from <http://websoilsurvey.sc.egov.usda.gov/App/HomePage.htm>
- USGS, (2014, Mar.). *USGS DS 240: Enhanced Historical Land-Use and Land-Cover Data Sets of the U.S. Geological Survey*. Retrieved from water.usgs.gov/GIS/dsdl/ds240/index.html
- VanDine, D. F. (1985). Debris-flows and debris torrents in the southern Canadian Cordillera. *Canadian Geotechnical Journal*, 22(1), 44-68.
- Vincent, R., Parker, K., Peterson, J., Welsh, M., Kersey, N., Scheinert, C., and Guevara, A. (2013). Integrated: multi-source lidar and imagery. *LiDAR Magazine* Vol. 3 no. 1, pp.

10-17. Retrieved from http://www.mckimcreed.com/media/resources/Integrated_Multi-Source%20LiDAR%20and%20Imagery.pdf

- Wasklewicz, T., Mihir, M., and Whitworth, J. (2008). Surface variability of alluvial fans generated by disparate processes, eastern Death Valley, CA. *The Professional Geographer*, 60(2), 207-223.
- Wasklewicz, T. A., & Staley, D. M. (2010, December). Monitoring debris-flow induced channel morphodynamics with terrestrial laser scanning, Chalk Cliffs, CO. In AGU Fall Meeting Abstracts (Vol. 1, p. 08).
- Webb, R.H., Magirl, C.S., Griffiths, P.G., and Boyer, D.E. (2008). Debris-flows and floods in southeastern Arizona from extreme precipitation in late July 2006: Magnitude, frequency, and sediment delivery, U.S. Geological Survey Open-File Report 2008-1274: Tucson, Arizona, United States Geological Survey, p. 95.
- Wehr, A. and Lohr, U. (1999). Airborne laser scanning—an introduction and overview. *ISPRS J Photogramm Remote Sens* 54:68–82.
- Welsh, A. and Davies, T. (2010). Identification of alluvial fans susceptible to debris-flow hazards. *Landslides*, 8:183-194.
- Whipple, K. X., and Dunne, T. (1992). The influence of debris-flow rheology on fan morphology, Owens Valley, California. *Geological Society of America Bulletin*, 104(7), 887-900.
- Wilford, D., Sakal, M., Innes J., Sidle R., & Bergerud, W. (2004). Recognition of debris-flow, debris-flood and flood hazard through watershed morphometrics. *Landslides*, 1:61-66.
- Wohl, E. E., & Pearthree, P. P. (1991). Debris-flows as geomorphic agents in the Huachuca Mountains of southeastern Arizona. *Geomorphology*, 4(3), 273-292.
- Wu, Y. H., Liu, K. F., & Chen, Y. C. (2013). Comparison between FLO-2D and Debris-2D on the application of assessment of granular debris-flow hazards with case study. *Journal of Mountain Science*, 10(2), 293-304.
- Youberg, A., Cline, M.L., Cook, J.P., Pearthree, P.A., and Webb, R.H. (2008). Geologic mapping of debris-flow deposits in the Santa Catalina Mountains, Pima County, Arizona: Arizona Geological Survey, scale 1:6,000.

Youberg, A. (2010). Methods for Evaluating Alluvial Fan Flood Hazards from Debris-flows in Maricopa County, Arizona. : 10-01. Arizona Geological Survey Open File Report.

Yu, F., Chen, C., Chen, T., Hung, F., and Lin, S. (2006). A GIS process for delimitating areas potentially endangered by debris-flow. *Natural Hazards*, 37:169-189.